

**PMP22-overexpressing mice
as a model for
Charcot-Marie-Tooth 1A neuropathy
implicate a role of immune-related cells**

Dissertation zur Erlangung des
naturwissenschaftlichen Doktorgrades
der Julius-Maximilians-Universität Würzburg

vorgelegt von
Bianca Dorothea Kohl
aus Rüdenuau

Würzburg, 2009

Eingereicht am: 03.08.2009

Mitglieder der Promotionskommission:

Vorsitzender: Prof. Dr. Martin Müller

Gutachter: Prof. Dr. Rudolf Martini

Gutachter: Prof. Dr. Erich Buchner

Tag des Promotionskolloquiums: 04.12.2009

Doktorurkunde ausgehändigt:

Eidesstattliche Erklärung

Hiermit erkläre ich, die vorliegende Arbeit selbständig angefertigt und keine anderen als die angegebenen Hilfsmittel verwendet zu haben.

Diese Arbeit hat weder in gleicher noch in ähnlicher Form in einem anderen Prüfungsverfahren vorgelegen.

Ich habe in keinem früheren Verfahren einen akademischen Grad erworben oder zu erwerben versucht.

Würzburg, 03.08.2009

Bianca Kohl

Für
Martin und meine Familie

1. Summary	8
2. Zusammenfassung	10
3. Introduction	12
3.1 The myelin sheath	12
3.1.1 Formation and structure of the myelin sheath	12
3.1.2 Proteins of the peripheral nervous system	14
3.2 Disorders of the peripheral nervous system	15
3.2.1 Polyneuropathies	15
3.2.2 Charcot-Marie-Tooth disease	16
3.2.3 PMP22 mutations as models for CMT1A	18
3.2.4 The immune system as a mediator of pathology in inherited demyelination	20
3.3 Aim of the study	22
4. Materials and methods	23
4.1 Equipment, reagents, solutions, buffers, media and antibodies	23
4.2 Mutant mice and genotyping	23
4.3 Cell culture	25
4.4 Bone marrow transplantation	25
4.5 Flow cytometry	26
4.6 Isolation of RNA and protein from peripheral nerves	26
4.7 Reverse transcription and quantitative real-time PCR	27
4.8 Western blot analyses	28
4.9 Immunohistochemical analyses	29
4.10 Electron microscopic analyses	31
4.11 Neurographic recordings	32
4.12 Functional tests	32
4.13 <i>In vivo</i> inhibition of the MEK1/2/ERK1/2 signaling cascade by CI-1040	33
4.14 Statistical analyses	33

5. Results -----	34 -
5.1 Morphological analyses of peripheral nerves of juvenile PMP22 mutant mice-----	34 -
5.1.1 Investigations of peripheral nerves of PMP22tg mice at the age P7 reveal no alterations in axonal sorting-----	34 -
5.1.2 Overexpression of PMP22 leads to thicker myelin sheaths in peripheral nerves of PMP22tg mice at the age P7 -----	36 -
5.2 The functional contribution of T-lymphocytes to the pathogenesis of PMP22tg mice-----	38 -
5.2.1 Pathological alterations are non-significantly increased in peripheral nerves of PMP22tg/RAG-1-/- mice at the age of 12 months-----	38 -
5.2.1.1 The absence of mature lymphocytes does not influence macrophage numbers within nervous tissue of PMP22tg mice -----	38 -
5.2.1.2 Peripheral nerves of PMP22tg/RAG-1-/- mice disclose a non-significant increase of pathological alterations at 12 months of age--	40 -
5.2.2 Deficiency of PD1 (PD-1-/-) in PMP22tg mice do not cause an aggravated neuropathological phenotype-----	43 -
5.2.2.1 The numbers of immune cells are not altered in peripheral nerves of PMP22tg BMC PD-1-/- compared to PMP22tg BMC wt----	43 -
5.2.2.2 The degree of pathological alterations is equal in nervous tissue of PMP22tg BMC PD-1-/- and of PMP22tg BMC wt -----	45 -
5.2.2.3 Sciatic nerve conduction properties are not altered in PMP22tg BMC PD-1-/- compared to PMP22tg BMC wt -----	47 -
5.2.2.4 PMP22tg BMC PD-1-/- exhibit stride properties similar to PMP22tg BMC wild type -----	48 -
5.3 The functional contribution of macrophages to the pathogenesis of PMP22tg mice-----	50 -
5.3.1 MCP-1 mRNA expression is increased in peripheral nerves of PMP22tg mice -----	50 -
5.3.2 Nervous tissue of PMP22/MCP-1 double mutants show differences in the demyelinating phenotype -----	51 -
5.3.2.1 MCP-1 deficiency causes a reduced number of macrophages in peripheral nerves of PMP22tg mutants compared to wild type mice -	52 -

5.3.2.2 PMP22/MCP-1 double mutant mice show different cytokine expression -----	54 -
5.3.2.3 Reduction and deficiency of MCP-1 leads to amelioration of disease in PMP22tg mice-----	56 -
5.3.2.4 Properties of axonal integrity are only improved in the complete absence of MCP-1 in PMP22tg mice -----	59 -
5.3.3 The MEK1/2/ERK1/2 signaling cascade is involved in the expression of MCP-1 in peripheral nerves of PMP22tg mice -----	63 -
5.3.3.1 The MEK1/2/ERK1/2 signaling cascade is activated in peripheral nerves of PMP22tg mice-----	63 -
5.3.3.2 <i>In vivo</i> inhibition of the MEK1/2/ERK1/2 signaling cascade leads to a reduction of macrophage numbers in nerves of PMP22tg mice----	66 -
Discussion -----	68 -
6.1 Pathological alterations in juvenile PMP22tg mice-----	68 -
6.2 Lymphocytes do not have a crucial role in the neuropathology of PMP22tg mice-----	71 -
6.3 Macrophages have a modulating capacity in the neuropathology of PMP22tg mice-----	73 -
6.4 PMP22tg and P0+/- mice: comparison of two models for inherited neuropathies-----	79 -
6.5 Closing remarks -----	81 -
Appendix	
A. Equipment and materials-----	84 -
A.1 Equipment -----	84 -
A.2 Reagents-----	85 -
A.3 Solutions, buffers and media -----	87 -
A.4 Antibodies for western blot analyses -----	90 -
B. References -----	91 -
C. Abbreviations -----	106 -
D. Curriculum vitae-----	109 -
E. List of Publications-----	110 -

Danksagung

Chapter 1

Summary

Charcot-Marie-Tooth disease (CMT) is a cohort of human hereditary disorders of the peripheral nervous system (PNS) which exhibit symptoms like sensory dysfunction, muscle weakness and gait disturbances. Different mutations are described as causation for this neuropathy, such as a duplication of chromosome 17 comprising the gene for the peripheral myelin protein-22 (PMP22). Based on different animal models former studies identified immune cells, i.e. macrophages and T-lymphocytes, as crucial mediators of pathology in these neuropathies. In this study, PMP22-overexpressing mice (PMP22tg, C61), serving as a model for a specific type of CMT – CMT1A – were crossbred with immune-deficient mutant mice to examine the impact of the immune system on nerve pathology.

Crossbreeding of PMP22tg mice with recombination activating gene-1 (RAG-1) deficient mice, lacking mature T- and B-lymphocytes, caused no striking alterations of pathogenesis in peripheral nerves of mutant mice. In contrast, crossbreeding of PMP22tg myelin mutants with mice deficient in the chemokine monocyte chemoattractant protein-1 (MCP-1, CCL2) caused an amelioration of the demyelinating phenotype of peripheral nerves when MCP-1 was either reduced or completely absent. Furthermore, functional investigations, i.e. neurographic recordings and examinations of the grip strength of the extremities, revealed an amelioration in PMP22tg/MCP-1^{-/-} mice in regard to a symptomatic improvement in the compound action muscle potential (CMAP) and stronger grip strength of the hindlimbs. Interestingly, peripheral nerves of PMP22tg mice showed an irregular distribution of potassium channels in presence of MCP-1, whereas the absence of MCP-1 in the myelin mutants rescued the ion channel distribution and resulted in a more wild type-like phenotype. Having shown the impact of MCP-1 as an important mediator of nerve pathology in PMP22/MCP-1 double mutants, the regulation of this chemokine became an important target for potential treatment strategies. We found that the signaling cascade MEK1/2/ERK1/2 was more strongly activated in peripheral nerves of PMP22tg mice compared to nerves of wild type mice. This activation corresponded to an increase in MCP-1 mRNA expression in peripheral nerves at the same age. Furthermore, a MEK1/2-inhibitor was used *in vivo* to confirm the regulation of MCP-1 by the MEK1/2/ERK1/2 pathway. After a treatment period of three weeks, a clear reduction of

ERK1/2-phosphorylation as well as a reduction of MCP-1 mRNA expression was observed, accompanied by a decline in macrophage number in peripheral nerves of PMP22tg mice.

These observations suggest that the expression of MCP-1 is crucial for the neuropathological progression in a mouse model for CMT1A. Therefore, this chemokine could provide a basis for a putative treatment strategy of inherited neuropathies.

Chapter 2

Zusammenfassung

Die Charcot-Marie-Tooth Erkrankungen (CMT) sind eine Gruppe von humanen, erblichen Erkrankungen des peripheren Nervensystems (PNS), welche Symptome wie sensible Störungen, Muskelschwäche und Gangstörungen verursachen können. Verschiedene Mutationen, z.B. eine Duplikation des Chromosoms 17, welches das Gen für das periphere Myelinprotein-22 (PMP22) enthält, sind als Ursache für diese Neuropathie beschrieben. Anhand verschiedener Tiermodelle wurde in früheren Studien gezeigt, dass Immunzellen, insbesondere Makrophagen und T-Lymphozyten, maßgeblich an der Pathogenese dieser Neuropathien beteiligt sind. In der vorliegenden Studie wurden PMP22-überexprimierende Mäuse (PMP22tg, C61) als Modell einer spezifischen CMT-Form – CMT1A – mit immun-defizienten Mutanten verkreuzt, um die modulierende Rolle des Immunsystems innerhalb der Pathogenese peripherer Nerven untersuchen zu können.

Die Verkreuzung von PMP22tg Mäusen mit „recombination activating gene-1“-defizienten Mutanten (RAG-1^{-/-}), die keine reifen T- und B-Lymphozyten besitzen, resultierte in keiner deutlich veränderten Pathologie der peripheren Nerven. Im Gegensatz hierzu führte die Verkreuzung der Myelinmutanten mit Mäusen, defizient für das Chemokin „monocyte chemoattractant protein-1“ (MCP-1), zu einer Abschwächung des demyelinisierenden Phänotyps in peripheren Nerven, wenn MCP-1 reduziert war oder völlig fehlte. Funktionelle Analysen, wie elektrophysiologische Messungen und Untersuchungen der Kraft in den Extremitäten, zeigten zudem in PMP22tg/MCP-1^{-/-} Mäusen eine symptomatische Verbesserung, was sich in einer höheren Amplitude (compound muscle action potential, CMAP) und einer erhöhten Kraft in den Hinterpfoten der Mäuse widerspiegelte. Interessanterweise zeigten periphere Nerven der PMP22tg Mäuse eine abnorme Verteilung von Kalium-Kanälen, wohingegen das Fehlen von MCP-1 in den Myelinmutanten zu einer Verteilung dieser Ionenkanäle führte, die ähnlich zu Wildtyp-Mäusen war. Da MCP-1 in den PMP22/MCP-1 Doppelmutanten einen deutlichen Einfluss auf die Pathogenese aufwies, wurde die Regulation dieses Chemokins im Hinblick auf mögliche Therapie-Ansätze untersucht. Diese Untersuchung zeigte, dass die MEK1/2/ERK1/2-Signalkaskade in peripheren Nerven von PMP22tg Mäusen stärker aktiviert wird als in Nerven von Wildtyp-Tieren. Die Aktivierung dieser Signalkaskade ging dabei mit einer erhöhten MCP-1 mRNA

Expression in peripheren Nerven von Tieren des gleichen Alters einher. Ergänzend wurde ein MEK1/2-Inhibitor *in vivo* verwendet, um die Regulation von MCP-1 durch die MEK1/2/ERK1/2 Kaskade zu bestätigen. Nach einer Behandlungszeit von drei Wochen wurde eine deutliche Reduktion der ERK1/2-Phosphorylierung, sowie eine Reduktion der MCP-1 mRNA Expression und eine geringere Makrophagen-Anzahl in peripheren Nerven von PMP22tg Mäusen detektiert.

Diese Untersuchungen zeigen, dass die Expression von MCP-1 entscheidend für den neuropathologischen Verlauf in einem Mausmodell für CMT1A ist. Somit bietet dieses Chemokin eine Basis für die Entwicklung neuer Behandlungsstrategien peripherer Neuropathien.

Chapter 3

Introduction

The nervous system is a complex communication system of the mammalian body which ensures the uptake of information from the environment and enables reactions to these stimuli. Hereby, the peripheral nervous system (PNS) forms the connective pathway between the single parts of the body and the central nervous system (CNS). Sensory neurons carry nerve impulses from a receptor to the CNS, where the information is processed (integration). Motor neurons reach the distal parts of the extremities by their processes (axons) which afford the signal transmission from the CNS to the effector organs, the muscles.

3.1 The myelin sheath

3.1.1 Formation and structure of the myelin sheath

In 1854, myelin was first mentioned by the pathologist Rudolf Virchow followed by a more detailed description by Louis-Antoine Ranvier in 1878. The myelin structure consists of a lipid-rich membrane which surrounds axons in many loops and functions like an electrical insulation. Therefore it is essential for the nerve conduction velocity. The myelin of the peripheral nervous system is formed by a specific type of glial cell, the Schwann cell, which obtained their name from the anatomist Theodor Schwann. A single axon is ensheathed by a series of Schwann cells which wrap their membrane around the axon in many layers. These myelin sheaths are intermittent at specific regions between two Schwann cells, the so called nodes of Ranvier which are important for the saltatory conduction of action potential. Here, the rapid transmission of signals within nerves is ensured by voltage-gated ion channels in unmyelinated regions of the axons. Only the basal lamina of the Schwann cells capped the nodes of Ranvier (Salzer, 1997), which are subdivided into three regions: the nodal, the paranodal and the juxtapanodal zone (Poliak and Peles, 2003). Sodium channels (mainly $Na_v1.6$ in motor fibers) are important for the depolarization and the genesis or transmission of the action potential and are located at the nodal regions. Here, the density of sodium

channels is much higher than in the internodes, the region between two nodes of Ranvier. Isoforms of Ankyrin-G and β IV-spectrin anchor the sodium channels to the actin cytoskeleton (Jenkins and Bennett, 2001, 2002). The paranodal zone is built up of loop-like myelin coils which contain cytoplasm (uncompacted myelin). This region contains septate junctions as a diffusion barrier for the membrane proteins of the juxtaparanodal region. In this latter region, potassium channels (Kv1.1 and Kv1.2) are accumulated and balance the concentration of extracellular potassium ions which are released during neuronal activity (Arroyo and Scherer, 2000). The axoglial contact is mediated by paranodin/contactin-associated protein-1 (Caspr-1) as well as Neurofascin-155 at the paranodal region and by Caspr-2 as well as TAG-1/axonin-1 at the juxtaparanodal zone (Rasband et al., 1999; Traka et al., 2002; Poliak and Peles, 2003). This separation of the different ion channels is a prerequisite for a successful transmission of nerve impulses.

The membrane potential of a cell during the resting state is called resting potential and it is determined by open potassium channels. During the resting potential, voltage-gated sodium channels are closed, but can be activated. Due to the depolarization, the conformation of the sodium channels is altered and sodium ions can stream into the axon. A specific region of the sodium channels, the inactivating domain, induces closing and thereby inactivation of the channels. Simultaneously, potassium ions effuse based on slow opening potassium channels. During the last phase, the repolarisation, the membrane potential converges the resting potential, the potassium channels are closed and the sodium channels are able to be activated again. Together, this specific structure with its separation of sodium and potassium channels assures that the action potential “jumps” from one node of Ranvier to the next and ensures a time and energy saving conduction.

As mentioned above, Schwann cells are the glial cells of the PNS and ensure different function besides the ensheathment of the axons. Further, they are important for trophic support, axonal regrowth after injury and phagocytosis of cell debris. In the peripheral nerves, the majority of axons are myelinated by Schwann cells, but there are also non-myelinating Schwann cells. Axons with small diameter ($<1\mu\text{m}$) are assembled to bundles by so-called non-myelinating Schwann cells (Remak fibers).

The ontogenetic origin of Schwann cells is the neural crest. During murine development at embryonic day 12 to 13 (E12 to 13), Schwann cell precursors are associated with axon bundles and are the source of immature Schwann cells (E13 to 15). At birth, the immature Schwann cells differentiate into either myelinating or non-myelinating Schwann cells, which

depends on the caliber of the associated axon, determined by the process of radial sorting (Jessen and Mirsky, 2005). In this process, Schwann cells are associated with a single, large diameter axon ($>1\mu\text{m}$) and start to enwrap it in form of a double-membrane structure, called mesaxon. During the developmental process, the cytoplasm of the Schwann cells is squeezed out and compact myelin is generated (Kettenmann and Ransom, 2005).

3.1.2 Proteins of the peripheral nervous system

The myelin sheath of the peripheral nervous system consists to 70% of lipids, whereas 30% are proteins which will be described in the following. Myelin proteins of the peripheral nervous system are myelin protein zero (MPZ or P0), peripheral myelin protein-22 (PMP22) and myelin basic protein (MBP) in the compact myelin as well as myelin associated glycoprotein (MAG) in the non-compact myelin. Further, the myelin-related gap junction protein Connexin-32 (Cx32 or GJB1) is also located in the non-compact myelin as well as in paranodal loops and Schmidt-Lanterman incisures (Scherer et al., 1995; Martini and Schachner, 1997). Besides the formation of the gap junctions, Cx32 is also important for the Schwann cell communication with axons (Scherer et al., 1995; Martini and Schachner, 1997; Balice-Gordon et al., 1998).

The major glycoprotein of the PNS is P0 with a frequency of approximately 50% (Greenfield et al., 1973; Niemann et al., 2006). This 28kDa protein is located only in the compact myelin (myelin loops without cytoplasm) and is important for both the formation of a normal myelin structure and stabilization due to homophilic interactions, as well as for the myelin compaction (Giese et al., 1992; Filbin and Tennekoon, 1993; Shapiro et al., 1996; Martini and Schachner, 1997). In addition, P0 can also interact with PMP22 by heterophilic binding to enable adhesion (D'Urso et al., 1999; Muller, 2000; Hasse et al., 2004). PMP22 is an integral membrane protein which is expressed mainly in Schwann cells with an amount of 2 to 5% of all myelin proteins. The function of this myelin protein has not been clearly identified yet, but it is likely to play a role in myelin maintenance, cell migration and differentiation, as well as in apoptosis (Brancolini et al., 1999; Sancho et al., 2001; Roux et al., 2005). The PMP22 protein belongs to the PMP22/EMP/MP20 protein family (Jetten and Suter, 2000) and is composed of 160 amino acids with 85% similarity between mouse, rat and human proteins (Manfioletti et al., 1990; Suter and Snipes, 1995b). It is a myelin-associated protein with four transmembrane domains (Suter and Snipes, 1995b; Muller,

2000). However, the occurrence of PMP22 is not restricted to myelin in the PNS. Earlier studies revealed that this protein is also an early component of the developing blood-nerve and blood-brain barrier (Notterpek et al., 2001; Roux et al., 2004). Nevertheless, the highest amount of PMP22 is found in the peripheral nervous system. Peripheral myelin sheaths also contain MBP, which plays an important role in the maintenance of the myelin and forms the major dense line together with P0 (Martini and Schachner, 1997; D'Urso et al., 1999; Shy, 2006). MAG as a further myelin protein of the PNS which is located at the inner and outer mesaxon (Trapp and Quarles, 1982) and functions as an adhesive molecule which is important during the development of the myelin sheaths (Quarles, 2007). Previously it was shown that MAG also promotes axonal stability and survival in cell culture and *in vivo* depending on the RGD domain around arginine 118 in the extracellular portion of MAG (Nguyen et al., 2009).

3.2 Disorders of the peripheral nervous system

3.2.1 Polyneuropathies

Polyneuropathies are disorders of the peripheral nervous system (PNS) which cause paraesthesia (sensory dysfunction), muscle atrophy, areflexia (disruption of reflexes), gait abnormalities and palsies of the distal extremities. The most common forms are the diabetic and the alcoholic neuropathy. Besides metabolic disorders, further reasons for polyneuropathies are infections (e.g. HIV infection or leprosy), ischemia or hereditary factors. The inherited forms are known as hereditary motor and sensory neuropathy (HMSN) or Charcot-Marie-Tooth disease (CMT). In specific cases of these inherited forms, only the sensory and autonomic system are affected, named hereditary sensory neuropathy (HSN) or hereditary sensory and autonomy neuropathy (HSAN). Here, the lack of pain perception of the patients can lead to frequent torridness and injuries. In HMSN or CMT, the dorsal flexor of the foot is initially affected which induces an impaired lifting of the foot and enables a fluent gait. The following sections will focus on the CMT disease regarding its classification as well as its causations.

3.2.2 Charcot-Marie-Tooth disease

In 1886, a form of a neuropathy characterized by muscular atrophy was first described by the physicians Jean-Martin Charcot and Pierre Marie in France as well as simultaneously by Howard Henry Tooth in England. CMT, also known as hereditary motor and sensory neuropathy (HMSN) or peroneal muscular atrophy is one of the most frequent inherited neurological disorders with a prevalence of one patient in 2.500 people (Skre, 1974). This hereditary neuropathy is very heterogeneous, clinically as well as genetically. The pathology affects either the myelin sheaths which function as an insulating layer of the nerve fibers or the axons directly as described before. The consequence of myelin damage (demyelination) is the disturbance of saltatory conduction and denervation or decomposition of the affected muscle. As mentioned above, one of the first symptoms is the structural foot deformities (high arched foot, hammertoes or extremely flat feet) which usually emerge in the late childhood or early adulthood. Later on, symptoms like muscle weakness, gait instability and foot drop develop. Nowadays, the diagnosis for CMT disorders is more confirmed by genetic analyses than by electromyography and nerve biopsies. To follow progression of CMT, a score is suggested to classify the severity of the ongoing disease (CMT neuropathy score or CMTNS; Shy et al., 2005). Many subtypes of CMT disorders are known which depend on their genetic mutations (Meyer Zu Horste and Nave, 2006; Nave et al., 2007, for review) and will be described in the following paragraph.

CMT type 1 (CMT1) is the most common form and affects approximately 80% of CMT patients (Suter and Snipes, 1995a). This subtype is also known as HMSN I and it is a predominantly demyelinating disease with reduced nerve conduction velocity (Harding and Thomas, 1980). Biopsies of sural nerves from CMT1 patients reveal demyelinating profiles and remyelinating clusters in terms of supernumerary Schwann cells (also called onion bulb formations) which are signs for ongoing de- and remyelination (Gabreels-Festen et al., 1992; Guenard et al., 1996; Thomas et al., 1996). CMT1 is inherited autosomal-dominantly. Different subtypes of CMT1 can be distinguished depending on the gene mutation.

CMT1A, affecting 70 to 80% of the CMT1 patients, is the most frequent form of CMT and is caused by a duplication of the region on chromosome 17 (17p11.2) which includes the gene encoding PMP22 (Vance et al., 1989; Lupski et al., 1991; Raeymaekers et al., 1991; Suter and Snipes, 1995a). The peripheral myelin protein-22 (PMP22) is an important component of the myelin sheaths of the peripheral nervous system as described in section 3.1.2. The

duplication of the gene leads to an overexpression of PMP22 and therefore to altered myelin sheaths with an average nerve conduction velocity of 20 to 25m/s. Patients suffer also from muscle weakness and atrophy of the distal limbs as well as of sensory loss. CMT1A is also called Roussy-Levy-Syndrome if clinical symptoms are accompanied by an essential tremor (shivering) and ataxia (disturbance of motion sequence; Zubair et al., 2008). Another neuropathy which is caused by a deletion of 17p11.2 – and thus a reduced protein level of PMP22 – is called hereditary neuropathy with liability to pressure palsies (HNPP) which characteristically shows tomacula (thickening of myelin sheaths) within peripheral nerves (Chance et al., 1993; Nicholson et al., 1994; Martini, 1997; Young et al., 1997). HNPP patients suffer from symptoms like paraesthesia, numbness and weakness after application of pressure or minimal trauma. However, these symptoms can regress after weeks or months.

Another subtype, CMT1B, affects 5 to 10% of CMT1 patients and is provoked by mutations in the gene encoding myelin protein zero (MPZ or P0; Hayasaka et al., 1993). CMT1B patients exhibit mostly point mutations in the MPZ gene which then lead to similar symptoms as in CMT1A patients, but the nerve conduction velocity can be more affected in some individuals (<20m/s). Other subtypes are known which include mutations for the lipopolysaccharide-induced tumor necrosis factor- α factor (LITAF; Street et al., 2003) and mutations in the zinc finger protein EGR2 (early growth response 2 or Krox20; Yoshihara et al., 2001) causing CMT1C and CMT1D, respectively. A further demyelinating subtype is CMT1X which is a dominant disorder linked to a mutation on chromosome Xq13.1. This neuropathy is caused by point mutations in the Cx32 gene (*GJB1*) and affects 10 to 15% of CMT patients (Bergoffen et al., 1993). The mutations in the *GJB1* gene leads to more severe symptoms in male CMT1X patients starting in late childhood whereas female patients develop mild symptoms or even no pathological alterations at all (Anzini et al., 1997; Martini, 1997; Scherer et al., 1998).

The second main type of CMT disorder is called CMT2 or HMSN II. It is mostly an axonal subtype of CMT diseases with normal or only slightly reduced nerve conduction velocities. The clinical symptoms are caused by axonal loss of peripheral nerves and peak in the second decade of life. Many subtypes are known with nomenclature by the letters from A to L. For example, a mutation on chromosome 1p36.2, which encodes the protein mitofusin (MFN)-2, leads to the subtype CMT2A2 (Ben Othmane et al., 1993; Zuchner et al., 2004). The protein MFN2 is a mitochondrial fusion protein, which is located in the outer

mitochondrial membrane and is important for the regulation of the mitochondrial network architecture by mitochondrial fusion (Zorzano et al., 2004).

A third main type of CMT disorder – called HMSN III, CMT3 or Dejerine-Sottas-Syndrome (DSS) – is mainly caused by point mutations in both PMP22 (DSS-A) and MPZ (DSS-B; Suter and Scherer, 2003; Al-Thihli et al., 2008). This rare subtype is characterized by slow progression, but severe pathology beginning in early childhood. Demyelination as well as axonal loss is frequent which causes a nerve conduction velocity of less than 12m/s.

Finally, one subtype will also be described which is autosomal recessive inherited and categorized as CMT4. Clinically, it is quite similar to CMT1. However, this HMSN subtype is characterized by severe neuropathological alterations with an early onset around the time point of birth (Suter and Scherer, 2003). Here, different mutations have been described which affect, amongst others, the ganglioside-induced differentiation-associated protein-1 (GDAP1; Pedrola et al., 2008) or the myotubularin-related protein-2 (MTMR2; Previtali et al., 2007). These subforms are referred to as CMT4A or CMT4B, respectively. Furthermore, mutations in the early growth response gene (EGR2, also known as Krox20) can cause the subtypes CMT4.

The classification of the CMT subtypes is referring to the nomenclature and descriptions of the Neuromuscular Disease Center, Washington University, St. Louis, USA (see <http://neuromuscular.wustl.edu/time/hmsn.html>).

3.2.3 PMP22 mutations as models for CMT1A

In general, to understand the detailed function of a protein, it is helpful to use animal models with an altered expression of the protein of interest. In the past, many studies focused on different mutations with a reduced or enhanced PMP22 protein expression as animal models for CMT1A. Twelve years ago, the protein PMP22 and the corresponding gene *gas-3* were first described as a disease-causing factor (Huxley et al., 1996; Magyar et al., 1996; Sereda et al., 1996). Huxley and colleagues generated different transgenic mouse models with increased PMP22 protein expression. In these experiments, it could be shown that there is a strong correlation between the level of PMP22-expression and the severity of demyelination. Thus, PMP22-overexpressing mice with seven copies of the human gene

(C22) develop a strong demyelination with a visible neuropathic phenotype. In contrast to this, heterozygous C61 mice with only four copies, showed a mild demyelination within peripheral nerves without any striking phenotype (Huxley et al., 1996; Huxley et al., 1998). In our laboratory, we were able to show that both, demyelinating hallmarks as well as hypermyelinated fibers increase with age in the C61 mutants (Kobsar et al., 2005).

In parallel, Sereda and colleagues generated transgenic rats with three extra copies of the murine PMP22 gene (Sereda et al., 1996). Whereas the homozygous animals developed a severe demyelination, heterozygous rats were less affected with symptoms reminiscent of the human CMT, like impairment of motor abilities, slowed nerve conduction velocity and demyelination with onion bulb formations. Additional PMP22 mutants with 16 to 30 extra copies are severely affected due to the failure of myelin formation (Magyar et al., 1996). Besides these transgenic models, there are spontaneous PMP22 mutants described in form of the Trembler (*Tr*) and Trembler-J (*Tr^J*) mice which contain missense point mutations of the PMP22 gene (Suter et al., 1992a; Suter et al., 1992b). In these mutations, the primary structure of PMP22 is altered, which causes a disturbance of the intracellular protein transport resulting in hypomyelination and increased Schwann cell number (Sancho et al., 2001). *Tr* mutants exhibit paralysis of the limbs and tremor (Suter et al., 1992a; Suter et al., 1992b). The *Tr^J* point mutation emerged independently from the *Tr* mutation (Henry et al., 1983). In the *Tr^J* mice, a leucine residue is substituted by a proline residue in the first transmembrane region of the PMP22 polypeptide. In contrast to the *Tr* mice, *Tr^J* mutants develop a less severe pathological phenotype with age and a reduced number of onion bulb formations. Furthermore, a current study focused on mechanisms which are closely linked to misfolding of PMP22 in the membrane of the endoplasmic reticulum (ER; Myers et al., 2008). Although the folded mutant forms of PMP22 from *Tr* and *Tr^J* mutants were similar to the folded wild type protein, the folded protein forms of the mutants seemed to be destabilized and unstable in case of the *Tr^J* mutant. In addition, there was no refolding observed for these two mutants. Therefore, the authors suggest that mutant PMP22 folds more slowly than wild type protein which causes a higher vulnerability to recognition by ER quality control and thus, almost complete targeting of the protein to degradative pathways.

Furthermore, studies with PMP22-deficient mutants allowed deeper insight in the function of the protein. Thus, PMP22-knockout (PMP22^{-/-}) mice revealed no altered integrity of the epithelium, but a slight delay in the initiation of myelination (Carenini et al., 1999). Even though PMP22 is a minor protein of the peripheral nervous system, many studies have elaborated the enormous impact of this protein.

3.2.4 The immune system as a mediator of pathology in inherited demyelination

Despite the altered protein expression in different mutations, the question arises by which mechanisms the myelin structure is damaged. Former studies could show that the immune system plays a crucial role in this process. Besides myelinated axons, peripheral nerves contain non-myelinated fibers (Remak bundles), blood vessels and different types of immune cells like macrophages, endoneurial fibroblasts, T-lymphocytes and mast cells. Macrophages which arise from monocytes are able to phagocytose pathogens or cellular debris. Further, these cells can act as antigen-presenting cells to induce response from lymphocytes as well as other immune cells. Different surface molecules like F4/80, CD11b or CD68 serve to identify macrophages. T-lymphocytes are classified by two different subpopulations, CD4-positive and CD8-positive T-cells. The main function of CD4-positive T-helper lymphocytes is the activation of other immune cells. If naïve CD4-cells are activated, they mainly differentiate into either T_{H1} -cells (enhancement of cell-mediated immune response) or cells of the T_{H2} -subtype (regulatory function). Naïve CD8-positive lymphocytes develop into cytotoxic T-cells after activation. Both, the CD4 and CD8-positive T-lymphocytes are the source of different cytokines or other soluble factors.

A series of studies allocated the functional role of immune cells in mouse models for myelin disorders and worked out the coherence of demyelination in peripheral nerves and the activity of immune cells. Two different myelin mutants of the PNS, the P0-heterozygous (P0+/-) mutants and the Cx32-deficient (Cx32-/-) mice, exhibit a demyelinating phenotype with an accumulation of F4/80-positive macrophages and CD8-positive T-lymphocytes with increased age, whereas CD4-positive T-cells were hardly detected in the nervous tissue (Schmid et al., 2000; Kobsar et al., 2002; Maurer et al., 2002). In addition, the dysmyelinating P0-homozygously deficient (P0-/-) mice, which reveal a disturbed myelin development, also display a higher number of macrophages and CD8-positive T-cells in peripheral nerves. Further, it could be shown that macrophages are able to ingest myelin debris, thus called foamy macrophages due to their appearance in electron microscopy (Giese et al., 1992; Martini et al., 1995).

Crossbreeding the myelin mutants with recombination activating gene-1 (RAG-1) deficient mice, (RAG-1-/-) which are lacking mature T- and B-lymphocytes, clarified the role of lymphocytes in the pathology of the investigated myelin mutations. Both demyelinating

myelin mutants (P0^{+/-} and Cx32^{-/-} mice) showed a clear amelioration of the pathological phenotype in nervous tissue of RAG-1^{-/-} double mutants and a reduced number of endoneurial F4/80-positive macrophages (Schmid et al., 2000; Kobsar et al., 2003). In contrast, the pathological phenotype was enhanced in nervous tissue of the dysmyelinating P0^{-/-} mice in absence of mature T- and B-lymphocytes concerning axonal loss, suggesting a neuroprotective role of lymphocytes in this model (Berghoff et al., 2005). These studies imply a crucial role of T-lymphocytes, dependent on the myelin mutation.

The functional impact of macrophages in pathogenesis of myelin mutant mice was also examined. For this purpose P0^{+/-} myelin mutants were crossbred with mice deficient for M-CSF, a macrophage directed cytokine (Carenini et al., 2001). In this case, a reduced number of macrophages and less demyelination could be shown in peripheral nerves of P0^{+/-} mice deficient in M-CSF indicative for an active role of macrophages during the pathomechanism of inherited demyelination.

To investigate a putative crosstalk between T-lymphocytes and macrophages, P0^{+/-} mice were crossbred with sialoadhesin (Sn)-deficient mice (Kobsar et al., 2006). Sialoadhesin, which stands for sialic acid-binding Ig-like Sialoadhesin, can be expressed on macrophages. P0^{+/-} mice devoid of sialoadhesin showed a reduced number of CD8-positive T-cells and macrophages in peripheral nerves, less severe demyelination and an amelioration of the nerve conduction velocity.

In addition, many studies focused on the question from which source these immune cells arise. Besides the intrinsic proliferation of resident cells, for example induced by M-CSF (Muller et al., 2007), immune cells, namely macrophages, might invade from the blood into peripheral nerves. This infiltration of macrophages is mediated by chemokines like the monocyte chemoattractant protein-1 (MCP-1). Thus, a reduction of 50% of MCP-1 by generation of P0/MCP-1 double mutant mice (P0^{+/-}/MCP-1^{+/-}) diminished the macrophage number in peripheral nerves and causes a clear amelioration of nerve pathology (Fischer et al., 2008b).

The impact of the immune system in models for peripheral neuropathies shows, that the immune system and the nervous system are interacting leading to endogenous mechanisms for de- and regeneration within peripheral nerves.

3.3 Aim of the study

PMP22-overexpressing mice (PMP22tg, C61) were investigated as a model for CMT1A regarding the role of immune cells in nerve pathology and clinical alterations. A previous study could show that macrophages are increased in femoral nerves of these mice and that the MCP-1 mRNA expression was also elevated (Kobsar et al., 2005). Therefore, we were interested in the role of macrophages as well as of T-lymphocytes in this mouse model and examined their function by crossbreeding the myelin mutants with the appropriate immune-deficient mice (MCP-1^{-/-} and RAG-1^{-/-} mutant mice, respectively). Further, we focused on the regulation of MCP-1 regarding signaling pathways to test a putative treatment strategy. Besides the functional role of immune cells, developmental aspects were investigated to clarify whether the overexpression of PMP22 causes early developmental alterations in peripheral nerves.

Chapter 4

Materials and methods

4.1 Equipment, reagents, solutions, buffers, media and antibodies

In the attached appendices, the used equipment (appendix A.1), reagents (appendix A.2), solutions and buffers (appendix A.3), as well as the antibodies applied in the western blot analyses (appendix A.4) can be perceived. Unless mentioned otherwise, standard material was employed for laboratory work.

4.2 Mutant mice and genotyping

Transgenic PMP22-overexpressing mice (PMP22tg) of the C61 strain carrying four copies of a human yeast artificial chromosome (YAC) clone encompassing the complete hPMP22 (Huxley et al., 1996; Huxley et al., 1998) were kept in our animal facilities. Mice were maintained on a mixed C57BL/6xCBA/Ca background and crossbred with MCP-1-mutant mice (PMP22/MCP-1; Lu et al., 1998) as well as with RAG-1-deficient (PMP22/RAG-1) mice (Mombaerts et al., 1992) to receive double mutants. In addition, PMP22 single mutants were backcrossed to a C57BL/6 background for six to eight generations. For all investigations only heterozygous PMP22-overexpressing mice and wild type littermates (PMP22wt) were used. All mouse strains used in this study were kept under specific pathogen-free conditions at the Department of Neurology, Julius-Maximilians-University, Wuerzburg, Germany. Animal experiments were approved by the local authorities (Regierung von Unterfranken)

Genotyping of all mutant mice was performed by polymerase chain reaction (PCR). For this purpose, genomic DNA was purified from tail biopsies using the DNeasy blood & tissue kit (Qiagen, Hilden, Germany) according to the manufacturer's guidelines. Genotypes of PMP22tg and wild type mice were identified by conventional PCR using the following oligonucleotides: 5-AACCGTGAAAAGATGACCC-3 and

5-TCGTTGCCAATAGTGATGACC-3 (MBA1 and MBA2 for wild type allele), 5-TCAGGATATCTATCTGATTCTC-3 and 5-AAGCTCATGGAGCACAAAACC-3 (2F and 2R for transgenic allele). The PCR was performed in a volume of 50µl according a standard protocol with an annealing temperature of 55°C and an elongation temperature of 72°C resulting in a 450bp fragment for wild type and in a 155bp fragment for transgenic allele, respectively.

The genotypes of the MCP-1 mutant mice (MCP-1+/+, MCP-1+/- and MCP-1-/-) were determined by the primer sequences 5-GGAGCATCCACGTGTTGGC-3 (MCP-1F), 5-ACAGCTTCTTTGGGACACC-3 (MCP-1R) and 5-AGGATCTCGTCGTGACCCATGGCGA-3 (IMRO 60) using an annealing temperature of 59°C and an elongation temperature of 72°C. After the PCR, a 888bp and a 1382bp amplificate were detected on agarose gels representative for wild type allele or knockout allele, respectively.

As a further PCR protocol we used oligonucleotides for PD-1 to control bone marrow chimerization experiments. The primer sequences 5-CCGCCTTCTGTAATGGTTTG-3 (PD-1-S), 5-TGTTGAGCAGAAGACAGCTAG-3 (PD-1-AS), 5-GCCCGGTTCTTTTTGTCAAGACCGA-3 (NEO-5) and 5-ATCCTCGCCGTCGGGCATGCGCGCC-3 (NEO-3) were applied in a conventional PCR with an annealing temperature of 54°C and an elongation temperature of 72°C resulting in amplification products of 600bp (wild type) and 400bp (neo cassette of PD-1).

To determine the specific genotype of RAG-1 mutant mice, fluorescence activated cell sorting (FACS) of peripheral blood cells was performed as described previously (Schmid et al., 2000; Kobsar et al., 2003). Peripheral blood cells were stained with rat anti-mouse CD4-PE (16µg/ml, clone GK1.5, Pharmingen, Heidelberg, Germany) and rat anti-mouse CD8-FITC (20µg/ml, clone 53-6.7, Pharmingen, Heidelberg, Germany) antibodies and examined using a FACScan (Becton Dickinson, Heidelberg, Germany). Immune-competent mice with CD4- and CD8-positive cells were categorized as RAG-1+/? mice, whereas immune-deficient mutants lacking mature CD4- and CD8-positive T-lymphocytes were denoted as RAG-1-/- mice.

4.3 Cell culture

To control the specificity of the antibodies used in western blot analyses, cell lysates of cultured NIH3T3 (mouse fibroblast cell line) were generated. For this, cells were cultured in DMEM (Invitrogen GmbH, Karlsruhe, Germany) with 10% fetal calf serum (FCS, Biochrom, Berlin, Germany) and 2mM glutamine (Invitrogen, Karlsruhe, Germany) in culture dishes. To generate specific control for unphosphorylated or phosphorylated proteins, cells were cultured in DMEM with 0.05% serum over night. The control for unphosphorylated proteins remained untreated, the control for phosphorylated proteins was stimulated with 10% FCS for 30 minutes on the next day, followed by trypsinization, washing with PBS and lysing in RIPA buffer. This lysates were used as controls for (p)ERK1/2, (p)STAT and (p)PKC α . As controls for (p)p38, (p)I κ B α and (p)JNK1/2, NIH3T3 cells were cultured as described above and irradiated with 100J/m² (UV Crosslinker 1800, Stratagene, La Jolla, CA, USA) followed by lysis in RIPA buffer.

4.4 Bone marrow transplantation

PMP22tg bone marrow chimeras (BMCs) were generated as previously described (Maurer et al., 2001; Ip et al., 2006; Kroner et al., 2008). PMP22tg mice were sub-lethally irradiated with 7.5 Gray at the age of 6 to 8 weeks and received bone marrow from either wild type ($n=7$) or from PD-1-deficient (PD-1 $^{-/-}$) mice ($n=6$) one day after irradiation. For this, bone marrow from donor mice (wild type or PD-1 $^{-/-}$ mice) was extracted from femoral bone marrow. After purification, approximately 2×10^7 cells were resuspended in 300 μ l PBS and injected intravenously into PMP22tg mice. Mice were then kept under normal conditions up to 6 months under weekly weight monitoring. To have a control for successful transplantation, spleen cells were analyzed by flow cytometry regarding CD4, CD8 and PD-1 positive cells. Additionally, conventional PD-1-PCR of spleen cell-DNA was performed to control the type of the received bone marrow.

4.5 Flow cytometry

To reassess the successful bone marrow transplantation in irradiated PMP22tg mice, splenocytes were used for flow cytometry. Purified splenocytes were stained with directly labeled antibodies (anti-CD4-PERCP, BD Bioscience Pharmingen, San Jose, CA, USA; anti-CD8-FITC, BD Bioscience Pharmingen, San Jose, CA, USA; anti-PD-1-PE eBioscience, San Diego, CA, USA) for 30 minutes in FACS buffer at 4°C. After washing and resuspending the cells in 500µl FACS buffer, the labeled splenocytes were examined by flow cytometry using CellQuestPro software. Isotype control antibodies were used to control the specific staining. Furthermore, the expression of PD-1 on immune cells of peripheral nerves, on stimulated and unstimulated splenocytes, as well as on stimulated peritoneal macrophages was determined by flow cytometry. Peripheral nerves (femoral, sciatic and plantaris nerves, as well as lumbar ventral roots) of 8-month-old PMP22tg mice and their wild type littermates ($n=2$, respectively) were prepared and nervous tissue was purified. Additionally, peritoneal macrophages were obtained using peritoneal lavage. For this, mice were sacrificed, the skin above the abdominal cavity was cut and approximately 5ml of sterile PBS were injected into the abdominal cavity. After a careful massage of the abdominal cavity the cell-containing PBS was soaked out. Peritoneal macrophages were then stimulated over night with 1µg/ml lipopolysaccharide (LPS) and labeled against different markers as noted below. Furthermore, purified splenocytes were activated under the same conditions over night by 1µg/ml LPS. All samples were labeled with the following antibodies: anti-CD11b-PERCP, BD Bioscience Pharmingen, San Jose, CA, USA; anti-PD-1-PE, eBioscience San Diego, CA, USA; anti-CD4-PERCP, BD Bioscience Pharmingen, San Jose, CA, USA; anti-CD8-APC, BD Bioscience Pharmingen, San Jose, Ca, USA and anti-B7H1-PE, eBioscience, San Diego, CA, USA.

4.6 Isolation of RNA and protein from peripheral nerves

Peripheral nervous tissue was prepared for RNA and protein extraction as described previously (Fischer et al., 2008a). Mice were deeply anesthetized and transcardially perfused for two minutes with PBS to avoid contamination with blood during preparation. Femoral quadriceps and saphenous nerves, as well as sciatic nerves were quickly but carefully dissected and immediately frozen in liquid nitrogen and stored at -80°C.

Total RNA was isolated from peripheral nerves using TRIzol® reagent (Invitrogen, Karlsruhe, Germany) according to the manufacturer's protocol. This reagent is a mono-phasic solution of phenol and guanidine isothiocyanate used for the single-step RNA isolation method developed by Chomczynski and Sacchi (Chomczynski and Sacchi, 1987). Towards the addition of TRIzol®, tissue was homogenized by an ultrathurax (ART Labortechnik, Muehlheim, Germany). Total RNA and proteins were isolated by Phenol-Chloroform extraction, phase separation and the RNA isolation by isopropanol precipitation and washing with 75% ethanol in DEPC-water, subsequently. The resulting RNA pellet was solubilized in 10µl DEPC-water. After a heating step (55°C 10 minutes), 0.5 to 1µg total RNA was transcribed into cDNA as described below.

Proteins were precipitated from the phenol-ethanol supernatant with isopropyl alcohol. After three washing steps with a solution of 0.3M guanidine hydrochloride in 95% ethanol, the protein pellets were solubilised in 100% ethanol for 20 minutes. The resulting protein pellets were dissolved in 1% SDS and sonicated if required. Towards the incubation for 5 minutes at 50°C, the protein content of the lysates was determined by Lowry assay as described below.

4.7 Reverse transcription and quantitative real-time PCR

An amount of 0.5 or 1µg total RNA was transcribed into cDNA using TaqMan Reverse Transcription Reagents in consideration of manufacturer guidelines (Applied Biosystem, Foster City, CA, USA). The resulting cDNA was examined with different TaqMan assays by semiquantitative real-time PCR (qRT-PCR) with a 7500 real-time PCR system (Applied Biosystems, Foster City, CA, USA).

For qRT-PCR with TaqMan universal PCR master mix (Applied Biosystems, Foster City, CA, USA), the following pre-developed TaqMan assays were used: 18s (4319413E), MCP-1 (Mm99999056_m1), IL-1β (Mm00434228_m1), IL-6 (Mm00446190_m1), LIF (Mm00434761_m1), M-CSF (Mm00432688_m1), TGFβ (Mm00441724_m1) and TNFα (Mm00443258_m1). All samples were measured in triplicates and finally analyzed in relation to 18s RNA content. All indicated values are standardized according to samples of wild type nerves.

4.8 Western blot analyses

Western blot technique was applied for detection of different kinases and their activation status. For this, lysates from peripheral nervous tissue of single mice were prepared as described above. To obtain equal protein amounts in the western blot analyses, protein content of the samples was determined by a Lowry protein assay (Sigma Aldrich Taufkirchen, Germany) using bovine serum albumine (BSA) as standard (Lowry et al., 1951). At last, 20 to 100µg protein per sample was used for western blotting as previously described (Fischer et al., 2008a). Shortly, after addition of Roti® Load buffer (1:3; Carl Roth, Karlsruhe, Germany), samples were denatured for three minutes at 95°C and added into a 10 or 12% polyacrylamide gel (SDS-Page) using a Biorad Mini-Protean® 3 electrophoresis module (Biorad Laboratories, Munich, Germany). Afterwards, the SDS-Page proteins were transferred on nitrocellulose membranes (Schleicher & Schuell BioScience, Keene, NH, USA) by a Biorad Mini Trans-Blot® module (Biorad Laboratories, Munich, Germany) at 400mA with the addition of an ice-cooling unit. To control the protein transfer afterwards, nitrocellulose membranes were stained with a reversible Ponceau S-solution for a maximum of five minutes.

The detection of proteins involved in signal transduction was implemented with specific antibodies against the phosphorylated as well as the non-phosphorylated protein (see appendix A.4) Unless described otherwise, nitrocellulose membranes were washed three times for 5 minutes with PBST, blocked with 5% milk powder in PBST for 30 minutes at room temperature and incubated with the primary antibody overnight at 4°C in 5% milk powder in PBST. On the next day, the membranes were washed again and incubated with the specific secondary antibody in 5% milk powder in PBST for 30 to 120 minutes at room temperature. The antibody binding was then visualized with ECL substrate reagent (GE Healthcare, Munich, Germany) for one minute and the resulting chemiluminescence was detected by Hyperfilm ECL (GE Healthcare, Munich, Germany). The examined phosphorylated proteins were normalized to the corresponding non-phosphorylated protein which served as a specific loading control. For this, the nitrocellulose membranes were incubated in stripping buffer for 30 to 60 minutes at room temperature after the detection of the phosphorylated form to remove the detected antibody. To have a control for the complete absence of the previously used antibody against the phosphorylated form, the nitrocellulose membrane was incubated with the specific secondary antibody for one hour at room temperature and the signal was detected as described above. Only nitrocellulose membranes with complete absence of the

signal for the phosphorylated form were used for detection with the non-phosphorylated total protein.

4.9 Immunohistochemical analyses

For identification and quantification of immune cells, immunohistochemical stainings with antibodies against different antigens were used. In order to prepare peripheral nervous tissue, mice were deeply anesthetized and transcardially perfused for three minutes with PBS. After removal of femoral or sciatic nerves, the tissue was embedded in O.C.T. matrix (DiaTec, Nuremberg, Germany), frozen in liquid nitrogen-cooled isopentane and cut into 10µm thick cross sections on a cryostat (Leica, Wetzlar, Germany).

The analyses of F4/80-positive macrophages and CD4- as well as CD8-positive T-lymphocytes were done by horseradish peroxidase-based immunohistochemistry as described previously (Carenini et al., 2001; Kobsar et al., 2005). After blocking with 5% normal bovine serum in 0.1M PBS, cross sections of femoral nerves were incubated with rat anti-mouse F4/80 (3µg/ml; Serotec, Eching, Germany), rat anti-mouse CD4 (1µg/ml; Serotec, Eching, Germany) and rat anti-mouse CD8 (5µg/ml; Serotec, Eching, Germany), respectively, overnight at 4°C in 1% normal bovine serum in 0.1M PBS. To optimize immunostaining against CD4 and CD8, sections were fixed in ice-cold acetone for 10 minutes before blocking solution and antibodies were added. In order to visualize the binding of primary antibodies, a biotinylated secondary antibody to rat IgG (1:300; rabbit anti-rat, Vektor Laboratories, Burlingame, CA, USA) was applied for one hour, followed by avidin-biotin reagent (Dako, Carpinteria, CA, USA) before incubation and staining with diaminobenzidine-HCl (DAB) and H₂O₂. As a negative control, the respective primary antibody was omitted using nerve cross sections, whereas sections of the spleen were included as a positive control for all immunohistochemical protocols.

For localization of the phospho-ERK1/2 signal, single fiber preparations of femoral quadriceps nerves were used, stained and evaluated on a laser scanning confocal microscope (DM RE-7 SDK, Leica, Germany). Therefore, mice were deeply anesthetized and perfused with 2% paraformaldehyde (PFA) in 0.1M PBS for 10 minutes and the femoral quadriceps nerves were dissected. After removal of the epineurium, each nerve was separated in single fibers at only one end to allow the appliance of a free-floating staining

technique. For double-staining, primary antibodies against S100 β as a Schwann cell marker (sheep anti-bovine S100 β , 1:100, Biocompare, South San Francisco, CA, USA) and phospho-ERK1/2 (rabbit anti-mouse phospho-ERK1/2, 1:100, Chemicon, Temecula, CA, USA) were incubated in 1% normal bovine serum on 0.1M PBS with 0.3% TritonX-100 for two hours at room temperature. Primary antibodies were detected with the specific secondary antibodies labeled with FITC (donkey anti-sheep IgG, 10 μ g/ml, Dianova, Hamburg, Germany) and Cy3 (goat anti-rabbit IgG, 1:300, Dianova, Hamburg, Germany). Additionally, cell nuclei were marked with the fluorescent stain 4',6-diamidino-2-phenylindole (DAPI, 1:1.000.000, Sigma Aldrich Taufkirchen, Germany). For positive controls, NIH3T3 cells were cultured on cover slips and were treated as described in section 4.3.

Furthermore, we used immunohistochemistry for cellular localization of MCP-1 in sciatic nerves of PMP22tg mice. Cross sections were incubated in ice-cold acetone and blocked with 5% normal bovine serum on 0.1M PBS with 0.3% TritonX-100. Primary antibody against MCP-1 (rabbit anti-mouse MCP-1, 4 μ g/ml, Peprotech, Hamburg, Germany) was added in 1% normal bovine serum on 0.1M PBS with 0.3% TritonX-100 over night and visualized with specific secondary antibody (goat anti-rabbit Cy3, 1:300, Dianova, Hamburg, Germany). Sections were investigated with an Axiophot 2 (Zeiss, Oberkochen, Germany).

To focus on axonal integrity in PMP22 mutant mice with different MCP-1 genotype, we examined the distribution of Na⁺ channels (rabbit anti-Nav1.6/SCN8A, 0.85 μ g/ml, Chemicon Temecula, CA, USA), K⁺ channels (rabbit anti-Kv1.2/Kcna2, 1:100, Biomol, Hamburg, Germany) and contactin associated protein (Caspr, 1:1000) by immunohistochemistry. This was performed on teased fiber preparations of sciatic and femoral quadriceps nerves from 6-month-old PMP22wt/MCP-1+/+ (*n*=3), PMP22tg/MCP-1+/+ (*n*=4), PMP22tg/MCP-1+/- (*n*=3) and PMP22tg/MCP-1-/- (*n*=3) as described previously (Ulzheimer et al., 2004). Expression of K⁺ channels was quantified by the presence or absence of Kv1.2, asymmetric as well as diffuse expression by localization with Caspr. For this, at least 120 nodes of Ranvier per mouse were examined.

In all quantifications, the investigator was not aware of the genotype of the mice.

4.10 Electron microscopic analyses

To examine PMP22-overexpressing mice during development, we focused on ultrathin sections of peripheral nerves from PMP22tg mice and their wild type littermates at postnatal day 7 (P7). For this, PMP22tg mice ($n=5$) and their wild type littermates ($n=5$) were sacrificed at postnatal day 7 (P7), the skin was cut ventral and dorsal at the inguinal region and the whole individuals were fixed in 2% paraformaldehyde, 2% glutaraldehyde in 0.1M cacodylate buffer over night at 4°C. Mouse tails were kept and fresh frozen for genotyping. The next day, femoral nerves composed of the femoral quadriceps and cutaneous saphenous branch, as well as sciatic nerves were prepared, followed by osmification and embedding in Spurr's medium. For all electron microscopic analyses, 70nm-thick sections were counterstained with lead citrate and investigated using a LEO 906 E electron microscope (Zeiss, Oberkochen, Germany) and associated software ITEM (Olympus Soft Imaging Solutions GmbH, Muenster, Germany). Femoral quadriceps, cutaneous saphenous and sciatic nerves were investigated with regard to myelin, sorting of the axons (ratio axon : Schwann cell = 1:1), axonal caliber and g-ratios. For g-ratio, 100 completely myelinated axons per mouse, in 1:1 ratio with Schwann cells, were examined.

Further, peripheral femoral nerves and lumbar ventral roots of adult mice were prepared for electron microscopy as described previously (Martini et al., 1995). Mice were deeply anesthetized and transcardially perfused for three minutes with phosphate-buffered saline (PBS) followed by a 15 minute-perfusion with 0.1M cacodylate buffer, pH 7.4, substituted with 4% paraformaldehyde and 2% glutaraldehyde. Afterwards, the tissue was post-fixed in the same buffer over night, osmificated with 2% osmiumtetroxide in 0.1M cacodylate buffer for two hours at room temperature, dehydrated in ascending acetone concentrations and embedded in Spurr's medium. For semithin analyses, 0.5µm-thick sections were stained with alkaline methylene blue and analyzed by light microscopy. Pathological profiles were quantified in ultra-thin sections of femoral nerves and ventral roots of adult PMP22 double mutants (PMP22/MCP-1 and PMP22/RAG-1) as well as the PMP22tg BMCs. In this regard, each nerve had been categorized with regard to the occurrence of axons devoid of myelin, thinly myelinated axons, hypermyelinated axons, supernumerary Schwann cells (onion bulb formations), foamy macrophages and g-ratios. In all experiments, the investigator was not aware of the genotype of the mice.

4.11 Neurographic recordings

The PMP22tg BMCs and the PMP22/MCP-1 double mutants were examined regarding their conduction properties of the sciatic nerve as described previously (Zielasek et al., 1996; Samsam et al., 2003). Briefly, mice were anesthetized with a neuroleptic / analgesic combination (Hypnorm, Janssen Pharmaceutica, Beerse, Belgium) and two stimulating electrodes were placed in the left sciatic notch and 2cm laterally for proximal stimulation. Further two electrodes were sited subcutaneously along the tibial nerve just above the ankle for distal stimulation. Supramaximal stimulation allowed the determination of compound muscle action potential (CMAP), duration of the CMAP, F wave latency as well as of the nerve conduction velocity (NCV). The PMP22/MCP-1 double mutants (6 and 12 months) were examined on the right side, in case of the PMP22tg BMC (8 months) both sides were measured. These experiments were arranged by Carsten Wessig who was not aware of the genotype of the mice.

4.12 Functional tests

Motor disturbances of PMP22tg BMCs were examined by gait studies as earlier described (Kunkel-Bagden et al., 1993; Kroner et al., 2008). In this experiment, the hind paws of mice were dyed with blue ink and mice were allowed to walk through a dark tunnel which was placed over pieces of paper. Three consecutive footprints were measured concerning different parameters like stride width, stride length on the right and left sides as well as stride rotation. To exclude any coherence of the body weight and possible stride abnormalities, mice were weighted on the same day.

To examine the muscle (grip) strength of PMP22/MCP-1 double mutants at the age of 5 to 6 months we performed grip strength tests of forelimbs as well as of hindlimbs. An automated grip strength meter (Columbus Instruments, Columbus, Ohio, USA) was used as described previously (Masu et al., 1993; Holtmann et al., 2005). Shortly, mice were trained to hold the grip bar. Afterwards, mice were dragged off the grip bar with constant strength and ten measurements per day were performed on three consecutive days. In addition, mice were weighed at the first day of testing.

4.13 *In vivo* inhibition of the MEK1/2/ERK1/2 signaling cascade by CI-1040

To test the functional relevance of the MEK1/2/ERK1/2 cascade *in vivo*, we performed inhibition studies with the MEK1/2 inhibitor CI-1040 (PD184352) which was kindly provided by Pfizer (New York, USA). Two months old PMP22tg mice and their wild type littermates were treated for 3 weeks by intraperitoneal injection of either 100mg/kg CI-1040 in dimethylsulfoxid (DMSO; PMP22tg mice: $n=6$, PMP22wt mice $n=4$) or DMSO alone as controls (PMP22tg: $n=5$, PMP22wt mice $n=4$). Due to the toxic side effects of DMSO, a maximal injection volume of 50 μ l was used and the body weight was monitored daily before injection. Hence, the correct dose of 100mg/kg was achieved by graduated dilutions. After 21 days, mice were sacrificed and sciatic nerves, femoral quadriceps and cutaneous saphenous nerves were dissected and conserved for RNA and protein purification. Additionally, femoral nerves were embedded in O.C.T. matrix (DiaTec, Nuremberg, Germany) and cut into 10 μ m thick cross sections on a cryostat (Leica, Wetzlar, Germany) for immunohistochemistry against the macrophage marker F4/80. Mice which showed an impaired health status were sacrificed earlier and not included into the results.

4.14 Statistical analyses

Statistical analyses were performed by using the unpaired two-tailed Student's *t*-test for comparison of immune cell number, number of supernumerary Schwann cells and foamy macrophages, electrophysiological parameters, mRNA expression and grip strength. The non-parametric Mann-Whitney-*U*-test was used for comparison of the numbers of neuropathological alterations and the distribution of K⁺ channels. Statistical significance is indicated with * $p<0.05$, ** $p<0.01$ and *** $p<0.001$, all data are reported as mean standard deviation (SD).

Chapter 5

Results

In 1999 it was shown that PMP22 is not involved in the initial ensheathment and separation of axons in sciatic nerves of C61 mutant mice at postnatal day 4 (P4) and postnatal day (P10-12; Robertson et al., 1999). Further, it was observed that C61 mice do not differ significantly from their wild type controls regarding the percentage of myelinated fibers. However, another PMP22-overexpressing mouse mutant with seven copies of the human gene (C22) revealed a lower proportion of single ensheathed myelinated fibers (Robertson et al., 1999). Therefore, to understand the pathological mechanisms in mutant animal models it can be helpful to examine the morphology during the development.

5.1 Morphological analyses of peripheral nerves of juvenile PMP22 mutant mice

In the present study, the morphology of peripheral nerves of PMP22tg mice and their wild type littermates were examined at postnatal day (P7) regarding different aspects. Axonal sorting in PMP22 mutant mice was analyzed to exclude potential developmental alterations due to the PMP22-overexpression in femoral and sciatic nerves. Furthermore, myelination of axons was examined regarding the thickness of the myelin sheaths and possible pathological alterations indicative for demyelination.

5.1.1 Investigations of peripheral nerves of PMP22tg mice at the age P7 reveal no alterations in axonal sorting

Electron microscopy was used to analyze the morphology of peripheral nerves of PMP22tg mice (C61) and their wild type littermates at the age of P7. Ultrathin cross sections of peripheral nerves were produced and analyzed regarding the axonal sorting (axon in 1:1-ratio with Schwann cells) as well as the axonal diameter.

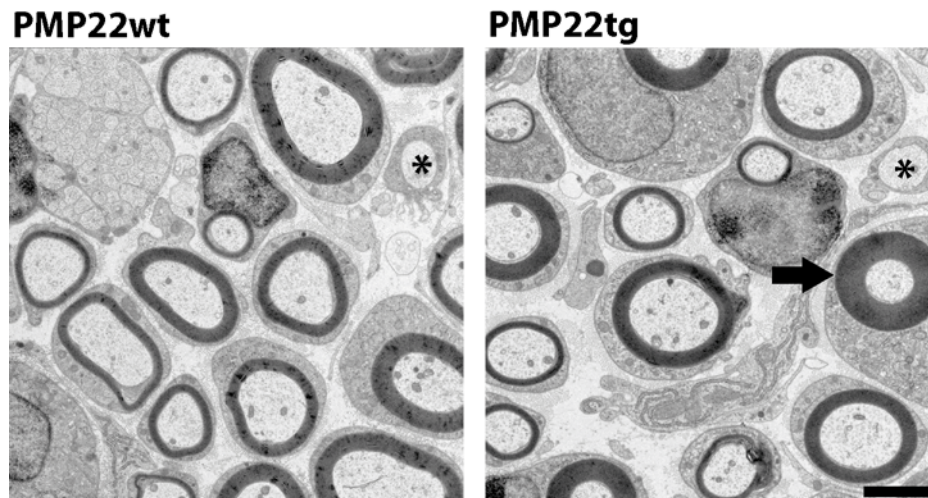


Figure 1: Electron micrograph images of femoral quadriceps nerve from PMP22wt and PMP22tg mice at P7.

Femoral quadriceps nerves of both genotypes, wild type and PMP22tg mice, showed axons in 1:1-ratio with Schwann cells. Note single separated axons, which are not surrounded with myelin (asterisk) and hypermyelinated axons in PMP22tg mice (arrow). Scale bar: 2 μ m.

The muscular quadriceps and the cutaneous saphenous branch of the femoral nerves, as well as the sciatic nerves, exhibited sorted and myelinated axons as well as axons devoid of myelin. Additionally, hypermyelinated axons were found in PMP22tg mice (**Figure 1**).

Quantification of the axons in 1:1-ratio with Schwann cells revealed no significant differences in femoral quadriceps, saphenous and sciatic nerves between PMP22tg mice and their wild type littermates. All examined peripheral nerves displayed comparable total numbers of myelinated axons as well as similar numbers of axons devoid of myelin (**Figure 2A**). The total number of axons in sciatic nerves was higher than in femoral quadriceps and saphenous nerves which are equivalent to the situation in adult peripheral nerves. The percentage of axons without myelin in comparison to the total number of axons was similar in femoral quadriceps, saphenous and sciatic nerves of wild type and PMP22tg mice indicative of no differences in axonal sorting (**Figure 2B**). The percentage of axons which were not surrounded with myelin was lower in femoral quadriceps nerves (10.7 ± 1.7 in PMP22wt and 11.8 ± 1.9 in PMP22tg) and sciatic nerves (12.1 ± 1.0 in PMP22wt and 15.7 ± 3.2 in PMP22tg) compared to cutaneous saphenous nerves (27.8 ± 5.8 in PMP22wt and 29.1 ± 2.7 in PMP22tg). Regarding the axon caliber, all three types of peripheral nerves consisted of similarly sized axons with a tendency to smaller caliber axons in cutaneous saphenous nerves of PMP22tg mutants compared to PMP22wt (**Figure 2C**).

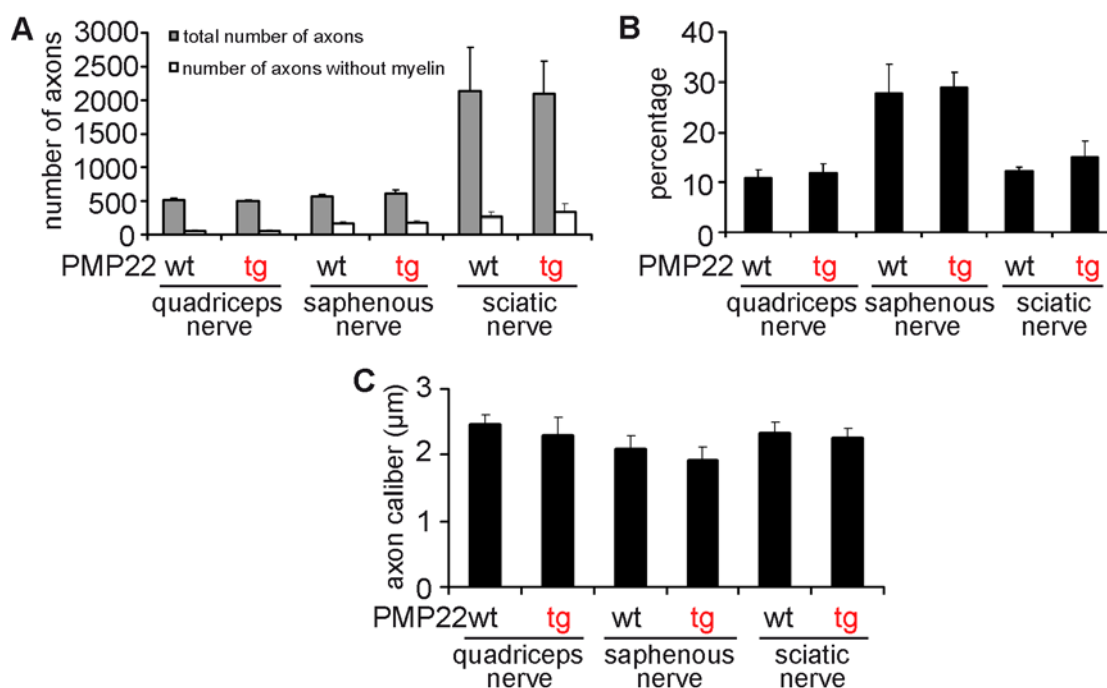


Figure 2: Morphometric analysis of PMP22tg mice and their wild type littermates at P7.

Axonal sorting and axonal diameter is not influenced by the overexpression of PMP22 ($n=5$) in peripheral nerves at P7 compared to wild type littermates ($n=5$). No significant difference was observed in the total number of axons surrounded with myelin in 1:1-ratio with Schwann cells (A, grey bars) or without myelin sheaths (A, white bars). The percentage of sorted axons (B), as well as the axon caliber (C) is illustrated for femoral quadriceps, cutaneous saphenous and sciatic nerves.

5.1.2 Overexpression of PMP22 leads to thicker myelin sheaths in peripheral nerves of PMP22tg mice at the age P7

In addition to analyzing the axonal sorting in PMP22tg mice at the age P7, we determined the g-ratio for 100 axons per nerve and mouse. The g-ratio is an established parameter for the thickness of the myelin sheath relative to the axonal size (Hildebrand and Hahn, 1978). It is determined by the ratio of axon circumference to fiber circumference. This means that the lower the value of the g-ratio, the thicker the myelin sheath surrounding the axon.

Interestingly, the measurement of the g-ratio revealed obvious differences in myelin thickness of peripheral nerves of PMP22tg and PMP22wt mice (**Figure 3**) which was recently published in collaboration with Dr. Elena M. Barbaria, Department of Neurology, Heinrich-Heine-University, Duesseldorf, Germany (Barbaria et al., 2008). In general, a trend towards

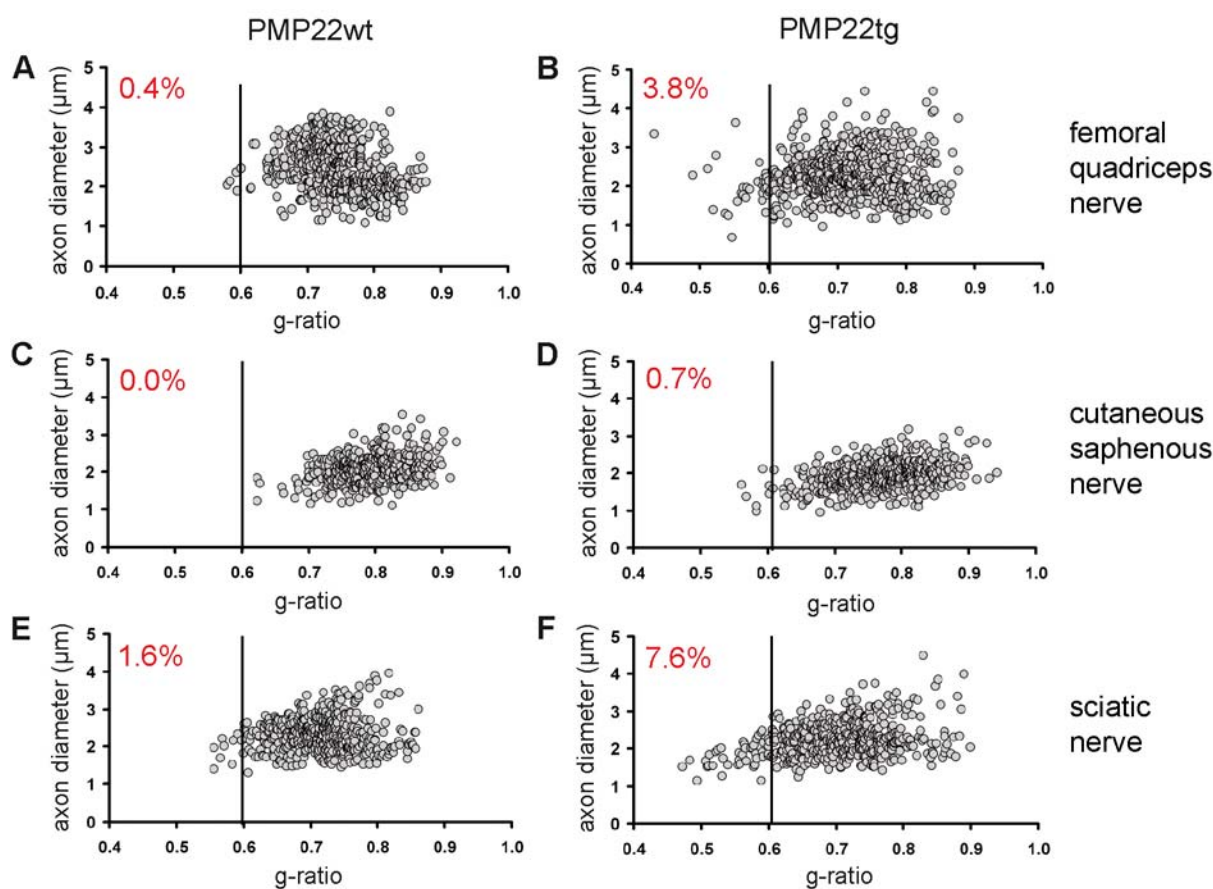


Figure 3: Measurement of g-ratios in peripheral nerves of PMP22 mutant mice at the age P7.

Already at P7, PMP22tg mice exhibited lower g-ratios indicative for thicker myelin sheaths in femoral quadriceps (A, B), cutaneous saphenous (C, D) and sciatic nerves (E, F) compared to nerves of their wild type littermates. For the determination of the g-ratio, 100 myelinated fibers per mouse and nerve were measured. The percentages of axons with a g-ratio lower than 0.6 relative to all investigated axons is indicated in red. These results allocate that the femoral quadriceps nerve, sciatic nerve and, to a smaller extent, the cutaneous saphenous nerve of P7 PMP22tg mice developed thicker myelin sheaths than the corresponding wild type nerves.

smaller caliber axons with thicker myelin sheaths in nerves of PMP22tg mice in comparison to nerves of wild type littermates was observed, especially in femoral quadriceps and sciatic nerves. Thicker myelin sheaths were found to a lesser extent in cutaneous saphenous nerves. This was also obvious if the percentage of axons with a g-ratio lower than 0.6 were determined. Femoral quadriceps nerves and sciatic nerves of PMP22tg mice showed 3.8% and 7.6% axons with a g-ratio lower than 0.6, respectively, and thus a higher proportion of thicker myelin sheaths than femoral quadriceps and sciatic nerves of PMP22wt (0.4% and 1.6%, respectively). Morphological alterations indicative of demyelination like thinly myelinated axons or supernumerary Schwann cells were not observed in PMP22 mutants at the age P7.

These results indicate that the overexpression of PMP22 leads to thicker myelin sheaths in femoral quadriceps nerves, sciatic nerves and to a lesser extent in cutaneous saphenous nerves of P7 PMP22tg compared to corresponding wild type littermates. Other developmental aspects like sorting of the axons were not affected.

5.2 The functional contribution of T-lymphocytes to the pathogenesis of PMP22tg mice

Previous studies showed a clear impact of T-lymphocytes on the pathology of myelin mutants of the peripheral nervous system (PNS, see section 3.2.4). Our group showed that in the absence of mature T- and B-lymphocytes the pathological phenotype of peripheral nervous tissue either could be ameliorated – like in the P0+/- and Cx32-/- mutants (Schmid et al., 2000; Kobsar et al., 2003) – or even aggravated as in the P0-/- mice (Berghoff et al., 2005). Furthermore, the number of F4/80-positive macrophages was also affected by the presence or absence of T-lymphocytes in peripheral nerves of the different myelin mutant mice. Based on these previous findings, the functional contribution of lymphocytes in nervous tissue of PMP22tg mice was examined. Therefore, two different experimental approaches were performed. Firstly, we crossbred PMP22tg mutants with RAG-1-/- mice lacking mature T- and B-lymphocytes. Secondly, we performed transfer of either PD-1-/- bone marrow or wild type bone marrow in irradiated PMP22tg mice and examined these bone marrow chimeras (BMCs) 6 months after transplantation.

5.2.1 Pathological alterations are non-significantly increased in peripheral nerves of PMP22tg/RAG-1-/- mice at the age of 12 months

5.2.1.1 The absence of mature lymphocytes does not influence macrophage numbers within nervous tissue of PMP22tg mice

While in other myelin mutants crossbreeding with RAG-1-/- mice resulted in a reduction of macrophage numbers in affected peripheral nerves (Schmid et al., 2000; Kobsar

5. Results

5.2 The functional contribution of T-lymphocytes to the pathogenesis of PMP22tg mice

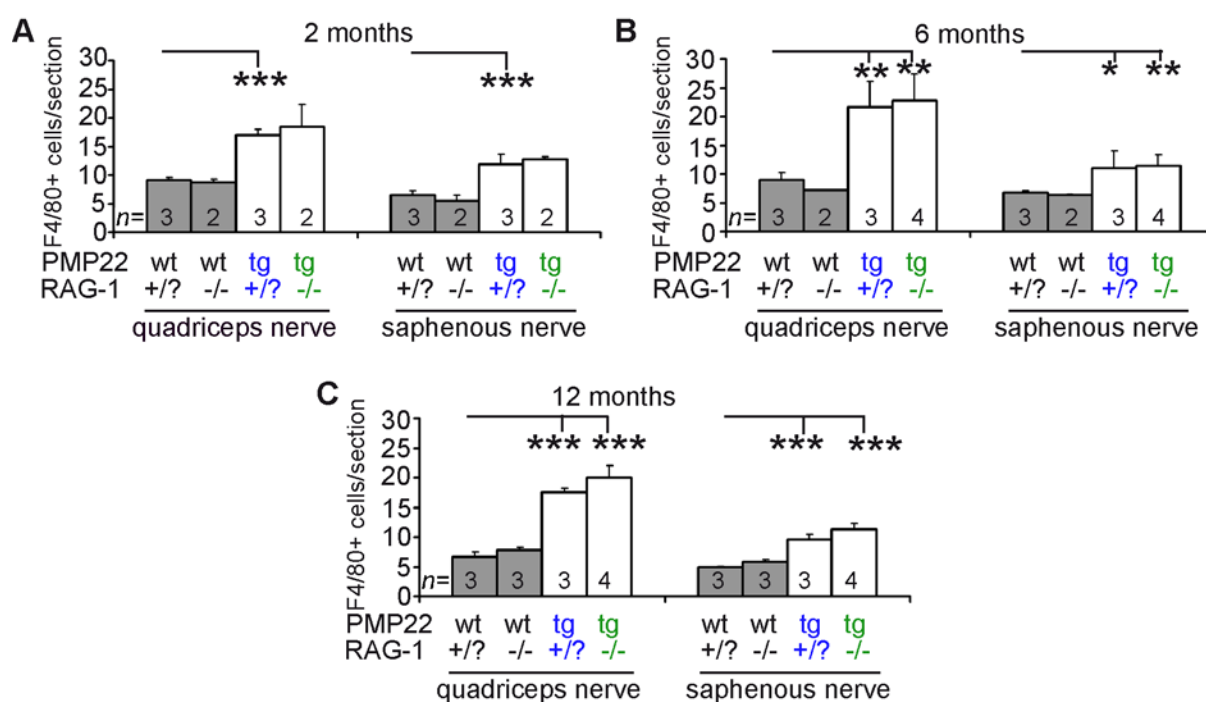


Figure 4: Quantification of F4/80-positive macrophages in femoral nerves of PMP22/RAG-1 double mutant mice.

Femoral quadriceps and cutaneous saphenous nerves showed increased numbers of F4/80-positive macrophages in PMP22tg mice at 2 (A), 6 (B) and 12 months of age (C). The RAG-1-deficiency had no effect on the macrophage number, neither in nerves of PMP22tg mice, nor in nerves of wild type mice compared to nerves of PMP22tg/RAG-1+/? and PMP22wt/RAG-1+/? , respectively. As expected, the number of F4/80-positive macrophages in wild type mice was not increased. * $p < 0.05$, ** $p < 0.01$; *** $p < 0.001$.

et al., 2003), these cells did not seem to be concerned by the RAG-1 genotype in nerves from PMP22tg mice (**Figure 4**). The number of F4/80-positive macrophages was already increased at the age of 2 months in femoral nerves of PMP22tg/RAG-1+/? mice and remained constant in 6 and 12 months old mutants (e.g. 17.0 ± 1.0 , 21.6 ± 4.5 and 17.6 ± 0.6 cells per section of femoral quadriceps nerves, respectively). This increase was not significantly altered in peripheral nerves of PMP22tg/RAG-1-/- mutants at 2 months, 6 months and 12 months (18.4 ± 3.9 , 22.7 ± 4.7 and 20.0 ± 2.0 cells per section of femoral quadriceps nerves). In peripheral nerves from PMP22wt/RAG-1-/- and PMP22wt/RAG-1+/? , no differences in macrophage numbers were obvious.

5.2.1.2 Peripheral nerves of PMP22tg/RAG-1^{-/-} mice disclose a non-significant increase of pathological alterations at 12 months of age

Next, the morphology of femoral quadriceps nerves was examined by electron microscopy. Here, the main focus was on the quantification of thinly and hypermyelinated axons, completely demyelinated axons, supernumerary Schwann cells (onion bulb formations) and foamy macrophages.

Ultrathin sections of femoral quadriceps nerves from 6-month-old double mutants displayed no obvious conspicuity comparing RAG-1^{+/?} mice and RAG-1^{-/-} mice (**Figure 5A**). In contrast to this, femoral quadriceps nerves of PMP22tg/RAG-1^{-/-} mice at the age of 12 months showed a tendency for thinner myelin sheaths compared to nerves from PMP22tg/RAG-1^{+/?} mice (**Figure 5A**). Quantification of pathological alterations in femoral quadriceps nerves revealed similar numbers of thinly myelinated axons, hypermyelinated axons as well as fibers devoid of myelin in PMP22tg/RAG-1^{+/?} and PMP22tg/RAG-1^{-/-} mice at the age of 6 months (**Figure 5B**). At the age of 12 months, nerves of PMP22tg/RAG-1^{-/-} mutant mice exhibited a slight aggravation of the diseased phenotype compared to PMP22tg/RAG-1^{+/?} mice which is depicted by a non-significant increase in the percentage of completely demyelinated fibers (**Figure 5B**). Additionally, there was a tendency towards a higher number of thinly myelinated axons in femoral quadriceps nerves of PMP22tg/RAG-1^{-/-} mice compared to PMP22tg/RAG-1^{+/?} mice at 12 months of age (**Figure 5B**). The number of hypermyelinated fibers as a typical hallmark for PMP22-overexpressing mice did not differ in peripheral nerves of PMP22tg mutants deficient or non-deficient for RAG-1. Similar to peripheral nerves of 6-month-old mice, the number of supernumerary Schwann cells was comparable in nerves from PMP22tg/RAG-1^{+/?} and PMP22tg/RAG-1^{-/-} mice at the age of 6 and 12 months (**Figure 5C**). The number of foamy macrophages was reduced in femoral quadriceps nerves of 12 months old mice relative to 6 months old mutant mice but was not altered in nerves of PMP22tg/RAG-1^{-/-} compared to PMP22tg/RAG-1^{+/?} mice (**Figure 5D**). Pathological alterations in peripheral nervous tissue of PMP22wt/RAG-1^{+/?} or PMP22wt/RAG-1^{-/-} were hardly ever detected and for this reason not quantified.

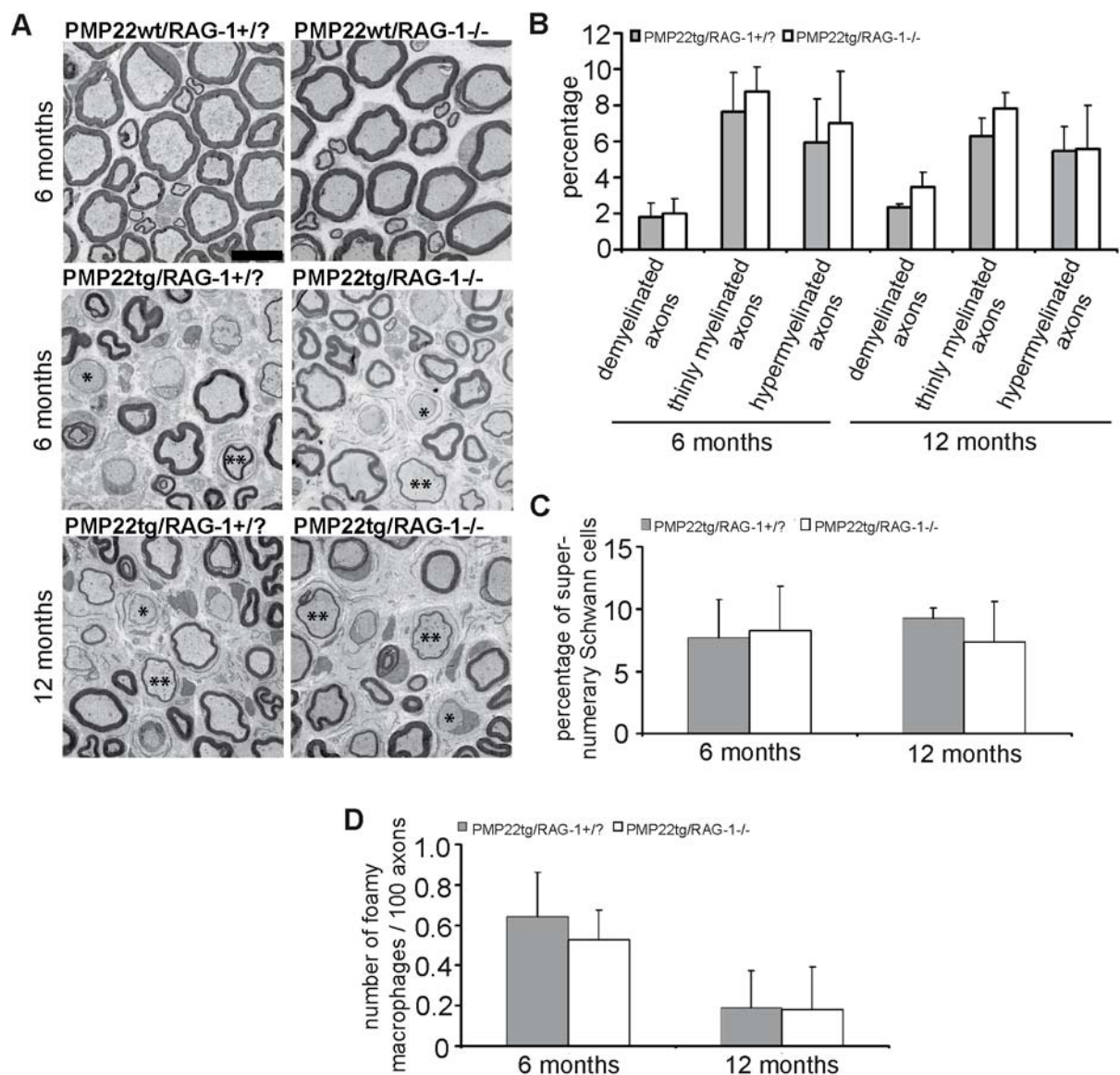


Figure 5: Morphometric analysis of femoral quadriceps nerves of 6 and 12 months old PMP22/RAG-1 double mutant mice.

Ultrathin sections of femoral quadriceps nerves of PMP22wt/RAG-1+/- and PMP22wt/RAG-1-/- did not reveal any signs of pathological alterations, whereas nerves of PMP22tg/RAG-1+/- and PMP22tg/RAG-1-/- mutants displayed axons devoid of myelin (asterisk) and thinly myelinated axons (double asterisks) at the age of 6 and 12 months (A). Quantification of pathological profiles exhibited a comparable percentage of demyelinated and thinly myelinated axons in nerves of 6-month-old double mutants (B). In femoral quadriceps nerves of 12-month-old PMP22tg/RAG-1-/-, the percentage of demyelinated and thinly myelinated axons was non-significantly increased compared to PMP22tg/RAG-1+/- mice (B). Interestingly, neither the number of hypermyelinated fibers (B), nor the number of supernumerary Schwann cells (C), nor the number of foamy macrophages (D) was affected by the RAG-1 genotype. Scale bar: 10 μ m.

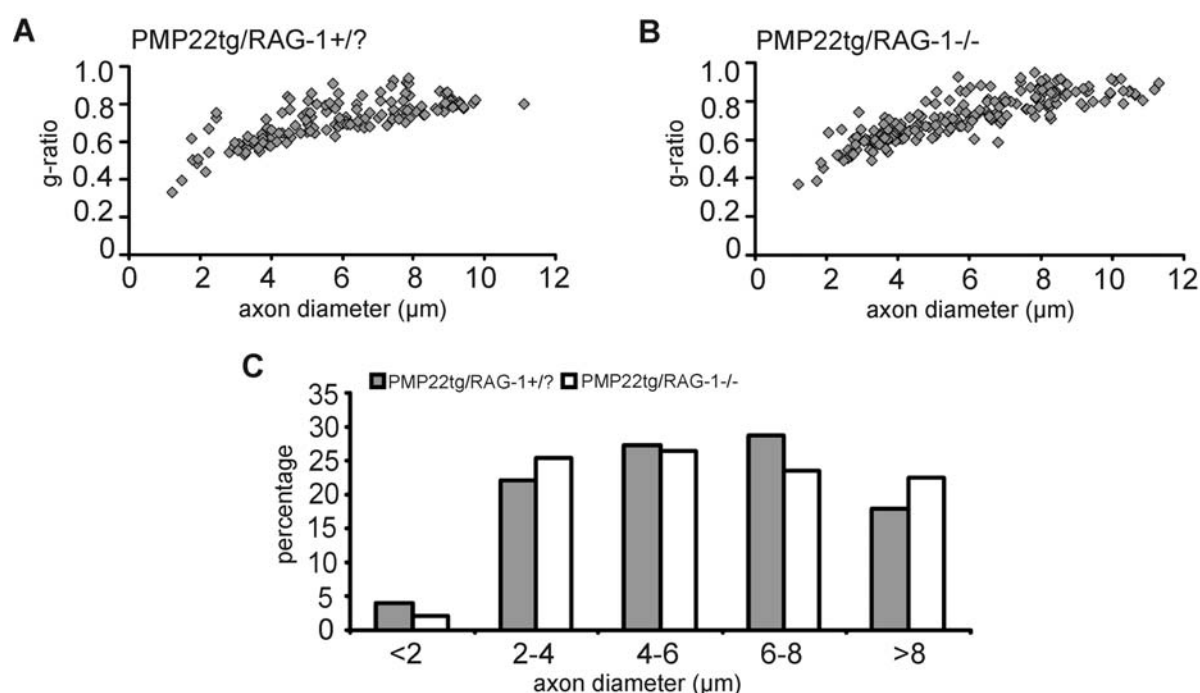


Figure 6: Measurement of axonal size in femoral quadriceps nerves from 12 month-old PMP22tg/RAG+/? and PMP22tg/RAG-1/- mice.

Illustration of g-ratios in correlation to the axonal diameter in femoral quadriceps nerves of 12-month-old PMP22tg/RAG-+/? and PMP22tg/RAG-1-/- mice (A, B). Nerves of PMP22tg/RAG-1-/- showed a tendency for a higher number of thinly myelinated axons with larger diameter as nerves from PMP22tg/RAG-1+/? mice. This is also indicated by the percentage of axonal size (C).

Furthermore, measurement of the g-ratio in femoral quadriceps nerves revealed a tendency for more larger caliber axons with thinner myelin sheaths (higher g-ratio values) in nerves of PMP22tg/RAG-1-/- mice compared to PMP22tg/RAG-1+/? mutant mice (**Figure 6A, B**). The percentage of larger caliber axons (>8μm) in nerves of PMP22tg/RAG-1-/- mice was non-significantly increased compared to nerves of PMP22tg/RAG-+/? mice (**Figure 6C**). Moreover, these large-caliber axons were predominantly surrounded with thin myelin sheaths.

In summary, these investigations revealed that PMP22tg/RAG-1-/- double mutants exhibited a non-significant tendency for an aggravation of the disease at the age of 12 months. Larger caliber axons in femoral quadriceps nerves from PMP22tg/RAG-1-/- mice were stronger affected than axons in nerves from PMP22tg/RAG-1+/? double mutants. In addition, the numbers of macrophages were not significantly altered in peripheral nerves of PMP22tg mice in presence or absence of T-lymphocytes.

5.2.2 Deficiency of PD1 (PD-1^{-/-}) in PMP22tg mice do not cause an aggravated neuropathological phenotype

To further analyze the impact of lymphocytes, we generated PMP22tg bone marrow chimeras (BMCs) by transplantation of either PD-1^{-/-} or wild type bone marrow as described in section 4.4.

“Programmed-death” (PD)-1 (CD279) is a co-inhibitory molecule which is expressed amongst others on activated T- and B-lymphocytes. It can interact with two ligands, PD-L1 (B7-H1, CD274) and PD-L2 (B7-DC, CD273), respectively (Okazaki et al., 2002; Okazaki and Honjo, 2007). A recent study from our group investigated the impact of PD-1 deficiency (PD-1^{-/-}) in nervous tissue of P0^{+/-}/RAG-1^{-/-} mice. In peripheral nerves of P0^{+/-}/RAG-1^{-/-} BMC PD-1^{-/-}, an impaired morphological phenotype and an increase of CD8-positive lymphocytes within peripheral nerves were observed in contrast to nerves of P0^{+/-}/RAG-1^{-/-} BMC wt (Kroner et al., 2008).

Therefore, we were interested in the role of T-lymphocytes in absence of PD-1 in peripheral nervous tissue of PMP22tg mice. As an initial step, we examined the expression of PD-1 and its ligand B7H1 (PD-1L) in PMP22 mutant mice. To investigate whether PD-1 and B7H1 is expressed in normal tissue, we performed flow cytometry with unstimulated splenocytes and nervous tissue of PMP22wt and PMP22tg mice. LPS-stimulated splenocytes and peritoneal macrophages were used as positive control. Hereby we found that PD-1 was expressed in nervous tissue of PMP22tg and their wild type littermates (**Figure 7A, B**, green line). In addition, expression of B7H1 was found in unstimulated splenocytes (**Figure 7C, D**; green line) of the mutants as well as to a lower amount in nervous tissue (data not shown).

5.2.2.1 The numbers of immune cells are not altered in peripheral nerves of PMP22tg BMC PD-1^{-/-} compared to PMP22tg BMC wt

To examine the putative role of PD-1 as a mediator of pathology in PMP22tg mice, we transplanted either PD-1-deficient (PD-1^{-/-}) or wild type bone marrow in sub-lethally irradiated myelin mutants. The successful transplantation was controlled by flow cytometry of peripheral blood and splenocytes for each individual. Only mice with usual amounts of CD4-positive and CD8-positive T-lymphocytes were included into the results.

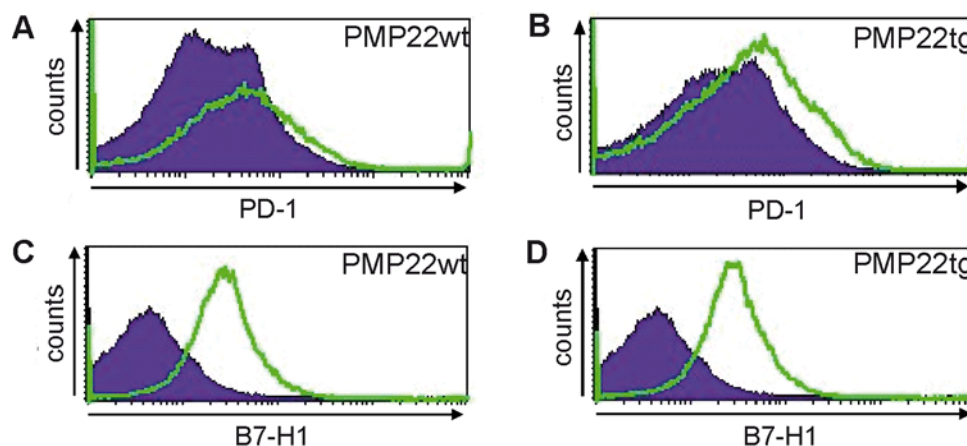


Figure 7: Analyses of expression of PD-1 and its receptor B7H1 in peripheral nerves and spleen by flow cytometry.

PD-1 is expressed in peripheral nerves of PMP22wt (A) and PMP22tg (B) which is indicated as the shift of PD-1-positive signal (green line) in comparison to the isotype control (blue area). Further, B7H1 is present in untreated splenocytes of PMP22wt (C) and PMP22tg mice (D, B7H1: green line, isotype control: blue area).

As a first indicator for a putative hyper-reactive immune system, we quantified F4/80-positive macrophages, as well as CD4- and CD8-positive T-lymphocytes by immunohistochemistry in femoral nerves of PMP22tg BMCs. Here, we found no differences regarding the investigated immune cells in nerves of PMP22tg BMC PD-1^{-/-} compared to PMP22tg BMC wt (**Figure 8**). Femoral nerves of PMP22tg mice which received wild type bone marrow exhibited macrophage numbers similar to nerves of PMP22tg mice transplanted with PD-1^{-/-} bone marrow (**Figure 8A**, 17.25 ± 1.77 and 17.35 ± 2.36 and 9.71 ± 1.31 and 9.80 ± 2.05 in femoral quadriceps nerves and cutaneous saphenous nerves, respectively). In addition, numbers of CD4- and CD8-positive T-lymphocytes were not altered by the PD-1-deficiency in peripheral nerves of PMP22tg mice 6 months after bone marrow transfer. Femoral quadriceps nerves displayed only few CD4-positive (**Figure 8B**) and CD8-positive immune cells (**Figure 8C**), whereas in cutaneous saphenous nerves nearly no T-cells were detectable. In nerves of PMP22tg BMC wt and PMP22tg BMC PD-1^{-/-}, the number of CD4-positive T-cells was similar with 0.1 ± 0.08 and 0.16 ± 0.06 cells per section. Similar results were achieved quantifying the number of CD8-positive lymphocytes (0.1 ± 0.07 and 0.13 ± 0.1 , respectively).

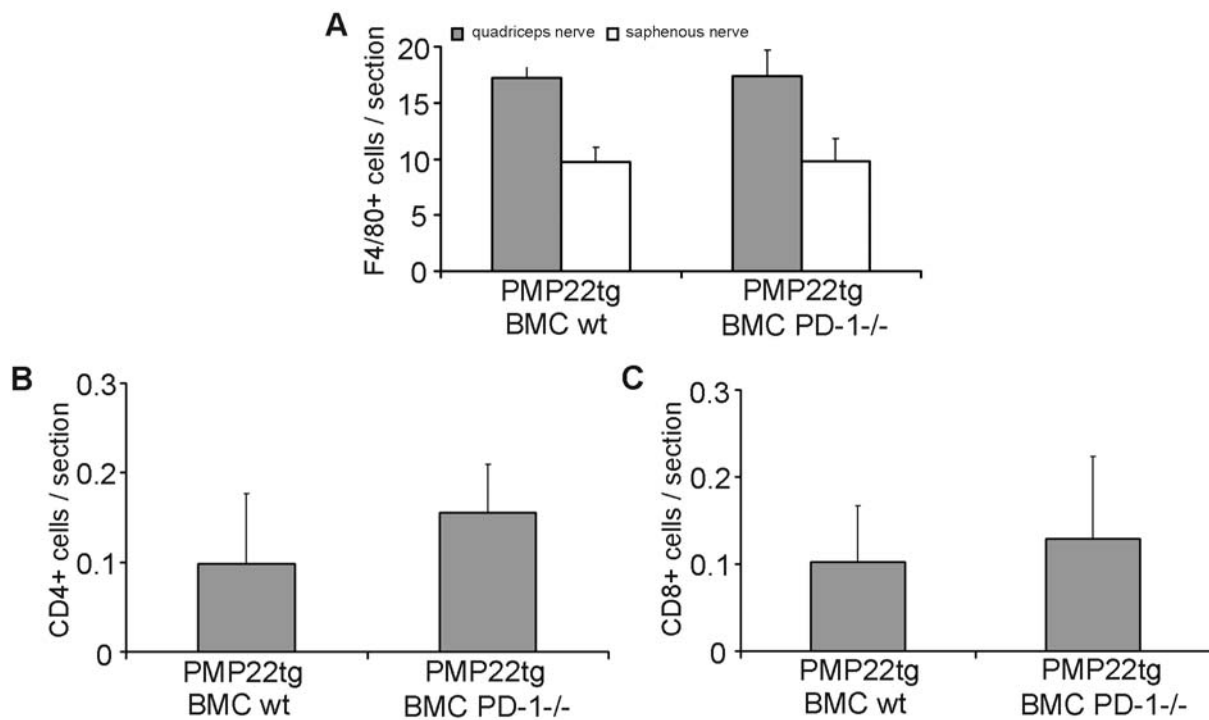


Figure 8: Quantification of immune cells in femoral nerves of PMP22tg bone marrow chimeras. F4/80-positive macrophages (A), CD4-positive T-lymphocytes (B) and CD8-positive T-cells (C) were not different in numbers in femoral nerves of PMP22tg mice which received PD-1^{-/-} bone marrow (PMP22tg BMC PD-1^{-/-}, *n*=6) in comparison to nerves of PMP22tg mice which received wild type bone marrow (PMP22tg BMC wt, *n*=7).

5.2.2.2 The degree of pathological alterations is equal in nervous tissue of PMP22tg BMC PD-1^{-/-} and of PMP22tg BMC wt

In a next step, morphological alterations in femoral nerves as well as lumbar ventral roots of PMP22tg bone marrow chimeras were quantified. Semithin sections of individuals displayed thinly and naked axons in femoral quadriceps nerves of PMP22tg BMC wt and PMP22tg BMC PD-1^{-/-} (**Figure 9A**) as well as in lumbar ventral roots (**Figure 9B**). By a semiquantitative test in which the investigator was not aware of the treatment of the bone marrow chimeras (“blinded” test), we examined the sections of femoral nerves and lumbar ventral roots by scoring the pathological alterations. Per definition, a score of 1 means no pathological alterations, where as a score of 5 implies massive damage. It was obvious that sections of femoral quadriceps nerves of both transplanted groups exhibited similar score (2.43 ± 0.53 and 2.80 ± 0.84 , **Figure 9C**). The scoring of lumbar ventral roots (**Figure 9D**) revealed a stronger pathology with more demyelinated axons than in femoral quadriceps

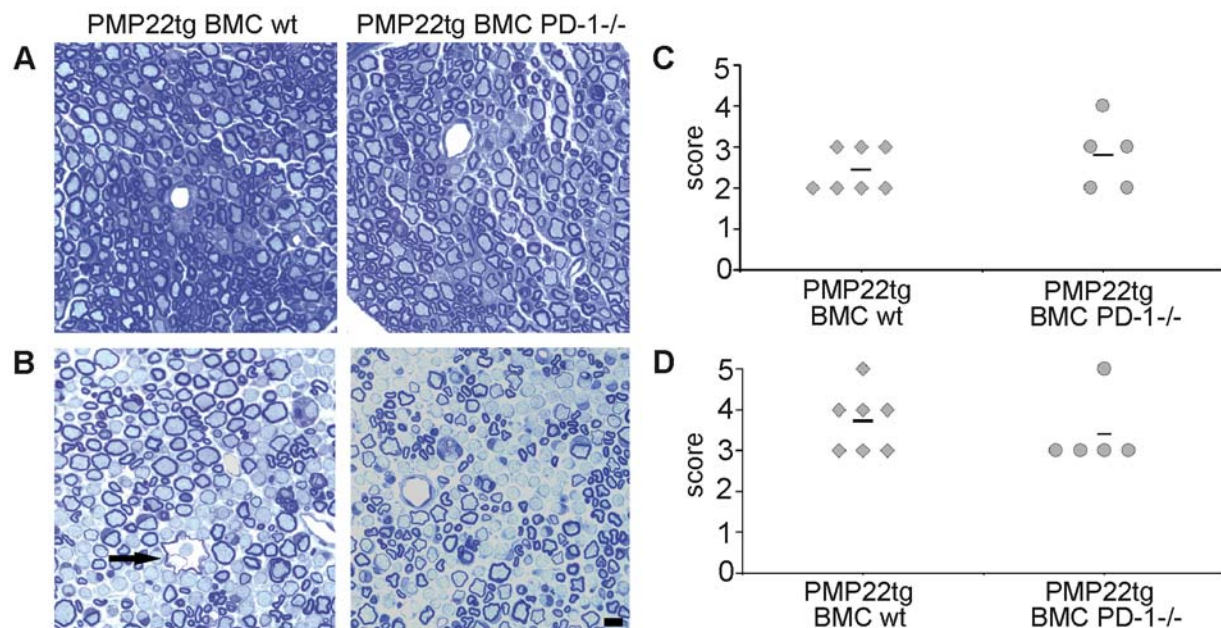


Figure 9: Analysis of semithin sections of nervous tissue from PMP22tg bone marrow chimeras.

Both, semithin sections of femoral quadriceps nerves (A) and lumbar ventral roots (B) from PMP22tg BMC wt and PMP22tg BMCs PD-1-/- showed similar pathological profiles which is also illustrated by semiquantitative scoring (C for femoral quadriceps nerves and D for lumbar ventral roots, respectively). A score of 1 depicts no pathological features, whereas a score of 5 means a massive damage. Thus, femoral quadriceps nerves were less affected than lumbar ventral roots and both, PMP22tg BMC wt and PMP22tg BMC PD-1-/- showed a comparable number of pathological profiles. Furthermore, vacuoles (arrow) were present in lumbar ventral roots from PMP22tg BMC wt and PMP22tg BMC PD-1-/- mice. Scale bar: 10 μ m.

nerve, but also no significant difference between PMP22tg BMC wt (3.71 ± 0.76) and PMP22tg BMC PD-1-/- (3.40 ± 0.89).

In a next step, we quantified the more strongly affected tissue – the lumbar ventral roots – by electron microscopy. The quantification of pathological profiles like demyelinated, thinly and hypermyelinated axons revealed no significant alterations in ventral roots of PMP22tg BMC PD-1-/- compared to PMP22tg BMC wt (**Figure 10A**). Remarkably, lumbar ventral roots showed a high percentage of completely demyelinated axons of approximately 30%. Furthermore, supernumerary Schwann cells as a sign for proliferation were not observed. Foamy macrophages were found at low levels with a non-significant tendency for fewer cells in PMP22tg mice which received PD-1-/- bone marrow (**Figure 10B**). In contrast to the femoral quadriceps nerves which exhibited nearly no vacuoles, lumbar ventral roots showed

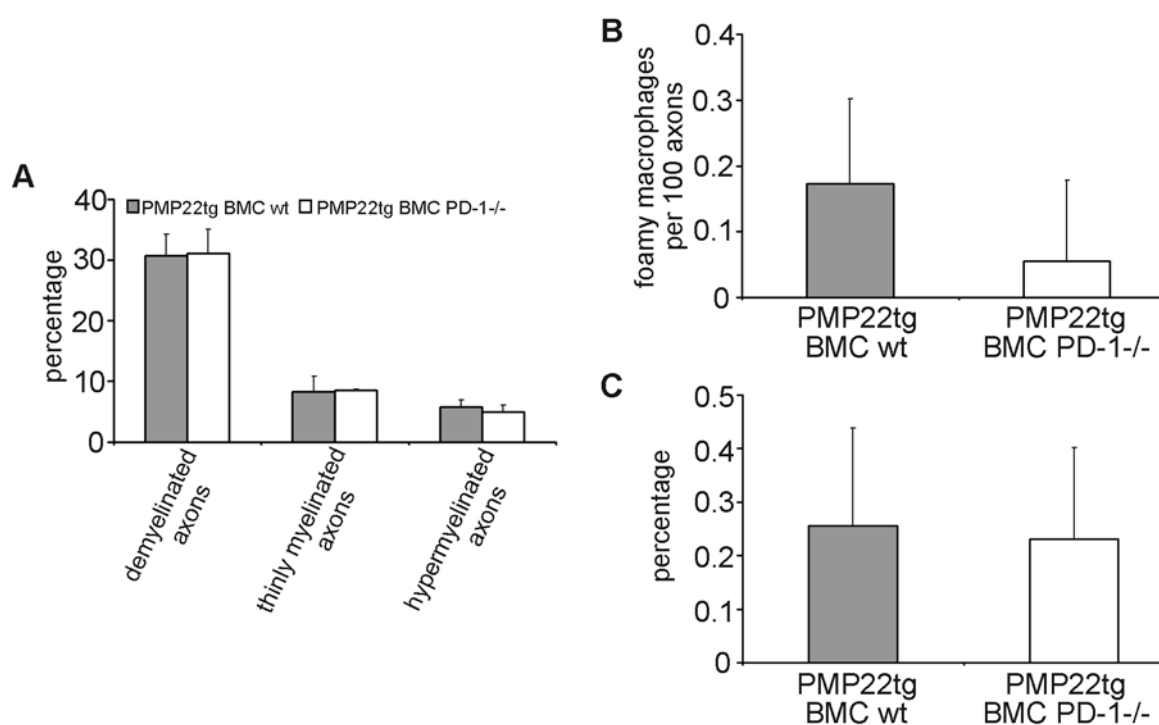


Figure 10: Quantification of pathological profiles in lumbar ventral roots of PMP22tg bone marrow chimeras.

Number of pathological alterations like demyelinated axons, thinly myelinated and hypermyelinated axons was similar in ventral roots of PMP22tg BMCs PD-1^{-/-} and PMP22tg BMCs wt (A). The number of foamy macrophages revealed a non-significant tendency to lower numbers in nervous tissue of PMP22tg BMCs PD-1^{-/-} (B) and vacuoles were similarly frequent in ventral roots of PMP22tg BMCs wt and PMP22tg BMCs PD-1^{-/-} (C).

periaxonal vacuoles with no difference in numbers between PMP22tg BMC PD-1^{-/-} and PMP22tg BMC wt (**Figure 10C**).

5.2.2.3 Sciatic nerve conduction properties are not altered in PMP22tg BMC PD-1^{-/-} compared to PMP22tg BMC wt

In complementary experiments we focused on functional tests regarding nerve conduction properties using neurographic recordings. Bone marrow chimeras were anesthetized with Hypnorm and electrophysiological examinations were enforced on both sciatic nerves per mouse 6 months after transplantation. Neither the compound muscle action potential (CMAP), nor the duration of CMAP, nor the F wave latency, nor the nerve conduction velocity indicated any altered nerve properties in PMP22tg bone marrow chimeras (**Table 1**). After distal stimulation, PMP22tg mice depicted the pre-described

	PMP22tg BMC wt	PMP22tg BMC PD-1 ^{-/-}
CMAP / proximal stimulation (mV)	3.8 ± 1.4	2.9 ± 1.4
CMAP / distal stimulation (mV)	4.2 ± 1.3	3.6 ± 1.8
duration of CMAP / proximal stimulation (ms)	3.7 ± 1.0	3.6 ± 0.4
duration of CMAP / distal stimulation (ms)	3.4 ± 1.2	3.4 ± 0.8
F wave latency (ms)	7.3 ± 1.0	6.6 ± 0.3
nerve conduction velocity (m/s)	30.3 ± 6.8	29.0 ± 5.1
<i>n</i> -numbers	5	3

Table 1: Neurographic recordings in PMP22tg bone marrow chimeras.

Conduction properties of sciatic nerves were not significantly altered in PMP22tg BMC PD-1^{-/-} mice compared to PMP22tg BMCs wt mice. This table indicates the mean values of both measurement of each mice, i.e. the right and the left extremities.

prolonged F wave latency and decelerated nerve conduction velocity (Kobsar et al., 2005). The CMAP was strikingly reduced with tendency for disperse responses. However, for all parameters, no differences were found between nerves of PMP22tg mice with wild type or PD-1^{-/-} bone marrow.

5.2.2.4 PMP22tg BMC PD-1^{-/-} exhibit stride properties similar to PMP22tg BMC wild type

As another performance test, we used the stride test to detect difficulties in walking or gait abnormalities. If mice would develop muscle weakness due to alterations within the nerves, it would be visible in the pattern of the footsteps. As mentioned in section 4.12, the hind paws of mice were dyed with ink and the mice were allowed to walk on papers in a dark environment. After three training runs, the tracks were conserved and investigated for four different parameters (**Figure 11A**). The distance between feet (a), the right (b) and left stride length (c), as well as the rotation angle of the gait (d) give information about altered walking abilities. This experiment revealed that PMP22tg mice showed no alterations regarding the stride length (**Figure 11B**) or the gait angle (**Figure 11C**) after the transplantation of either wild type or PD-1^{-/-} marrow. To exclude any differences in body size, mice were weighted on the same day (**Figure 11D**).

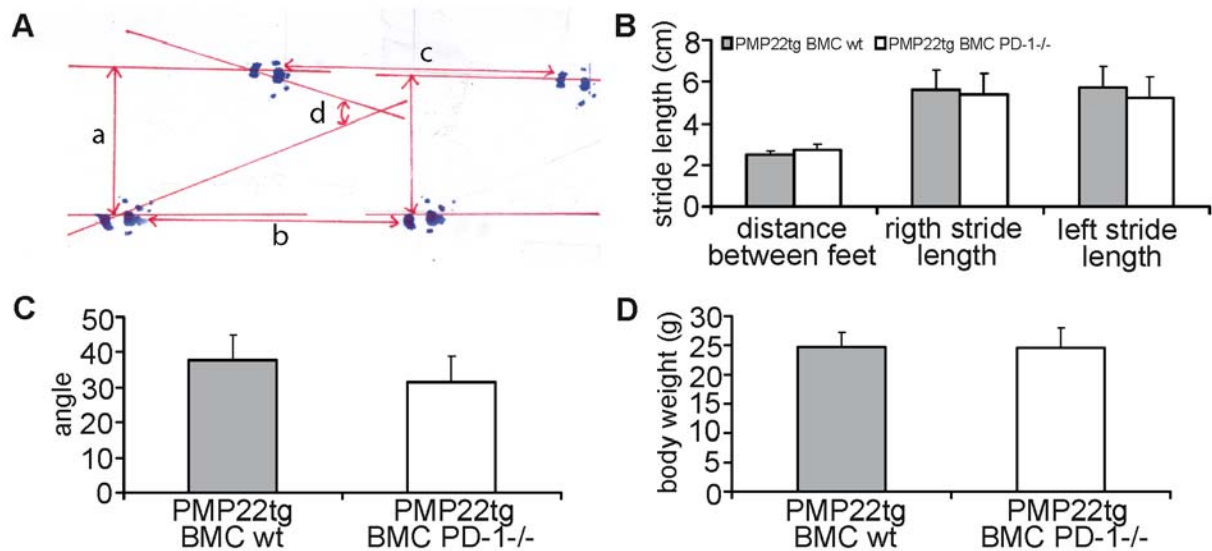


Figure 11: Stride test of PMP22tg bone marrow chimeras.

Schematic overview of one PMP22tg BMC mouse (A) illustrates the measured parameters, i.e. the distance between feet (a), the stride length of the right (b) and the left feet (c), as well as the angle of the gait (d). The distance between feet, right stride length and the left stride length were not different in PMP22tg BMC wt and PMP22tg BMC PD-1^{-/-} mice (B). In addition, PMP22tg BMC PD-1^{-/-} mice showed an angle of the gait comparable to PMP22tg BMC wt mice (C). In both groups, individuals were of similar body weight (D).

These experiments show that – as opposed to the P0^{+/-} bone marrow chimeras – the pathology in peripheral nerves of PMP22tg BMCs was not altered as figured out by immunohistochemical and electron microscopic analyses as well as by performance testing. In PMP22tg mice, the PD-1-deficiency did not induce an aggravation of the demyelinating phenotype of peripheral nerves or disturbances of motor performance.

5.3 The functional contribution of macrophages to the pathogenesis of PMP22tg mice

5.3.1 MCP-1 mRNA expression is increased in peripheral nerves of PMP22tg mice

PMP22tg mice exhibit a demyelinating phenotype with an early onset at the age of 2 months and pathological alterations in motor quadriceps as well as in cutaneous saphenous nerves (Kobsar et al., 2005). Kobsar and colleagues found an elevated macrophage number in femoral quadriceps and cutaneous saphenous nerves and an increase in MCP-1 mRNA expression in sciatic nerves of PMP22tg mice compared to wild type littermates. Further studies in our lab could identify MCP-1 as a mediator of pathology in peripheral nerves of another myelin mutant, the P0^{+/-} mice (Fischer et al., 2008b; Fischer et al., 2008a). In this mouse model, MCP-1 was upregulated in Schwann cells and it was shown to be important for macrophage immigration into peripheral nerves (Fischer et al., 2008b). Based on these observations, the expression of MCP-1 in femoral nerves of PMP22tg mice and its regulation within peripheral nerves were examined.

As a first step, semi-quantitative real-time PCR (qRT-PCR) was performed to investigate MCP-1 expression in femoral quadriceps nerves and cutaneous saphenous nerves. To confirm the increase of MCP-1 mRNA in sciatic nerves of PMP22tg mice, we also performed qRT-PCR analyses in femoral nerves. As expected, MCP-1 mRNA expression was 3-fold increased in sciatic nerves of PMP22tg mice compared to wild type littermates (**Figure 12A**; (Kobsar et al., 2005)). At the age of 2 months, MCP-1 mRNA was increased more than 2-fold in motor quadriceps nerves of PMP22tg mutants compared to wild type mice (**Figure 12B**). The cutaneous saphenous nerves of these mice exhibited only a non-significant elevation of MCP-1 mRNA relative to PMP22wt (**Figure 12C**). Furthermore, the cellular localization of MCP-1 was examined by immunohistochemistry on sciatic nerve cross sections of 2-month-old mice, which revealed a myelin-associated staining in PMP22wt mice (**Figure 12D**). The intensity of the MCP-1 signal seemed to be increased in sciatic nerves of PMP22tg mutants and also Schwann cell-associated (**Figure 12E**). Cross sections of PMP22tg/MCP-1^{-/-} mice ($n=3$) which were used as negative control exhibited only a weak background staining (data not shown).

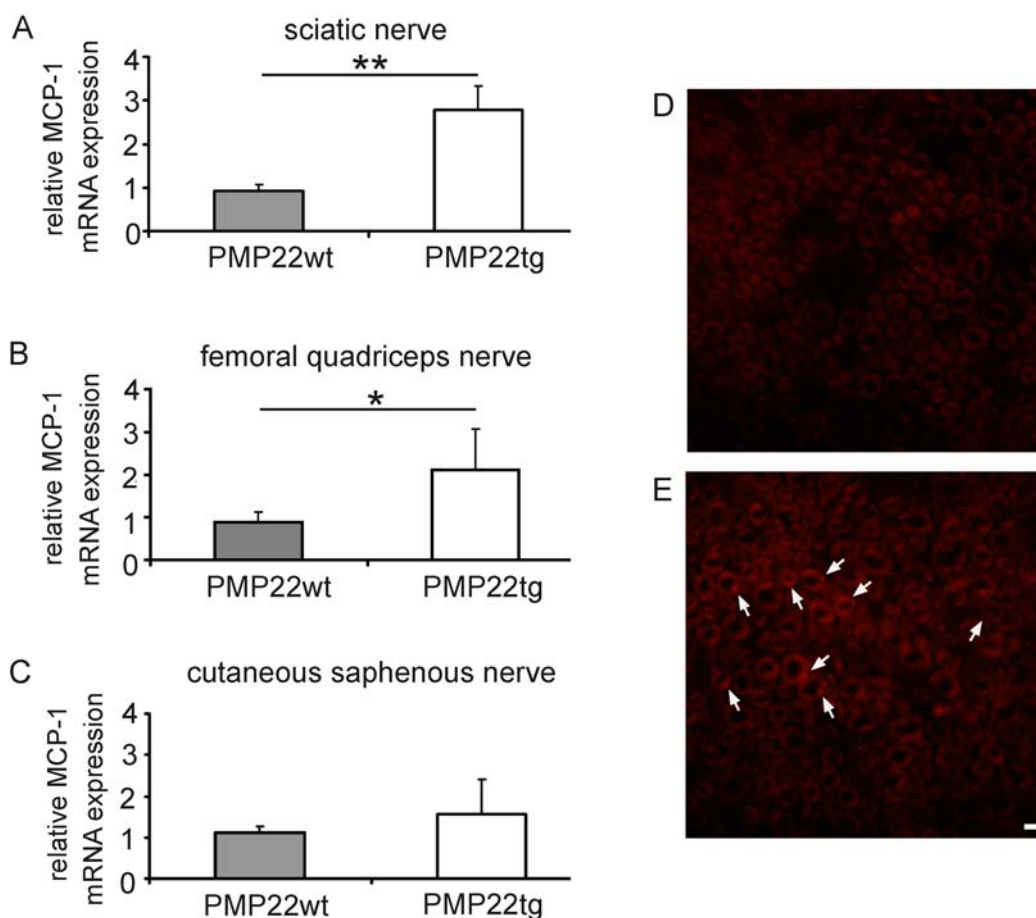


Figure 12: Analysis of MCP-1 mRNA and localization of MCP-1 protein in peripheral nerves of 2-month-old PMP22 mutant mice.

Increased MCP-1 mRNA expression was detected in sciatic nerves (A) as well as in femoral quadriceps nerves (B) of PMP22tg ($n=4$) relative to nerves of PMP22wt mice ($n=3$) by qRT-PCR. Cutaneous saphenous nerves (C) reveals only a slight increase in MCP-1 mRNA of PMP22tg ($n=3$) in comparison to PMP22wt mice ($n=2$). Localization of MCP-1 (red) in sciatic nerves of PMP22wt ($n=3$, D) and PMP22tg mice ($n=4$, E) by immunohistochemistry. Note the Schwann cell-associated staining with high intensity in PMP22tg mutants (arrows) which was not observed in PMP22wt mice. * $p<0.05$, ** $p<0.01$, scale bar: 10 μ m.

5.3.2 Nervous tissue of PMP22/MCP-1 double mutants show differences in the demyelinating phenotype

Former studies showed that P0 $^{+/-}$ mice crossbred with MCP-1 mutant mice revealed pathological alterations, i.e. an improvement of the pathological phenotype of peripheral nerves from P0 $^{+/-}$ /MCP-1 $^{+/-}$ mice. Surprisingly, the numbers of axons devoid of myelin and thinly myelinated axons were clearly reduced in peripheral nerves of P0 $^{+/-}$ /MCP-1 $^{+/-}$ (Fischer et al., 2008b). In contrast, peripheral nervous tissue of P0 $^{+/-}$ /MCP-1 $^{-/-}$ displayed an

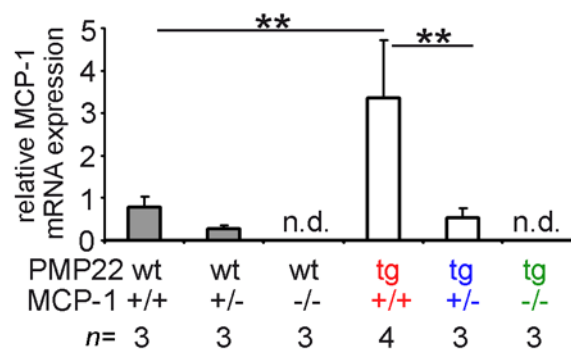


Figure 13: Analysis of MCP-1 mRNA expression in sciatic nerves of PMP22/MCP-1 double mutant mice at the age of 2 months by qRT-PCR.

Semiquantitative real-time PCR of nerve lysates from PMP22/MCP-1 double mutant mice revealed an elevated MCP-1 expression in sciatic nerves of PMP22tg/MCP-1+/+ mice compared to PMP22wt/MCP-1+/+ mutants similar to PMP22 single mutant mice. This increase is clearly diminished by MCP-1 heterozygosity in myelin mutant mice (PMP22tg/MCP-1+/- mice). As expected, no MCP-1 expression was detected in nerves of PMP22wt/MCP-1-/- and PMP22tg/MCP-1-/- (n.d. = not detectable). ** p<0.01.

increased numbers of pathological alterations. To analyze the impact of MCP-1 in PMP22tg mice, myelin mutants were crossbred with MCP-1-deficient mice (Lu et al., 1998) and peripheral nervous tissue of double mutants were examined at different ages.

5.3.2.1 MCP-1 deficiency causes a reduced number of macrophages in peripheral nerves of PMP22tg mutants compared to wild type mice

As a first step, we examined the MCP-1 mRNA expression in sciatic nerves of PMP22 mutant mice crossbred with MCP-1 deficient mice. Whereas 2-month-old PMP22tg/MCP-1+/+ showed a 3-fold increase of MCP-1 mRNA similar to PMP22tg mice, the expression of MCP-1 was clearly reduced in PMP22tg/MCP-1+/- . In complete absence of MCP-1 in PMP22wt and PMP22tg mice, no MCP-1 mRNA was detectable by qRT-PCR (**Figure 13**).

Next, immunohistochemical stainings against the macrophage marker F4/80 as well as the T-cell markers CD4 and CD8 on cross sections of peripheral nerves from PMP22/MCP-1 double mutants at the age of 2, 6 and 12 months were performed. For first immunohistochemical analyses, the number of F4/80-positive macrophages in femoral

5. Results

5.3 The functional contribution of macrophages to the pathogenesis of PMP22tg mice

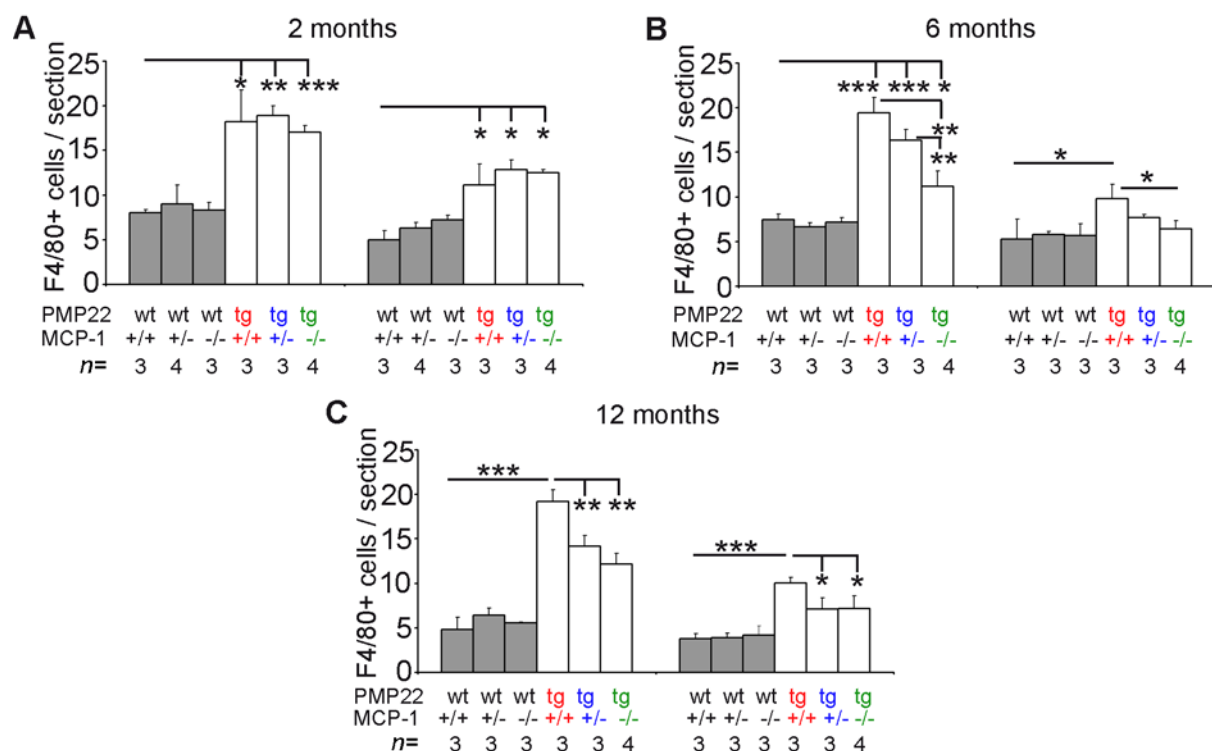


Figure 14: Quantification of F4/80-positive macrophages in femoral nerves of PMP22/MCP-1 double mutants at 2, 6 and 12 months of age.

The number of F4/80-positive macrophages per section was increased in femoral nerves of PMP22tg/MCP-1+/+, PMP22tg/MCP-1+/- as well as in nerves of PMP22tg/MCP-1-/- mice at the age of 2 months (A). The reduction (MCP-1+/-) or the complete absence of MCP-1 (MCP-1-/-) led to a decline in macrophage numbers in nerves of PMP22tg/MCP-1+/- and PMP22/MCP-1-/- mutant mice at the age of 6 months (B) as well as of 12 months (C). * p<0.05; ** p<0.01; *** p<0.001.

nerves was determined. Femoral nerves of PMP22tg/MCP-1+/+ and PMP22tg/MCP-1+/- mice showed an elevation in macrophage number already at the age of 2 months in femoral quadriceps and saphenous nerves (**Figure 14A**). Interestingly, there were also more macrophages in nerves of PMP22tg/MCP-1-/- in comparison to PMP22wt/MCP-1+/+ mice (**Figure 14A**). A similar number was detected in nerves of 6- and 12-month-old mice in PMP22tg/MCP-1+/+, whereas macrophages were reduced in femoral nerves of PMP22tg/MCP-1+/- and PMP22tg/MCP-1-/- mutants (**Figure 14B, C**). In peripheral nerves of PMP22wt/MCP-1+/- and PMP22wt/MCP-1-/- mice, the macrophage number did not increase. Thus, this data clarify the strong correlation of the increase in macrophage number and the elevated MCP-1 expression in both the femoral quadriceps and the saphenous nerves of PMP22tg mice.

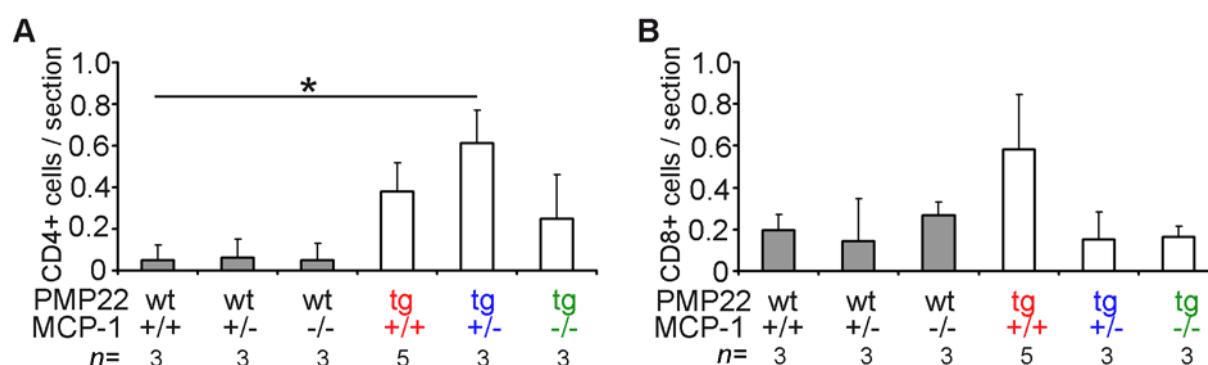


Figure 15: Quantification of CD4- and CD8-positive macrophages in femoral quadriceps nerves of PMP22/MCP-1 double mutants at 12 months of age.

CD4-positive T-lymphocytes were more frequent in femoral quadriceps nerves of PMP22tg/MCP-1+/+, PMP22tg/MCP-1+/- and PMP22tg/MCP-1-/- mice compared to wild types (A). In nerves of PMP22tg/MCP-1+/- mutants, the highest number of CD4-positive T-lymphocytes was found. The numbers of CD8-positive T-cells were only slightly increased in femoral quadriceps nerves of PMP22tg/MCP-1+/+ mutants in comparison to nerves of PMP22wt/MCP-1+/+ mice (B). * $p < 0.05$.

Next, we focused on the quantification of CD4- and CD8-positive T-lymphocytes in femoral nerves of PMP22/MCP-1 double mutants at the age of 12 months. The number of T-lymphocytes in femoral quadriceps nerves was smaller than the number of F4/80-positive macrophages. CD4-positive T-cells were slightly increased in femoral quadriceps nerves of PMP22tg/MCP-1+/+, PMP22tg/MCP-1+/- and PMP22tg/MCP-1-/- compared to wild type littermates which reached statistical significance for the PMP22tg/MCP-1+/- mutants (**Figure 15A**). In contrast, CD8-positive T-cells were non-significantly elevated in femoral quadriceps nerves of PMP22tg/MCP-1+/+ at the age of 12 months in comparison to wild type mice, PMP22tg/MCP-1+/- and PMP22tg/MCP-1-/- mice (**Figure 15B**).

5.3.2.2 PMP22/MCP-1 double mutant mice show different cytokine expression

In order to identify further possible immune modulators besides MCP-1, mRNA expression of macrophage-colony stimulating factor (M-CSF), tumor necrosis factor- α (TNF α), interleukin-6 (IL-6), leukaemia inhibitory factor (LIF), tumor growth factor- β (TGF β) and interleukin-1 β (IL-1 β) in peripheral nerves of 2 months old double mutants was examined by qRT-PCR. M-CSF mRNA was 1.6-fold upregulated in femoral quadriceps nerves of PMP22tg/MCP-1+/+ at the age of 2 months, whereas the expression was lower in nerves from PMP22tg/MCP-1+/- similar to the expression in wild type nerves (**Figure 16A**). This increased expression of M-CSF mRNA in nerves from PMP22tg/MCP-1+/+ was also evident

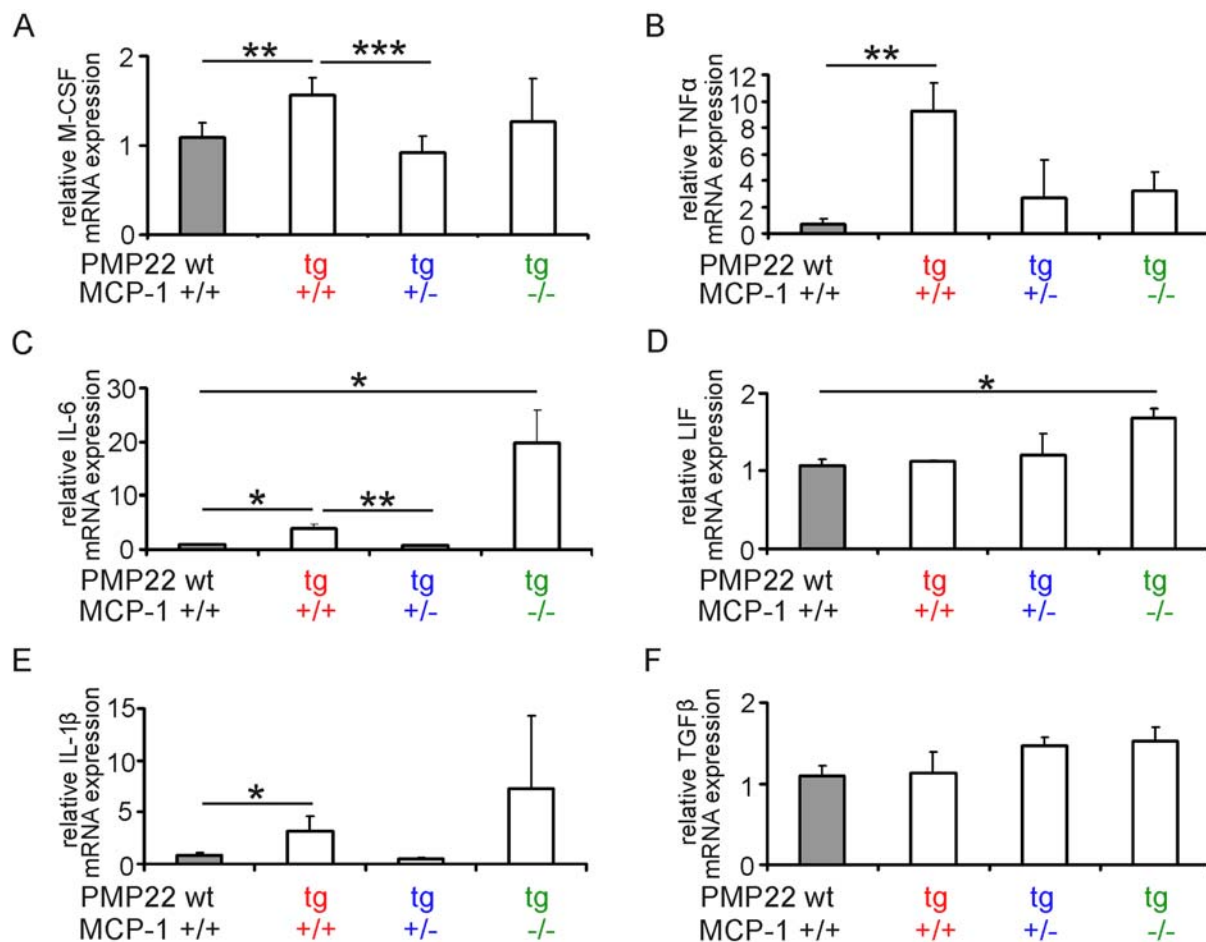


Figure 16: Cytokine expression in peripheral nerves of PMP22 mutant mice at the age of 2 months.

mRNA expression of different cytokines was analyzed in femoral quadriceps (A) and sciatic nerves (B-F) of 2-month-old PMP22/MCP-1 double mutants by qRT-PCR. M-CSF mRNA was significantly increased in nerves of PMP22tg/MCP-1+/+ ($n=4$). M-CSF mRNA expression in nerve lysates of PMP22tg/MCP-1+/- ($n=3$) and PMP22tg/MCP-1-/- ($n=3$) mice showed no significant differences to the expression in nerves from PMP22wt/MCP-1+/+ mice ($n=3$, A). TNF α mRNA expression was highest in sciatic nerves of PMP22tg/MCP-1+/+ (B). In contrast, IL-6 (C), LIF (D) and IL-1 β (E) mRNA expression were increased in sciatic nerves of PMP22tg/MCP-1-/- mice. Quantification of TGF β mRNA showed no significant alterations in nerves of PMP22tg/MCP-1 double mutant mice (F). * $p < 0.05$; ** $p < 0.01$; *** $p < 0.001$.

at the age of 6 months (data not shown). Furthermore in sciatic nerves of PMP22tg/MCP-1+/+, TNF α and IL-6 mRNA was increased in comparison to nerves from wild type (Figure 16B, C). However, the highest IL-6 mRNA expression was found in PMP22tg/MCP-1-/- double mutants (Figure 16C). Additionally, LIF and IL-1 β mRNA were also upregulated in PMP22tg/MCP-1-/- compared to wild type nerves (Figure 16D, E). In

comparison to nerves from wild type mice, TGF β mRNA was not strikingly altered in PMP22tg mice by the MCP-1 deficiency (**Figure 16F**).

5.3.2.3 Reduction and deficiency of MCP-1 leads to amelioration of disease in PMP22tg mice

Morphological alterations indicative of demyelination were quantified using electron microscopy in femoral quadriceps, cutaneous saphenous nerves and lumbar ventral roots of PMP22tg/MCP-1+/+, PMP22tg/MCP-1+/- and PMP22tg/MCP-1-/- mutants at the age of 6 and 12 months.

Ultrastructural analysis of peripheral nerves of PMP22/MCP-1 double mutants at the age of 6 months revealed a clear amelioration of the pathological phenotype in PMP22tg/MCP-1+/- mice and a slight reduction of nerve pathology in PMP22tg/MCP-1-/- compared to nerves of PMP22tg/MCP-1+/+ mutants (**Figure 17A**). In 12-month-old mice, all femoral nerves of PMP22tg/MCP-1 double mutants displayed pathological alterations like demyelinated axons and thinly myelinated fibers (**Figure 17B**).

Quantification of pathological profiles revealed a reduction of demyelinated and thinly myelinated axons in femoral quadriceps nerves from 6-month-old PMP22tg/MCP-1+/- and PMP22tg/MCP-1-/- mice compared to PMP22tg/MCP-1+/+ (**Figure 17C**). Furthermore, the improvement of the morphological phenotype of peripheral nerves from PMP22tg/MCP-1+/- mice was also obvious by determination of the g-ratio which displayed a lower number of thinly myelinated and demyelinated axons compared to nerves of PMP22tg/MCP-1+/+ (**Figure 17D**). In 12-month-old mutants, pathological profiles like demyelinated and thinly myelinated axons were increased in femoral quadriceps nerves of PMP22tg/MCP-1+/- and PMP22tg/MCP-1-/- mice compared to 6 months old mice, but still reduced in comparison to nerves from PMP22tg/MCP-1+/+ mutants (**Figure 17C**). Interestingly, the number of hypermyelinated fibers as a typical feature for peripheral nerves of PMP22tg mice was not affected by the MCP-1 genotype which was already observed in nerves of PMP22tg/RAG-1-/- mice (see section 5.2.1.2). In addition, no differences were found in the number of supernumerary Schwann cells between nervous tissue of the different double mutants (**Figure 17E**). Regarding foamy macrophages, femoral quadriceps nerves of PMP22tg/MCP-1+/- showed a non-significant tendency towards less cells compared to

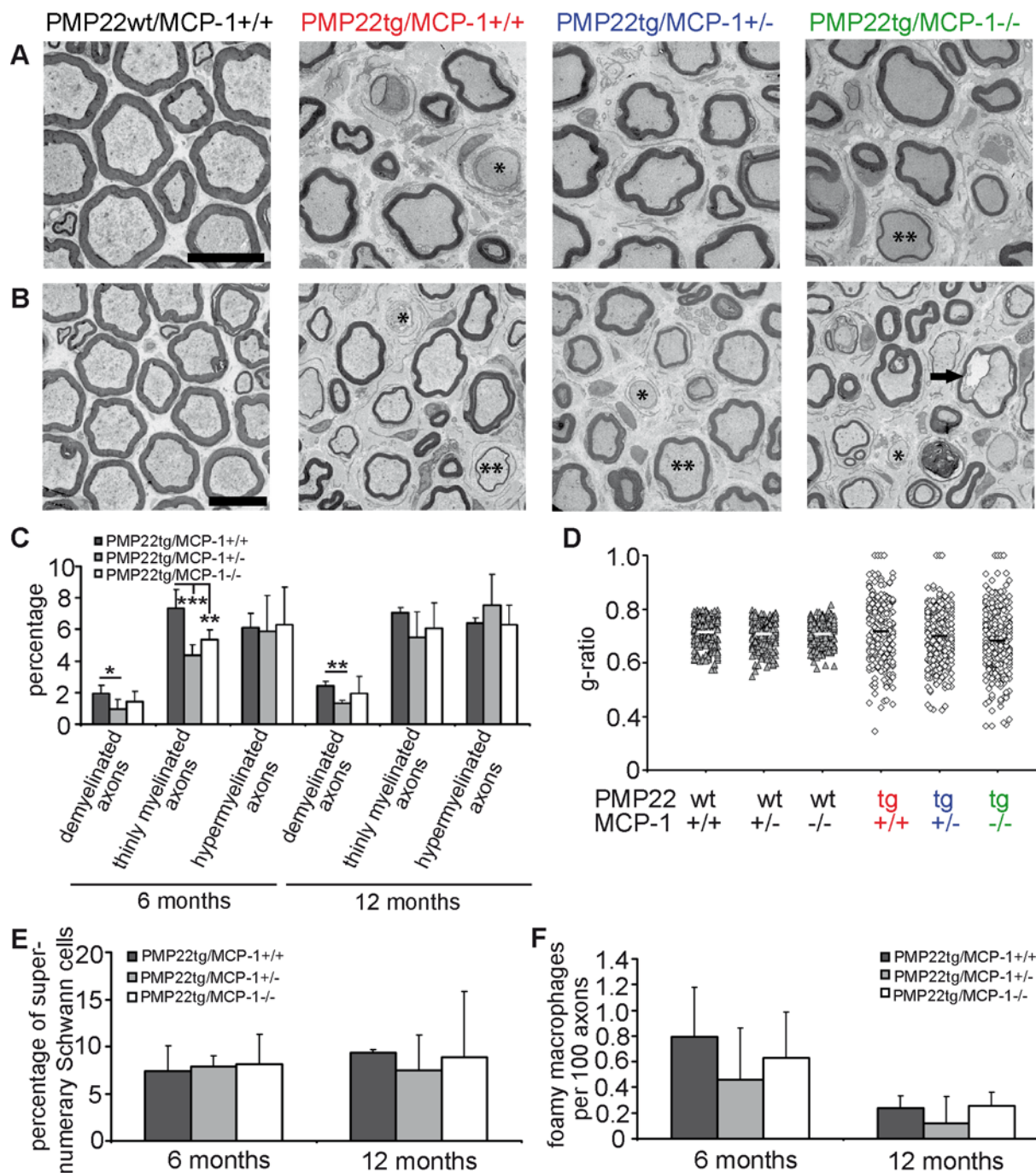


Figure 17: Morphometric analysis of femoral nerves from PMP22/MCP-1 double mutant mice at 6 and 12 months of age.

Electron micrographs of femoral quadriceps nerves of 6 months (A) and 12 months (B) old PMP22/MCP-1 double mutant mice showed demyelinated axons (asterisk), thinly myelinated axons (double asterisks) and vacuoles (arrow). Femoral quadriceps nerves exhibit reduced demyelination in PMP22tg/MCP-1+/- and PMP22tg/MCP-1-/- in comparison to PMP22tg/MCP-1+/+ mice at the age of 6 months (C). Hypermyelinated fibers were not affected by the MCP-1 genotype. Determination of the g-ratio reflected the milder pathology in peripheral nerves of PMP22tg/MCP-1+/- mutant mice at the age of 6 months (D, $n=3-4$). Quantification of supernumerary Schwann cells (E) and foamy macrophages (F) in femoral quadriceps nerves of PMP22tg/MCP-1 at the age of 6 and 12 months by electron microscopy. Scale bar: 10 μ m. * $p<0.05$, ** $p=0.05$, *** $p<0.005$.

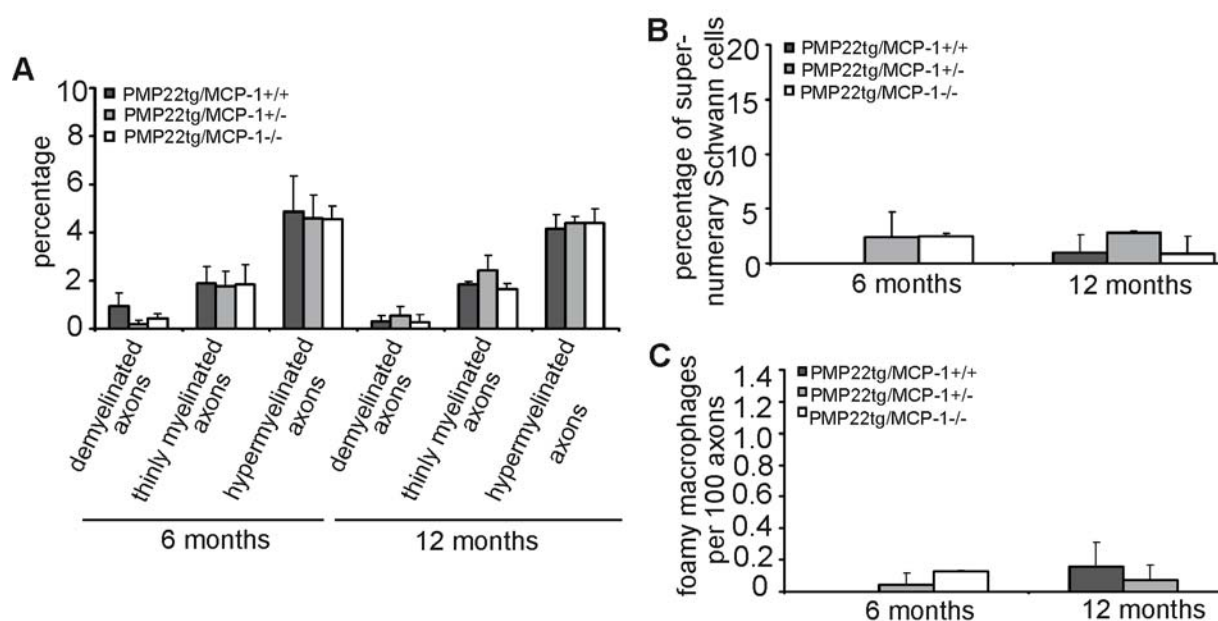


Figure 18: Morphometric analysis of cutaneous saphenous nerves from 6 and 12 months old PMP22tg/MCP-1 double mutant mice.

Pathological profiles like de- and thinly myelinated axons as well as hypermyelinated fibers are obvious in cutaneous saphenous nerves from PMP22tg/MCP-1 double mutant mice (A). Supernumerary Schwann cells (B) and foamy macrophages (C) are rarely seen in cutaneous saphenous nerves of all genotypes.

nerves of PMP22tg/MCP-1+/+ and PMP22tg/MCP-1-/- mice (**Figure 17F**). Furthermore it is to note that the cutaneous saphenous nerves displayed also pathological alterations like demyelinated axons and thinly or hypermyelinated fibers which were less numerous than in femoral quadriceps nerves (**Figure 18**). The deficiency of MCP-1 in wild types did not lead to pathological alterations in peripheral nerves at any age and were therefore not quantified.

We further analyzed lumbar ventral roots of 6- and 12-month-old PMP22/MCP-1 double mutants by electron microscopy. In lumbar ventral roots, the number of demyelinated fibers was increased in comparison to femoral quadriceps nerves (**Figure 19**). Quantification of pathological alterations confirmed a high percentage of completely demyelinated axons in nerves of all PMP22tg/MCP-1 mutant mice. Interestingly, the percentages of thinly myelinated axons and of hypermyelinated axons were similar to those in femoral quadriceps nerves. At 6 months of age, no significant differences were observed between the genotypes. Lumbar ventral roots of PMP22tg/MCP-1-/- at the age of 12 months revealed a non-significant increase of demyelinated fibers in comparison to ventral roots of PMP22tg/MCP-1+/- and PMP22tg/MCP-1+/- mice. Foamy macrophages were equally

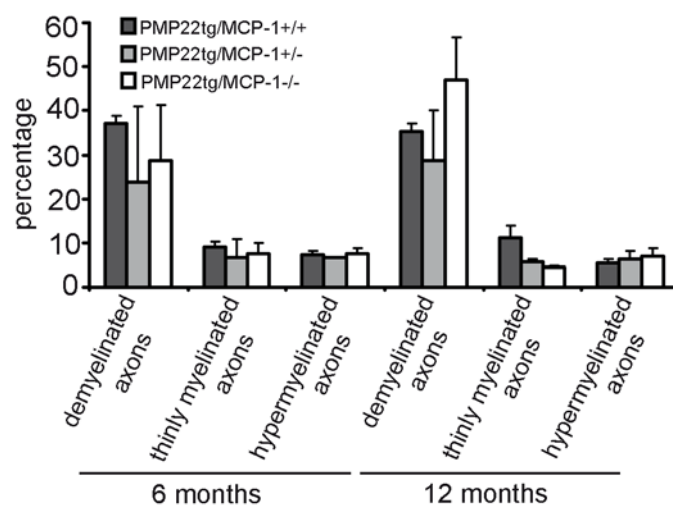


Figure 19: Morphometric analysis of lumbar ventral roots of PMP22/MCP-1 double mutant mice at the age of 6 and 12 months.

Lumbar ventral roots of PMP22tg/MCP-1+/+, PMP22tg/MCP-1+/- and PMP22tg/MCP-1-/- displayed a high number of demyelinated axons at 6 and 12 months of age ($n=3$, respectively). Here, all genotypes exhibited comparable numbers of pathological alterations.

distributed at low number in nervous tissue of 6 months old double mutants (approximately 0.3 – 0.4 foamy macrophages per 100 axons for each genotype) and were completely absent in ventral roots of 12-month-old PMP22tg/MCP-1-/- mice (data not shown).

5.3.2.4 Properties of axonal integrity are only improved in the complete absence of MCP-1 in PMP22tg mice

To detect abnormalities in motor performance, neurographic recordings of distal nerves and grip tests were performed to examine functional consequences of the demyelinating phenotype in PMP22tg mice with different MCP-1 genotypes.

Neurographic recordings were performed for 6 and 12-month-old PMP22wt/MCP-1+/+, PMP22tg/MCP-1+/+, PMP22tg/MCP-1+/- and PMP22tg/MCP-1-/- mice. Distal stimulation in PMP22wt mice at the age of 6 months led to normal compound muscle action potentials (CMAP) with normal values (**Table 2**). In contrast, PMP22tg/MCP-1+/+ mutants showed a reduction in CMAP, a prolonged duration of CMAP, an increased F wave latency and a slowed nerve conduction velocity (NCV) in comparison wild type mice. Whereas the NCV was similar in all PMP22tg/MCP-1 mutants, the CMAP, the duration of CMAP and the

5. Results

5.3 The functional contribution of macrophages to the pathogenesis of PMP22tg mice

	PMP22wt MCP-1+/+	PMP22tg MCP-1+/+	PMP22tg MCP-1+/-	PMP22tg MCP-1-/-
CMAP / proximal stimulation (mV)	13.8 ± 3.2	2.6 ± 0.4*	1.9 ± 0.5	6.5 ± 1.7*§
CMAP / distal stimulation (mV)	15.1 ± 3.3	3.0 ± 0.1*	4.5 ± 0.7	6.9 ± 2.1*§
duration of CMAP / proximal stimulation (ms)	1.7 ± 0	3.0 ± 0.5*	3.2 ± 0.1	2.4 ± 0.2*§
duration of CMAP / distal stimulation (ms)	1.7 ± 0.1	3.4 ± 0.7*	3.2 ± 0.2	2.3 ± 0.1*§
F wave latency (ms)	4.1 ± 0.1	6.3 ± 0.3*	7.9 ± 0.8	7.5 ± 0.6*
nerve conduction velocity (m/s)	43.9 ± 1.7	25.2 ± 3.5*	26.8 ± 4.1	29.1 ± 4.3*
<i>n</i> -numbers	3	4	2	4

Table 2: Neurographic recordings of 6-month-old PMP22/MCP-1 double mutant mice.

Note that PMP22/MCP-1-/- revealed an amelioration in the compound muscle action potential (CMAP) as well as in the duration of the CMAP compared to PMP22tg/MCP-1+/+ mice. * Significant differences compared to PMP22wt/MCP-1+/+ mice. § Significant differences compared to PMP22tg/MCP-1+/+ mice. $p < 0.05$, Student's *t*-test.

	PMP22wt MCP-1+/+	PMP22tg MCP-1+/+	PMP22tg MCP-1+/-	PMP22tg MCP-1-/-
CMAP / proximal stimulation (mV)	8.0 ± 2.8	2.8 ± 0.7	3.6 ± 2.3	3.7 ± 1.2
CMAP / distal stimulation (mV)	10.7 ± 4.0	3.7 ± 1.3	3.9 ± 1.9	4.5 ± 1.6
duration of CMAP / proximal stimulation (ms)	1.9 ± 0.3	3.5 ± 0.2	3.4 ± 0.5	3.3 ± 0.3
duration of CMAP / distal stimulation (ms)	1.9 ± 0.4	3.2 ± 0.3	2.9 ± 0.4	2.9 ± 0.3
F wave latency (ms)	4.8 ± 0.2	7.0 ± 0.4	8.5 ± 2.2	7.7 ± 0.8
nerve conduction velocity (m/s)	34.2 ± 4.2	26.0 ± 3.4	26.9 ± 1.4	27.7 ± 4.0
<i>n</i> -numbers	2	2	3	2

Table 3: Neurographic recordings of 12-month-old PMP22/MCP-1 double mutant mice.

Regardless of the few individuals in each group, the beneficial effect of the MCP-1 deficiency was not visible at older age compared to 6-month-old mice.

F wave latency were improved in 6-month-old PMP22tg/MCP-1-/- compared to PMP22tg/MCP-1+/+ mutants. Furthermore, we investigated 12-month-old double mutants regarding the nerve conduction properties (**Table 3**). Here, the beneficial effect of the absence of MCP-1 in PMP22tg mice were less obvious and did not reach statistical significance due to the fewer individuals in each group.

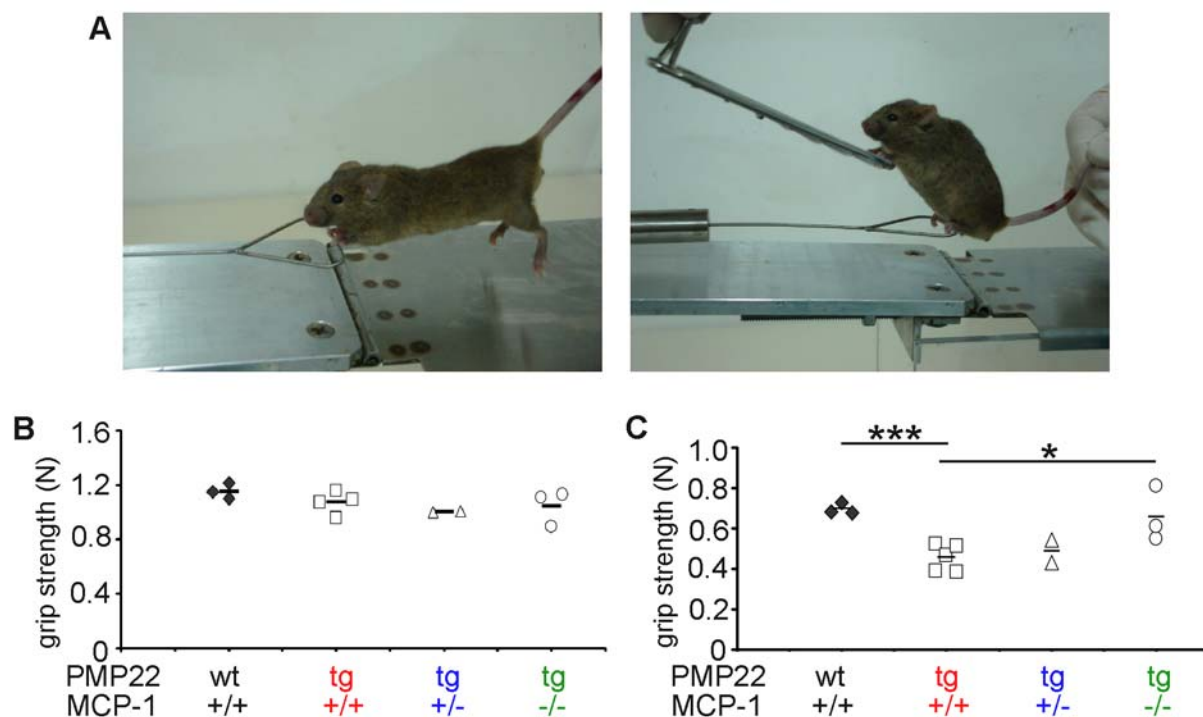


Figure 20: Grip strength tests of forelimbs and hindlimbs from PMP22/MCP-1 double mutant mice at the age of 5 to 6 months.

PMP22/MCP-1 double mutant mice were tested for the grip strength of the forelimbs as well as of the hindlimbs (A). Measurement of the grip strength of the forelimbs exhibited no striking differences between the genotypes (B). Interestingly, PMP22tg/MCP-1+/+ mice show an impaired motor strength of the hindlimbs compared to PMP22wt/MCP-1+/+, whereas PMP22tg/MCP-1-/- mice exhibited an improvement of grip strength comparable to PMP22wt/MCP-1+/+ mice (B). Each indicated value represents one tested individual; bars represented the mean values of the specific genotypes. * $p < 0.05$, ** $p < 0.01$, *** $p < 0.001$.

In addition, grip tests were performed with PMP22/MCP-1 double mutants to examine the grip strength of their forelimbs and their hindlimbs (**Figure 20A**). The grip strengths of the forelimbs were not significantly different between the genotypes (**Figure 20B**). However, the strengths of the hindlimbs showed obvious differences in the PMP22/MCP-1 double mutants (**Figure 20C**). The average grip strength of PMP22tg/MCP-1+/+ were significantly reduced compared to PMP22wt/MCP-1+/+ mice. Interestingly, PMP22tg/MCP-1-/- mutant mice exhibited a stronger grip strength of the hindlimbs compared to PMP22tg/MCP-1+/+ and PMP22tg/MCP-1+/- double mutants which was quite similar to PMP22wt/MCP-1+/+ mice.

To elucidate the finding of the functional recovery of PMP22tg in complete absence of MCP-1, we focused next to the examination of the nodes of Ranvier as an important structure for saltatory conduction. Here, we used markers for the nodal, paranodal as well as

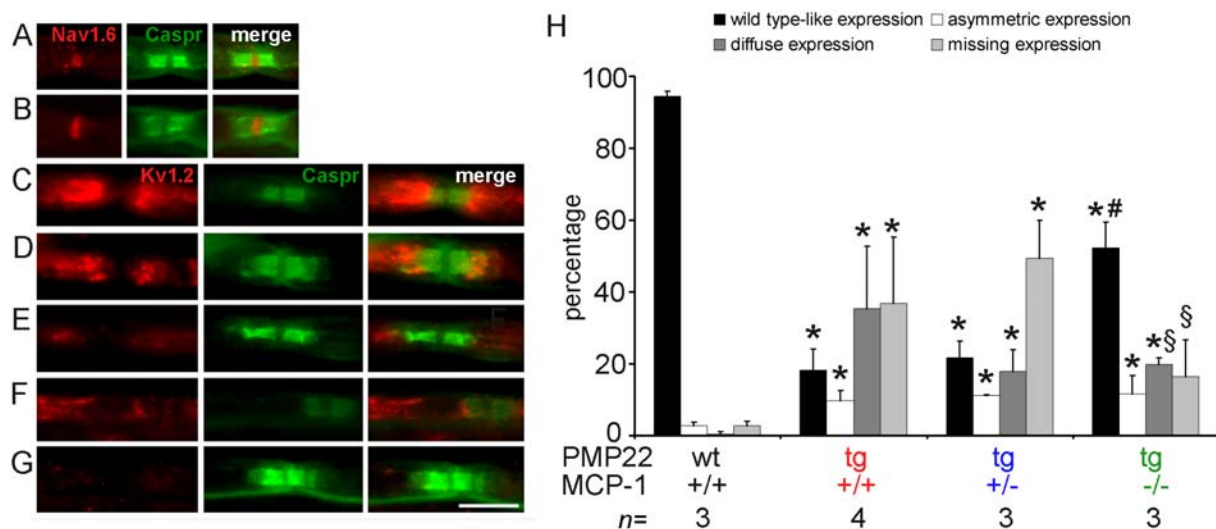


Figure 21: Analysis of ion channel distribution of teased fiber preparations of PMP22/MCP-1 double mutant mice at the age of 6 months.

Immunohistochemistry for anti-Nav1.6, anti-Kv1.2 (red, respectively) and anti-Caspr (green) of teased fiber preparations of 6-month-old PMP22/MCP-1 mutant mice (A – G, scale bar: 10 μ m). Nav1.6 expression is comparable in wild type (A) and PMP22tg/MCP-1+/+ mice (B). Kv1.2 is symmetrically distributed in juxtaparanodal regions of fibers from wild type mice (C). In addition to wild-type like expression (D), an asymmetric distribution (E) and a diffuse expression (F) is also found in teased fibers of PMP22tg/MCP-1+/+ mice. Further, some fibers do not show any Kv1.2 expression (G). Quantification of Kv1.2 distribution in teased fiber preparations of MCP-1 mutant mice revealed significant differences in the distribution of Kv1.2 (H). In complete absence of MCP-1, PMP22tg mice (PMP22tg/MCP-1-/-) showed a more wild type-like expression of Kv1.2 in peripheral nerves. * Significant differences compared with PMP22wt/MCP-1+/+ mice. # Significant differences compared with PMP22tg/MCP-1+/+ and PMP22tg/MCP-1+/- mice. § Significant differences compared with PMP22tg/MCP-1+/+ mice. $p < 0.05$.

juxtaparanodal regions to investigate the distribution of voltage-gated sodium channels of the Nav-type (Nav1.6), contactin-associated protein (Caspr) and potassium channels (Kv1.2). Teased fiber preparations of femoral quadriceps nerves from 6-month-old PMP22tg/MCP-1+/+ mice revealed a distribution of sodium channels comparable to wild type mice (**Figure 21A, B**). It is to note that PMP22tg/MCP-1+/- and PMP22tg/MCP-1-/- also showed normal sodium channel expression (data not shown). Interestingly, PMP22tg/MCP-1+/+ exhibited besides wild type-like potassium channels (Kv1.2) expression also juxtaparanodal potassium channels which were asymmetrically or diffusely distributed or even completely absent (**Figure 21C – G**). Quantification of these alterations revealed that both, PMP22tg/MCP-1+/+ and PMP22tg/MCP-1+/- mice exhibited only 20% of nodes of Ranvier with wild type-like distribution of potassium channels (**Figure 21H**). Interestingly, In PMP22tg/MCP-1-/- mutant mice, more than half of the juxtaparanodes showed wild type-like

potassium channel distribution (52%). No striking differences were found for the asymmetric distribution of potassium channels in PMP22tg/MCP-1+/+, PMP22tg/MCP-1+/- and PMP22tg/MCP-1-/- mice. However, the diffuse expression and the number of absent potassium channels were clearly diminished in PMP22tg in the absence of MCP-1 (PMP22tg/MCP-1-/- mice). The immunohistochemistry against Caspr serves as localization of the nodes of Ranvier and were comparable in all genotypes.

These results corroborate the role of MCP-1 as an important mediator of nerve pathology in PMP22tg mice. Here, MCP-1 deficiency can lead to reduced numbers of macrophages, to a distinct expression of cytokines, to an amelioration of the demyelinating disease in peripheral nerves and to an improved functional outcome in a mouse model of CMT1A.

5.3.3 The MEK1/2/ERK1/2 signaling cascade is involved in the expression of MCP-1 in peripheral nerves of PMP22tg mice

Due to the crucial role of MCP-1 in the pathogenesis of PMP22 mutant mice, the regulation of this chemokine was examined. Previous studies showed that different kinases can be responsible for the induction of MCP-1. Out of these, JNK, p38, I κ B α and STAT1 α have been described as regulators for MCP-1 expression (Goebeler et al., 2001; Boekhoudt et al., 2003; Sheng et al., 2005; Waetzig et al., 2005; Yoo et al., 2005). In addition, Fischer and colleagues examined the role of MCP-1 in a model for CMT1B – the P0+/- mice – and showed that MCP-1 is regulated at least in part by the MEK1/2/ERK1/2 signaling cascade (Fischer et al., 2008a). To identify the responsible signaling cascade in the PMP22 mutants, western blot analyses for different kinases with lysates of femoral quadriceps, cutaneous saphenous and sciatic nerves were performed.

5.3.3.1 The MEK1/2/ERK1/2 signaling cascade is activated in peripheral nerves of PMP22tg mice

To investigate whether signaling cascades like JNK, p38, I κ B α , STAT1 α as well as PKC α can have a regulatory function for MCP-1 in nerves of PMP22tg mice, specific antibodies against these kinases were used. Analyses of protein lysates from nerves of 2-month-old mice did not reveal an altered activation status of JNK, I κ B α and PKC α in

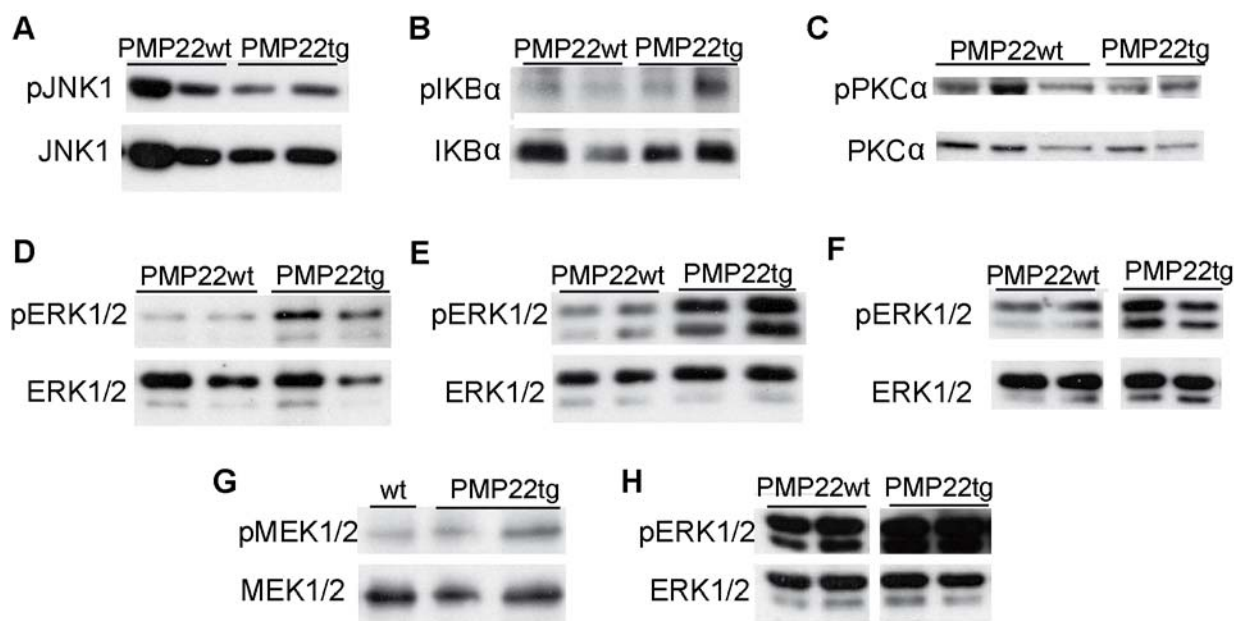


Figure 22: Western blot analyses of peripheral nerve lysates of PMP22 myelin mutant mice at different ages.

Signaling proteins like JNK1 (A, 46 kDa), IKBα (B, 37 kDa) and PKCα (C, 76 kDa) did not show a stronger phosphorylation in femoral quadriceps nerves of 2-month-old PMP22tg mice ($n=6$) compared to nerves from PMP22wt ($n=5$). Stronger phosphorylation of ERK1/2 (pERK1/2, 44/42 kDa) was visible in femoral quadriceps (D), cutaneous saphenous (E) and sciatic nerves (F) of 2-month-old PMP22tg mice ($n=6$) compared to PMP22wt ($n=5$). Furthermore, the upstream kinase of ERK1/2, namely MEK1/2 (45 kDa), was activated more strongly in femoral quadriceps nerve of PMP22tg mice at the age of 2 months (G). The increased pERK1/2 expression in nervous tissue of PMP22tg mice was obvious until the age of 6 months in comparison to nervous tissue of PMP22wt mice (H). Staining with antibodies to unphosphorylated proteins served as loading control.

PMP22tg compared to PMP22wt mice (**Figure 22A – C**). In addition, higher activation of STAT1α could not be observed in peripheral nerves of PMP22tg mice, whereas the phosphorylated form of p38 was hardly detectable in femoral quadriceps nerves of PMP22tg or wild types. In order to identify the underlying signaling cascade for the upregulation of MCP-1 in PMP22tg mice by western blot analyses, peripheral nerves of mice at the age of 1, 2 and 6 months were analyzed regarding the phosphorylation of ERK1/2 and its upstream signaling protein, MEK1/2. For the first time, a stronger phosphorylation of ERK1/2 was detectable in femoral quadriceps, cutaneous saphenous and sciatic nerves of PMP22tg mice at the age of 2 months (**Figure 22D – F**). Also, MEK1/2 was phosphorylated more strongly in femoral quadriceps nerves of 2-month-old PMP22tg mice compared to nerves from wild type littermates (**Figure 22G**). Higher activation of ERK1/2 was detected additionally in nerves from PMP22tg mice at the age of 6 months (**Figure 22H**).

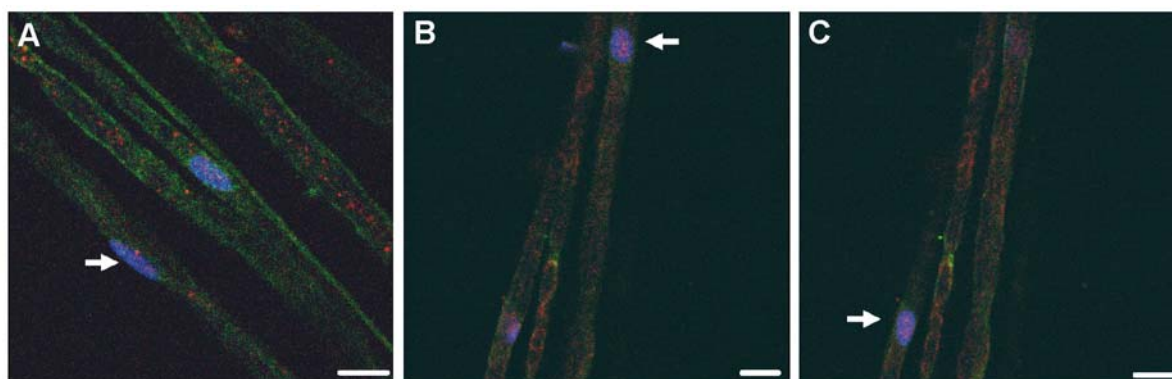


Figure 23: Localization of phosphorylated ERK1/2 in teased fiber preparations of 2-month-old PMP22 myelin mutant mice by immunohistochemistry.

Single fiber preparations of femoral quadriceps nerves from 2-month-old PMP22wt mice ($n=3$) revealed a weak non-nuclear phospho-ERK1/2 labeling (A, red), whereas in teased fiber preparations of PMP22tg mice the pERK1/2 signal was located within the nucleus (DAPI, blue; arrow) of Schwann cells (green; $n=3$; B, C). Scale bar: 10 μ m.

Next, we were interested in the cellular localization of the phosphorylated ERK1/2 proteins. Therefore, we performed immunohistochemistry on teased fiber preparations. Single fiber preparations of femoral quadriceps nerves of PMP22wt revealed a predominantly cytoplasmic phospho-ERK1/2-positive signal. In single fiber preparations of PMP22wt mice, only a weak phospho-ERK1/2 staining was located within nuclei of Schwann cells (**Figure 23A**). This was less intensive than the staining against phosphorylated ERK1/2 proteins in teased fibers of femoral quadriceps nerves from PMP22tg mice. Single fibers of femoral quadriceps nerves from PMP22tg mice exhibited a strong nuclear localization of phosphorylated ERK1/2 proteins and a less intensive cytoplasmic staining (**Figure 23B, C**).

In summary, these data revealed that the MEK1/2/ERK1/2 signaling cascade is active in mutant Schwann cells in peripheral nerves of PMP22tg mutants. Interestingly, the stronger phosphorylation of ERK1/2 was found in both, the femoral quadriceps as well as the saphenous nerve which suggested a direct link between the expression of MCP-1 and the activation of ERK1/2. Moreover, this signaling cascade is active at a time at which MCP-1 expression is observed. This identification of a putative relevant signaling cascade for the expression of MCP-1 suggested *in vivo* approaches to test the direct link between ERK1/2 activation and MCP-1 expression.

5.3.3.2 *In vivo* inhibition of the MEK1/2/ERK1/2 signaling cascade leads to a reduction of macrophage numbers in nerves of PMP22tg mice

To validate our hypothesis that the MEK1/2/ERK1/2 signaling cascade is responsible for the regulation of the MCP-1 expression, the MEK1/2-inhibitor CI-1040 (PD184352), which was kindly provided by Pfizer (New York, USA), was applied *in vivo*.

For this, daily injection of CI-1040 in DMSO (100mg/kg, i.p.) were performed for a period of three weeks and femoral and sciatic nerves were analyzed regarding the phosphorylation of ERK1/2, MCP-1 mRNA expression as well as the number of F4/80-positive macrophages.

Importantly, in femoral quadriceps nerves of CI-1040-treated mice, reduced phosphorylation of ERK1/2 proteins was detected in comparison to sham-treated mice (**Figure 24A**). As expected, sham-treated PMP22tg mice revealed a stronger ERK1/2-phosphorylation in femoral quadriceps nerves compared to nerves of sham-treated wild type littermates at the same age (**Figure 24A**).

Next, we performed qRT-PCR to examine the level of MCP-1 mRNA expression in nerves from CI-1040 and sham-treated mice. Interestingly, the expression of MCP-1 mRNA was approximately 50% reduced in nerves of CI-1040-treated PMP22tg mice compared to the DMSO controls (**Figure 24B**) showing a direct correlation between ERK1/2 activation and MCP-1 mRNA expression in peripheral nerves of PMP22tg mice as a model for CMT1A.

To further analyze the impact of MCP-1, F4/80-positive macrophages in peripheral nerves of CI-1040-treated mice were examined in comparison to sham-treated controls. Importantly, F4/80-positive macrophages were less frequent in femoral nerves of CI-1040-treated PMP22tg in comparison to nerves of sham-treated mice (**Figure 24C**).

It is to note that only one of 6 PMP22tg mice which received CI-1040 did not exhibit a reduction in ERK1/2 phosphorylation in femoral quadriceps nerves. Interestingly, this unaltered increase in ERK1/2-phosphorylation was correlated with a higher MCP-1 mRNA expression and an increased F4/80-positive macrophage number in femoral quadriceps nerves. Hence, this individual supports the observation that MCP-1 is regulated by the MEK1/2/ERK1/2 pathway and that it has a mediatory role regarding the macrophage number within peripheral nerves.

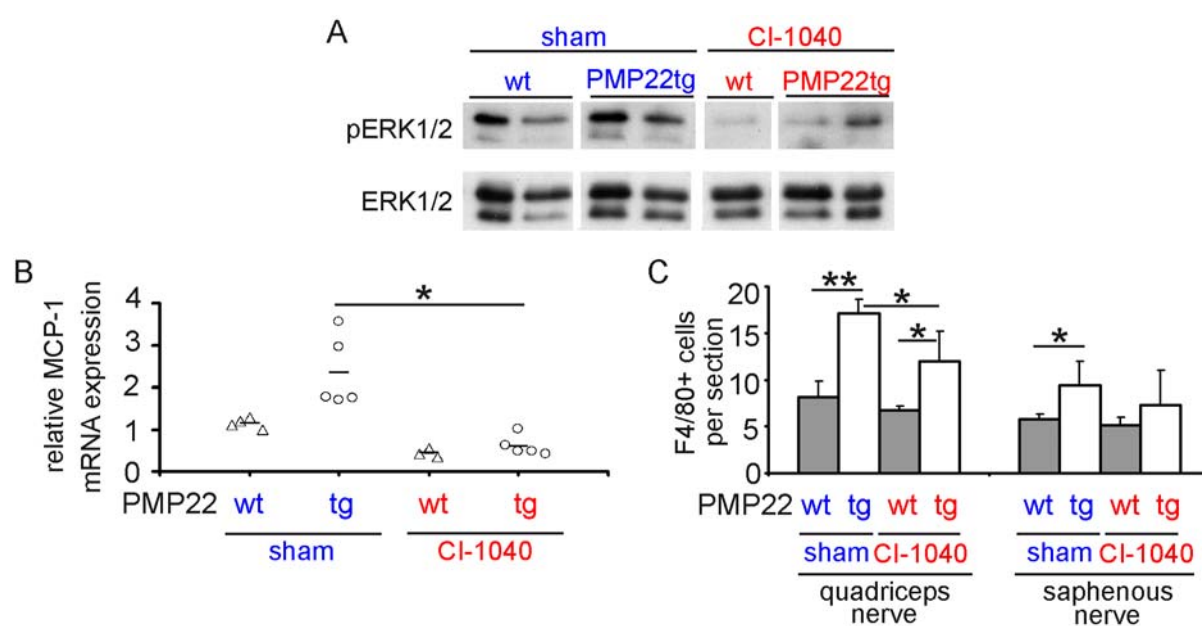


Figure 24: Daily CI-1040 treatment diminish ERK1/2-phosphorylation and MCP-1 mRNA expression in peripheral nerves of PMP22tg mice.

Western blot analyses of femoral quadriceps nerve lysates from CI-1040-treated (red) and sham-treated (blue) PMP22 mutant mice at the age of 2 months 3 weeks after treatment. Note the decreased phosphorylation of ERK1/2 (44/42 kDa) in the CI-1040-treated PMP22 mutants compared to sham-treated mice (A). qRT-PCR of MCP-1 mRNA revealed elevated amount of MCP-1 mRNA in femoral quadriceps nerves of sham-treated PMP22tg mice, whereas MCP-1 mRNA is reduced in nerves of CI-1040-treated PMP22tg mice (B). Furthermore, the number of F4/80 macrophages was reduced in peripheral nerves of PMP22tg mice which receive CI-1040 (C). * $p < 0.05$, ** $p < 0.01$.

In summary, it can be concluded that the *in vivo* inhibition of the MEK1/2/ERK1/2 signaling pathway by daily injection of CI-1040 caused a reduction in ERK1/2 phosphorylation, a decline in MCP-1 expression and as a consequence a decreased number of F4/80-positive macrophages in femoral nerves of PMP22tg mice.

Chapter 6

Discussion

It is known that macrophages play a crucial role in the pathogenesis of hereditary neuropathies (Martini et al., 2008 for review). In the present study we could show that the monocyte chemoattractant protein-1 (MCP-1) is upregulated in peripheral nerves of PMP22tg mice, which represent a model for CMT1A, compared to wild type littermates. Further, MCP-1 is Schwann-cell derived and it is regulated by the MEK1/2-ERK1/2 signaling pathway promoting the increase of macrophages in the myelin mutant nerves. This finding is strengthened by the pharmacological intervention with the MEK1/2-inhibitor CI-1040 as well as by the crossbreeding of PMP22tg mice with MCP-1 deficient mutants. Blocking the phosphorylation of ERK1/2 lowered the MCP-1 mRNA expression and also the macrophage number in CI-1040 treated PMP22tg mice compared to sham-treated controls. In PMP22/MCP-1 double mutant mice, the reduction or absence of MCP-1 caused a reduction of macrophage number and an amelioration of the pathological phenotype. Importantly, the complete absence of MCP-1 in PMP22tg mice increased the compound muscle action potential (CMAP) and the grip strength of the hindlimbs in comparison to PMP22tg/MCP-1+/+ mutants. In strong correlation to this functional recovery, we found a more regular localization of axonal potassium channels (Kv1.2) in nerves of PMP22tg/MCP-1-/- mice than in PMP22tg/MCP-1+/+ mutant nerves.

6.1 Pathological alterations in juvenile PMP22tg mice

Human neuropathies like Charcot-Marie-Tooth diseases are caused by genetical alterations and defects in Schwann cells which lead to de- or dysmyelination of peripheral nervous tissue. As a consequence, axonal transport, phosphorylation of neurofilaments and the organization of ion channels can be disturbed, which induces axonal loss (Niemann et al., 2006).

The Schwann cell-expressed protein PMP22 is constantly synthesized and rapidly degraded to 80% due to inefficient folding (Pareek et al., 1997). Under specific conditions, the inhibition

of the proteosomal transduction pathway provokes an accumulation of PMP22 in specific compartments of the cytoplasm, the aggresomes (Notterpek et al., 1999; Fortun et al., 2005). Furthermore, overexpression of PMP22 can also lead to an accumulation of this myelin protein which causes cellular stress and an altered Schwann cell metabolism (Hanemann et al., 2000; Muller, 2000). The hypothesis that mutations in genes expressed by myelinating Schwann cells cause CMT1 was first strengthened by a study of Aguayo and colleagues. In their study, transplantation of nerve segments from *Trembler* mice into sciatic nerves of wild type mice induced abnormal myelination of host axons which regenerated into the nerve segments of the *Trembler* mice (Aguayo et al., 1977). These data confirmed the hypothesis that the mechanisms of demyelination can be intrinsic to Schwann cells.

As a typical hallmark of CMT1A patients, hypermyelinated fibers within peripheral nerves have been described (Gabreels-Festen et al., 1992). Animal models like the PMP22-overexpressing rat or the adult heterozygous PMP22-overexpressing mouse (C61) exhibit these pathological alterations as well within peripheral nervous tissue (Sereda et al., 1996; Martini, 1997; Kobsar et al., 2005). In the present study we observed that the overexpression of PMP22 induced thicker myelin sheaths already at early age. Peripheral nerves of juvenile PMP22tg mice at postnatal day 7 (P7) exhibited thicker myelin sheaths reflected by lower g-ratio values. Interestingly, hypermyelinated fibers were more frequent in femoral quadriceps and sciatic nerves than in cutaneous saphenous nerves of PMP22tg mice. It is conceivable that the less prominent hypermyelination in cutaneous saphenous nerves was due to development stages. The myelination of axons depends on the axonal diameter and larger caliber axons are myelinated first (Voyvodic, 1989). Thus, one could assume that the cutaneous saphenous nerves have potentially a “delay” in myelination due to its composition of smaller caliber axons. As another possibility for the development of hypermyelinated fibers in femoral quadriceps and sciatic nerves, the increased expression of the α -chemokine CXCL14 in such nerves of PMP22tg mice could be proposed. CXCL14 belongs to the CXC chemokines (Hromas et al., 1999) and is also called breast and kidney-expressed chemokine (BRAK; Hromas et al., 1999; Frederick et al., 2000) or B-cell- and monocyte-activating chemokine (BMAC; Sleeman et al., 2000). Neither the exact function, nor its receptor have been identified so far. Anyhow, it is known that CXCL14 is expressed in normal non-lymphoid tissues, brain and muscles (Sleeman et al., 2000) as well as in dermal fibroblasts (Kurth et al., 2001). So far, CXCL14 has been described to have chemoattractant capability for dendritic cells *in vitro* (Shurin et al., 2005) and to be upregulated in infiltrating inflammatory cells (Frederick et al., 2000). In PMP22tg mice at the age P7, the expression of CXCL14

mRNA is increased in nerve lysates of femoral quadriceps and sciatic nerves relative to wild type mice, but not in cutaneous saphenous nerves (Barbaria et al., 2008). Moreover, CXCL14 mediates Schwann cell differentiation and myelin gene expression *in vitro* whereby a coherence of the expression of this chemokine and the hypermyelination in peripheral nerves of PMP22tg mice could be possible by triggering differentiation of Schwann cells *in vivo* (Barbaria et al., 2008).

Aside from the thicker myelin sheaths as pathological alterations, peripheral nerves of PMP22tg mice at P7 exhibited neither signs for demyelination, nor alterations regarding the development compared to wild type littermates. Both, the axonal caliber and the axonal sorting which is indicated by the 1:1-ratio of axons with Schwann cells revealed no developmental delay or disturbance in peripheral nerves of PMP22tg mice similar to nerves from wild type mice. This finding is in line with the observation of normal axon-Schwann cell ratio in young CMT1A patients (Hanemann et al., 1997). Further we presume that the presence of axons devoid of myelin at this age is rather due to the ongoing sorting and myelination process than to a hallmark of demyelination. First signs of demyelination are observed in peripheral nerves of PMP22tg mice at the age of 2 months (Kobsar et al., 2005).

Different studies strengthened the hypothesis that demyelinating neuropathies start with defects in Schwann cells. As mentioned above, the consequences are altered phosphorylation of neurofilaments, disturbed axonal transport, axonal loss and infiltration of immune cells. Due to disturbances in the axonal transport, distal nerve segments are more affected than proximal nerves (Martini and Toyka, 2004; Niemann et al., 2006). The expression of PMP22 transcripts is not well understood but it is known that PMP22 can be regulated on both transcriptional and posttranscriptional levels (Suter et al., 1994; Bosse et al., 1999). Once PMP22 is incorporated into the myelin membranes, it forms heterophilic bindings with P0 to stabilize the myelin compaction. Disorganization of these interactions – e.g. by altered PMP22 expression – causes destabilization of the myelin compaction and, hence, demyelination (Muller, 2000).

6.2 Lymphocytes do not have a crucial role in the neuropathology of PMP22tg mice

Besides Schwann cells as the primarily affected cell type in models for inherited neuropathies, immune cells, i.e. macrophages and T-lymphocytes, have an important impact on the pathogenesis (Ip et al., 2006). Macrophages are increased within peripheral nerves of P0+/- mice before massive demyelination becomes obvious. In contrast, CD8-positive T-lymphocytes are found in higher number at later stages with ongoing demyelination (Schmid et al., 2000; Carenini et al., 2001; Kobsar et al., 2002). Crossbreeding of the P0+/- myelin mutants with mice deficient of mature T- and B-lymphocytes clarified the functional contribution of these cells to pathological mechanisms. The absence of T-lymphocytes in peripheral nerves of P0+/- leads to an amelioration of the pathological phenotype (Schmid et al., 2000). This indicates that T-lymphocytes have a detrimental role in this mouse model for CMT1B.

The present study should clarify the functional contribution of immune cells, i.e. macrophages and T-lymphocytes, on the pathogenesis in peripheral nerves of PMP22-overexpressing mice. The crossbreeding of PMP22 myelin mutants with RAG-1-deficient mice reveals findings contrary to the observations in peripheral nerves of P0+/-/RAG-1-/- mice. For a first read-out, we quantified the number of F4/80-positive macrophages within femoral nerves of PMP22/RAG-1 double mutants. Here, the early increase of macrophage number relative to wild types in femoral nerves of 2-month-old PMP22tg/RAG-1+/? mice was also observed in nerves of PMP22tg/RAG-1-/- mice. In femoral nerves of 2, 6 and 12 months old double mutants, the total number of macrophages was unexpectedly quite similar in peripheral nerves of both genotypes. The elevation of the macrophage number in nerves of PMP22tg mice relative to nerves of wild types at the age of 2 months with no further intense increase at higher age reflects the early pathological mechanisms in PMP22tg mice. Additionally, the number of foamy macrophages containing myelin debris was not altered in nerves of PMP22tg/RAG-1-/- mice compared to nerves of PMP22tg/RAG-1+/? double mutants. Furthermore, quantification of pathological profiles by electron microscopy revealed a similar severity of nerve pathology in both the PMP22tg/RAG-1-/- and the PMP22tg/RAG-1+/? mice at the age of 6 months. Femoral nerves of 12-month-old PMP22tg/RAG-1-/- showed a non-significant tendency for an increased number of completely demyelinated and thinly myelinated axons in contrast to PMP22tg/RAG-1+/?

mice. This non-significant aggravation of disease in nerves of PMP22tg/RAG-1^{-/-} was mainly observed for axons with larger caliber. Interestingly, the number of hypermyelinated fibers as a typical hallmark for PMP22tg as well as the number of supernumerary Schwann cells is not influenced by the absence of T- and B-lymphocytes.

These data indicate that the primary nerve pathology in PMP22tg mice is independent from T-lymphocytes. As already described, other myelin mutants – the P0^{+/-} mice – show an amelioration of the pathological phenotype when crossbred with RAG-1^{-/-} mice (Schmid et al., 2000). Similar results are also observed in peripheral nerves of Cx32/RAG-1^{-/-} double mutants (Kobsar et al., 2003). Thus, T-lymphocytes play a detrimental role in these two different models for CMT1B and CMT1X, respectively. In contrast, the dysmyelinating P0^{-/-} mice as a model for a severe form of DSS, exhibit a severe aggravation of nerve pathology after crossbreeding with RAG-1^{-/-} mice (Berghoff et al., 2005). In peripheral nerves of P0^{-/-}/RAG-1^{-/-} mice, an increased axonal loss is observed and the number of macrophages is still elevated in contrast to a decline of the macrophage number within age in P0^{-/-}/RAG-1^{+/?} mice. Thus, for this model it has been discussed that the aggravation of the pathological phenotype could either be provoked by a more aggressive population of macrophages or by the loss of lymphocytes which have a neuroprotective function. In the present study, the absence of T-lymphocytes causes only a non-significant tendency for an increase in pathological alterations in PMP22tg mice with a nonspecific impact.

As a second experimental setup for examination of the functional role of T-lymphocytes, PMP22tg mice were sub-lethally irradiated and transplanted with either PD-1-deficient or wild type bone marrow. PD-1 is a co-inhibitory molecule which is expressed on the surface of lymphocytes and plays an important role for tissue homeostasis (Liang et al., 2003; Okazaki and Honjo, 2007; Sharpe et al., 2007). PD-1^{-/-} mice exhibit an elevated number of B-lymphocytes and develop different autoimmune disorders which depend on the genetic background (Nishimura et al., 1998). The transfer of PD-1^{-/-} bone marrow into P0^{+/-}/RAG-1^{-/-} mice led to an elevated number of CD8-positive T-lymphocytes and an aggravation of nerve pathology compared to P0^{+/-}/RAG-1^{-/-} mice which received wild type bone marrow (Kroner et al., 2008). The authors presume that systemic clonal expansions of T-lymphocytes and increased secretion of pro-inflammatory cytokines like interferon- γ (IFN γ) contribute to this phenotype. Furthermore, P0^{+/-}/RAG-1^{-/-} BMC PD-1^{-/-} exhibited an impaired motor performance regarding broader distance between feet indicating the inability to carry their weight properly.

In contrast to P0+/-/RAG-1-/- BMC PD-1-/-, the bone marrow chimerization of 2-month-old PMP22tg mice caused neither an increase of immune cells (i.e. macrophages and T-lymphocytes), nor an aggravation of the pathological phenotype, nor disturbed motor performance. To investigate whether PD-1 and its ligand B7H1 (PD-1-L) were expressed in normal tissue (tissue from PMP22wt and PMP22tg mice) we performed flow cytometry with unstimulated splenocytes and nervous tissue. For this, LPS-stimulated splenocytes and peritoneal macrophages were used as positive control. Thus, PD-1 is expressed in nervous tissue of PMP22tg and their wild type littermates. In addition, expression of B7H1 is found in unstimulated splenocytes of the mutants as well as, to a lower amount, in nervous tissue. Although PD-1 is expressed in tissue of PMP22 mutant mice, its absence does not cause an alteration of the pathological mechanism contrary to the P0+/-/RAG-1-/- BMC PD-1-/. This further strengthens the view that the primary development of pathological mechanisms in nervous tissue of PMP22tg mice is not influenced by T-lymphocytes.

6.3 Macrophages have a modulating capacity in the neuropathology of PMP22tg mice

During the last years, different studies focused on the coherence of genetic defects in Schwann cells and the mechanisms leading to myelin degeneration (Martini et al., 2008 for review). In 1850, Waller described interactions between Schwann cells and macrophages which led to rapid removal of myelin debris (Waller, 1850). Schwann cells are able to express different cyto- and chemokines during Wallerian degeneration, which induce either the attraction of immune cells or the phagocytosis of degenerated myelin. The macrophage galactose-specific lectin-2 (MAC-2) can be expressed by Schwann cells and causes the phagocytosis of myelin debris by these cells (Saada et al., 1996). This mechanism is activated when only a reduced number of macrophages or no macrophages are present (Beuche and Friede, 1985; Bruck et al., 1996). MCP-1 is a chemokine expressed by Schwann cells already 24h after nerve injury (Toews et al., 1998; Taskinen and Roytta, 2000; Tofaris et al., 2002; Kleinschnitz et al., 2004; Perrin et al., 2005; Cheepudomwit et al., 2008). The increase of MCP-1 occurs before macrophages immigrate into peripheral nerves which indicates that MCP-1 can be directly responsible for the degeneration of myelin by hydrolysis (De et al., 2003). It has been shown that phospholipases, especially phospholipase A₂

(PLA₂), can induce the breakdown of the myelin as a lipid-rich membrane and MCP-1 is able to induce the expression of PLA₂ (Murakami et al., 1997; Lopez-Vales et al., 2008).

In this study, we were interested in the functional contribution of macrophages in the demyelinating phenotype of PMP22tg mice. A previous study showed that MCP-1 is increased in the sciatic nerve of 2-month-old PMP22tg mutants relative to nerves of wild type mice (Kobsar et al., 2005). In the present study we found also a higher expression of MCP-1 mRNA in the femoral quadriceps nerves as well as in the cutaneous saphenous nerves of PMP22tg mice. This elevated MCP-1 mRNA expression is in line with an increased number of macrophages and pathological alterations in both branches of the femoral nerve from PMP22tg mice compared to wild types.

Crossbreeding of the PMP22 myelin mutants with mice deficient of MCP-1 clarified the role of this chemokine. At the age of 2 months, femoral quadriceps and saphenous nerves of PMP22tg mice – MCP-1 deficient or not – exhibited an elevated number of macrophages compared to wild type littermates. This elevation of macrophages persisted in nerves of older PMP22tg/MCP-1^{+/+} mice, whereas the macrophage number declined in femoral nerves of PMP22tg/MCP-1^{-/-} mice with increasing age. This suggests that MCP-1 does not exclusively regulate macrophage attraction and immigration into peripheral nerves. One could assume that in the absence of MCP-1 the increased macrophage number could also emerge due to other cytokines. Using qRT-PCR we found that IL-6 and LIF mRNA were upregulated in nerves of PMP22tg/MCP-1^{-/-} whereas M-CSF mRNA was increased in nerves of both PMP22tg/MCP-1^{+/+} and PMP22tg/MCP-1^{-/-} mice. Therefore, the elevated macrophage number in femoral nerves of 2-month-old PMP22tg/MCP-1^{-/-} mice could arise due to the increased expression of M-CSF, IL-6 and LIF. M-CSF is important for survival, proliferation and differentiation of mononuclear phagocytes (Stanley et al., 1997). Thus, it is possible that intrinsic macrophages within nerves of PMP22tg/MCP-1^{-/-} proliferate due to the increase of M-CSF mRNA, thereby increasing the total number despite the absence of MCP-1. Interestingly, the M-CSF mRNA expression in nerves of PMP22tg/MCP-1^{+/+} mice was similar to the expression in wild type nerves, suggesting that the reduced level of MCP-1 is still sufficient to attract macrophages into peripheral nerves. Another explanation for the macrophage-increase in peripheral nerves of PMP22tg/MCP-1^{-/-} mice is the elevated expression of IL-6 and LIF mRNA. Tofaris and colleagues showed that Schwann cells are able to secrete MCP-1 and LIF in an autocrine manner which are 60 to 70% and 30 to 40% chemoattractant for macrophages, respectively (Tofaris et al., 2002). IL-6 per se does not

have chemoattractant capacity, but it is able to induce the expression of LIF mRNA in cultured Schwann cells (Tofaris et al., 2002). Hence, the high level of IL-6 mRNA in peripheral nerves of PMP22tg/MCP-1^{-/-} compared to all other genotypes could induce the elevation of LIF mRNA and consequently the immigration of blood-derived macrophages into peripheral nerves. With increasing age, it is indicated by the decreased immune cell number that the attraction of blood-derived macrophages in PMP22tg/MCP-1^{-/-} mice is diminished or the proliferation of intrinsic cells is reduced. Another reason could also be ongoing apoptosis within peripheral nerves due to limited lifespan of macrophages.

Previously, different studies focused on the role of macrophages and the differentiation of resident and infiltrating cells in peripheral nerves. It is known that resident macrophages are located throughout the endoneurium in healthy PNS (Griffin et al., 1993; Mueller et al., 2003). Due to a permanent turnover, up to 60% of resident macrophages are renewed by hematogenous macrophages within three months (Vass et al., 1993; Maurer et al., 2003). The ability of macrophages to infiltrate peripheral nerves has been studied under various conditions by mice expressing green fluorescent protein (GFP). In 1997, a transgenic mouse line was generated that contains the GFP under the control of a chicken β -actin promoter (Okabe et al., 1997). Hereby, the GFP-positive bone marrow, which is under normal conditions responsible for the green bioluminescence of the jellyfish *Aequorea victoria*, is located in most tissues of the transgenic mice. Therefore, transplantation of GFP-positive bone marrow allows the distinction between resident (GFP-negative) and infiltrating hematogenous (GFP-positive) cells. Transplantation of GFP into irradiated P0^{+/-} mutant mice revealed that approximately 60% of endoneurial macrophages were GFP-positive indicating the immigration of these cells (Maurer et al., 2003). In 2008, Fischer and colleagues transplanted GFP-chimeric bone marrow into P0/MCP-1 double mutant mice and examined the role of MCP-1 in macrophage immigration (Fischer et al., 2008b). Hereby, they demonstrated that MCP-1 is able to attract macrophages into normal peripheral nerves. In absence of MCP-1, the number of infiltrating GFP-positive macrophages was reduced. Once immigrated into peripheral nerves, hematogenous monocytes are – in addition to resident macrophages – able to damage myelin structures (Maurer et al., 2003).

To confirm this hypothesis also for the PMP22tg mice, continuative studies would be required. For this, it would be worthwhile to examine the protein expression of relevant cytokines like M-CSF, MCP-1 or TNF α in addition to the mRNA expression in this study to

get more insight into the functional relevance of these factors. Further it would be interesting to focus on examinations of GFP-bone marrow chimeric PMP22 mutant mice.

Analyses of the morphological phenotype of peripheral nervous tissue from PMP22/MCP-1 double mutant mice reveal an amelioration of the demyelinating phenotype by reduction or complete absence of MCP-1. In nerves of PMP22tg/MCP-1+/- as well as of PMP22tg/MCP-1-/- mice, the numbers of demyelinated and thinly myelinated fibers were clearly reduced which was also reflected by the measurement of the g-ratio. Here, the reduction of MCP-1 by 50% leads to the mildest demyelinating phenotype within peripheral nerves. The strongest pathological phenotype was observed in nerves of PMP22tg/MCP-1+/+ mice which also contain the highest number of total macrophages and of foamy macrophages indicative for phagocytosing activity. In contrast, the number of foamy macrophages in nerves of PMP22tg/MCP-1+/- and PMP22tg/MCP-1-/- was lower than in PMP22tg mice with complete MCP-1 expression. However, the number of supernumerary Schwann cells, indicative of proliferation of these cells, was not altered in PMP22/MCP-1 double mutant mice. Interestingly, the percentage of hypermyelinated fibers as typical sign of pathology in PMP22tg mice was not influenced by the MCP-1 genotype. This was also observed in peripheral nerves of PMP22/RAG-1. It is of note that a similar observation was also made in Cx32-deficient mice as a model for the X-linked form of CMT1. Here, the number of typical periaxonal swellings was independent of immune cells (Kobsar et al., 2003).

At the age of 12 months, the number of pathological alterations increased in nerves of PMP22tg/MCP-1+/- and PMP22tg/MCP-1-/- mice, but the tendency observed in 6-month-old mice was still present. This indicates that the reduction and complete absence of MCP-1 can evoke a transient ameliorated phenotype in PMP22tg mice which is less striking in nerves of older double mutants. Lumbar ventral roots of PMP22/MCP-1 double mutants exhibit a stronger pathology and a higher percentage of demyelinated fibers in PMP22tg mice regardless of the MCP-1 genotype.

In addition to the number of macrophages, the number of CD4- and CD8-positive T-lymphocytes was quantified in peripheral nerves of PMP22/MCP-1 mice. Due to the finding that PMP22tg mice in absence of mature T- and B-lymphocytes (PMP22tg/RAG-1-/-) do not reveal a significant number of pathological alterations, it is likely that T-lymphocytes play an ancillary role in the pathology of these myelin mutant mice. In nerves of PMP22tg/MCP-1+/-

mice, it was observed that the number of CD4-positive T-lymphocytes was non-significantly increased in comparison to PMP22tg/MCP-1+/+ and PMP22tg/MCP-1-/- mice. This was also observed in nerves of P0+/-/MCP-1+/- mutants (Fischer, 2008c). Despite the low number of these cells, the most frequent CD8-positive T-lymphocytes were found in femoral quadriceps nerves of PMP22tg/MCP-1+/+ mice whereas the PMP22tg/MCP-1+/- and PMP22tg/MCP-1-/- mutants showed a cell number comparable to wild types. Therefore, we concluded that T-lymphocytes have a late beneficial role in the pathological mechanism of PMP22-overexpressing mice demonstrated by the PMP22tg/RAG-1-/- double mutants. Macrophages seem to be independent from T-lymphocytes during the neuropathy of PMP22tg mice.

In 2005, Kobsar and colleagues also examined PMP22tg mutant mice regarding the number of CD8-positive T-lymphocytes and found an almost 7-fold up-regulation in femoral quadriceps nerves of 14-month-old myelin mutant mice (Kobsar et al., 2005). In this study, only a 3-fold increase of CD8-positive T-lymphocytes could be observed in femoral quadriceps nerves from 12-month-old PMP22tg/MCP-1+/+ mice. This discrepancy could possibly be explained by the hygiene standards of the different animal facilities.

Due to the amelioration of the morphology in PMP22tg mice with reduced or completely absent MCP-1, we were also interested in the functional recovery of the double mutants. Surprisingly, neurographic recordings revealed an ameliorated phenotype regarding the CMAP in PMP22tg/MCP-1-/- in contrast to PMP22tg/MCP-1+/+ mice at the age of 6 months. This functional recovery was also confirmed by grip strength test. Importantly, the PMP22tg/MCP-1+/+ mice exhibited an impaired grip strength of the hindlimbs, whereas the grip strength of the PMP22tg/MCP-1-/- was comparable to wild type mice. Due to the strong correlation between the increased CMAP amplitude and the grip strength in PMP22tg/MCP-1-/-, we examined the nodes of Ranvier as the most important structure for saltatory conduction by immunohistochemistry. The nodes of Ranvier per se, as well as the internodal length flanked by normally localized Caspr-protein, seemed to be not altered in PMP22tg mice. Interestingly, the distribution of potassium channels (Kv1.2) was irregular in teased fiber preparations of PMP22tg/MCP-1+/+ and PMP22tg/MCP-1+/- mutants compared to wild types whereas sodium channels were unaltered in nerves of all genotypes. Moreover, teased fiber preparations of PMP22tg/MCP-1-/- mutants exhibited a potassium channel distribution which was more wild type-like than in PMP22tg/MCP-1+/+ and PMP22tg/MCP-1+/- . Thus, we propose that there is a direct link between the refractory period or rather the release of action potentials and the distribution of potassium channels. If

one would assume that nerve fibers of PMP22tg mice suffer from a prolonged refractory period due to the altered potassium channel distribution, it would be possible that these mice are not able to generate action potentials as fast as wild type mice. This impairment would then be reflected in the decreased grip strength of PMP22tg mice. Furthermore it is possible that there is coherence between macrophage activation and the altered axonal integrity in the myelin mutants. So, one could propose that macrophage activation by MCP-1 might be deleterious for axon integrity. A detrimental factor for the axonal integrity could be TNF α , which is involved in axonal damage in inflammatory neuropathies (Stubgen, 2008 for review). In nerves of PMP22tg/MCP-1+/+ mice, TNF α is highly expressed suggesting a more activated and a more aggressive population of macrophages. Interestingly, TNF α mRNA was less reduced in PMP22tg/MCP-1-/- mice which show a more regular potassium channel distribution. Further, one would propose that anti-inflammatory cytokines like TGF β , which are elevated in nerves of PMP22tg/MCP-1+/- and PMP22tg/MCP-1-/- mice, induce an inactivation of macrophages and therefore a less aggressive phenotype. Due to the fact that CCR2, the main receptor for MCP-1, is expressed on neurons, it is also possible that MCP-1 has a direct detrimental effect on neuronal profiles (Jung et al., 2008; Melik-Parsadaniantz and Rostene, 2008). Whether there is such a direct deleterious effect of MCP-1 still has to be determined by a current analysis of embryonic motoneurons *in vitro*.

Therefore, the expression of MCP-1 is determining the pathological severity in PMP22tg mice. To find a putative treatment strategy, we investigated the cellular regulation of MCP-1 expression. Western blot analyses revealed that the MEK1/2/ERK1/2-cascade is activated in those nerves of PMP22tg mice that show an increased MCP-1 mRNA expression, i.e. sciatic, femoral quadriceps and saphenous nerves. This activation is timely correlated with the increase of macrophages and the demyelinating alterations in peripheral nerves of 2-month-old PMP22tg mice. In addition, the increased ERK1/2 phosphorylation was found in nuclei of Schwann cells of PMP22tg mice, co-localizing with MCP-1 expression which was also found Schwann cell- and myelin-associated. This confirmed the hypothesis that the initial immune regulation is Schwann cell-mediated. To further strengthen the hypothesis that the MEK1/2/ERK1/2-signaling cascade is the regulator for the MCP-1 expression, we used CI-1040 as a MEK1/2-inhibitor *in vivo*. After a systemic treatment with the MEK1/2-inhibitor CI-1040, we found a reduced ERK1/2-phosphorylation and a lower expression of MCP-1 mRNA, which finally led to a reduced number of macrophages in peripheral nerves of inhibitor-treated PMP22tg mice compared to sham-treated PMP22tg mutants. One individual which did not show a reduced ERK1/2 phosphorylation did also not exhibit a lower

expression of MCP-1 mRNA or a reduced macrophage number, accenting the relevance of the MEK1/2/ERK1/2 signaling pathway for the increase of MCP-1 mRNA. Importantly, decreased numbers of macrophages in mice with inhibited MCP-1 expression might show a direct correlation of MCP-1 expression and macrophage presence in peripheral nerves.

However, it is to note that the MCP-1 expression did not correlate with the increased phosphorylation of ERK1/2 at every time point. MCP-1 expression in sciatic nerves of PMP22tg mice seemed already at postnatal day 7 to be non-significantly upregulated compared to wild type littermates. An increased phosphorylation of ERK1/2-proteins could not be detected in such nerves relative to wild type littermates. However, a regulation of MCP-1 by this signaling cascade already at this juvenile age could not be excluded due to the important role of ERK1/2 in cell differentiation and development. Thus, due to ongoing development, ERK1/2 could also be highly active in nerves of both wild types and PMP22tg mice. The spatial correlation of the elevated MCP-1 expression and the increased ERK1/2-phosphorylation is in strong coherence with the upregulation of macrophages and demyelinating profiles in nerves of PMP22tg mice compared to wild types. It is known that the regulation of ERK1/2 itself is affected by the duration of its activation and a chronic activation of ERK1/2 is found in neurodegenerative diseases (Colucci-D'Amato et al., 2003).

6.4 PMP22tg and P0+/- mice: comparison of two models for inherited neuropathies

In the last years, different mouse models for inherited neuropathies were examined in our laboratory, e.g. PMP22-overexpressing (PMP22tg) and P0-heterozygous (P0+/-) mice as models for CMT1A and CMT1B, respectively. Interestingly, some findings in these two myelin mutant mice showed distinctive similarities.

Not only peripheral nerves of PMP22tg mice exhibited an elevated expression of MCP-1 but also nerves of P0+/- mice (Fischer et al., 2008a). In both myelin mutants, the upregulation of this chemokine was found before macrophage numbers were increased or any signs of demyelination were obvious. In addition, the macrophage numbers were clearly reduced in myelin mutant mice with reduced or complete absent MCP-1 at 6 months of age. Both PMP22tg mice and P0+/- mice, showed macrophages in close contact with visually normal

myelin suggesting phagocytosing activity (Carenini et al., 2001; Kobsar et al., 2005). Interestingly, the number of foamy macrophages was in direct correlation with the demyelinating phenotype in nerves of PMP22tg mice at the age of 6 months. The total number of macrophages is indirectly correlated to the functional performance, i.e. PMP22tg/MCP-1^{-/-} with the lowest number of macrophages showed an increased CMAP, enhanced grip strength and a more wild type-like potassium channel distribution in teased fiber preparations. These data suggest that macrophages are the source of different cytokines and other factors (i.e. nitric oxide) which influence the pathological outcome. Alternatively, different macrophage populations within the nerves of different genotypes are conceivable. Indeed, former reports focused on different macrophage subsets in mice. Sunderkötter and colleagues described three subpopulations of mouse monocytes which are mainly distinguishable by different expression of the surface markers Ly6C (ER-MP20; Sunderkötter et al., 2004). Immature Ly-6C^{high} monocytes resembling bone marrow monocytes are characterized by a higher expression of L-selectin (CD62L) compared to the Ly-6C^{low} subset (Juttila et al., 1988). This inflammatory Ly-6C^{high} monocyte subpopulation was recruited into acute inflammation in contrast to the Ly-6C^{low} monocytes. A further study described six monocyte-related populations, three each in murine peripheral blood and bone marrow (Schlueter and Glasgow, 2006). All subpopulations have in common the expression of F4/80 which is indicative for the myeloid nature of these cells.

In the present study, we showed that the MEK1/2/ERK1/2 pathway promotes the increase of MCP-1 mRNA. Inhibition of MCP-1 expression might directly decrease the macrophage number in peripheral nerves of PMP22tg. Similar results were found previously in the P0+/- mice (Fischer et al., 2008b; Fischer et al., 2008a). In both myelin mutants, blocking of the MEK1/2/ERK1/2 signaling cascade resulted in a decreased expression of MCP-1 and in a reduced macrophage number. The reduction of this chemokine by crossbreeding the myelin mutants with MCP-1 mutant mice caused a clear amelioration of the pathological phenotype in nerves of P0+/-/MCP-1+/- (Fischer et al., 2008b) as well as in PMP22tg/MCP-1+/- mice. A third myelin mutant, the Cx32-deficient mice, showed similar results regarding the morphology, the phosphorylation of ERK1/2 and the effect of MCP-1 expression (Groh et al., unpublished). This suggests a widespread pathomechanism in three different mouse models of inherited neuropathies.

The reduction of MCP-1 by 50% in both myelin mutant mice (i.e. PMP22tg and P0+/- mice) resulted in a clear amelioration of the demyelinating phenotype. In the complete absence of

MCP-1, the P0+/- mutants revealed – in contrast to PMP22tg/MCP-1-/- mice – an aggravation in the demyelinating phenotype (Fischer et al., 2008b). Due to the fact that different pro- and anti-inflammatory cytokines are upregulated in P0+/-/MCP-1-/- and PMP22tg/MCP-1-/-, it is possible that the genetic loss of MCP-1 resulted in compensatory mechanisms in the mutant Schwann cells which causes a different cytokine expression. As a consequence, macrophages are activated and myelin is degenerated by secondary immune-dependent mechanisms.

A further striking difference between PMP22tg mice and P0+/- myelin mutants is the presence of pathological alterations in cutaneous saphenous nerve of PMP22tg mice. Former studies showed that sensory nerves and dorsal roots of P0+/- mice as well as of other myelin mutants are protected from degeneration (Martini et al., 1995; Shy et al., 1997). The reasons for this are not well known. Interestingly, cutaneous saphenous nerves of P0+/- mice showed neither an increased ERK1/2 phosphorylation, nor an upregulated MCP-1 expression, nor a higher macrophage number. Contrarily, all these pathological alterations were found in cutaneous saphenous nerves of PMP22tg mice which led finally to demyelination of sensory fibers. These findings in sensory nerves of PMP22tg mice emphasize the role of MCP-1 and macrophage activity in the pathomechanism of a mouse model for CMT1A.

In PMP22tg/MCP-1 mutant mice we could show that there is a strong correlation between the CMAP, the grip strength and the organization of potassium channels. To which extent these findings are also present in the P0+/-/MCP-1 has to be determined.

6.5 Closing remarks

Taking into account the results of the present study, we can ascertain that the overexpression of PMP22 leads to an early hypermyelination at P7 which induces cellular stress within Schwann cells and the expression of MCP-1 by these cells. Thereby, both branches of the femoral nerve, i.e. femoral quadriceps and cutaneous saphenous nerve are affected. Further, the reduction of MCP-1 causes a considerably amelioration of the myelin pathological phenotype, whereas the complete absence of MCP-1 improves the axonal integrity and motor performance. This improved functional capacity is in direct correlation with a more wild type-like distribution of potassium channels. Moreover, the MCP-1

expression in PMP22tg mice is regulated by the MEK1/2/ERK1/2 signaling cascade and could serve as a putative factor for a treatment strategy. Importantly, T-lymphocytes play only – if at all – a minor role in the neuropathy of PMP22tg mice.

Former reports concerning examinations in human biopsies showed also a potential role of macrophages in the demyelinating mechanisms (Vital et al., 1992; Shy et al., 2002; Vital et al., 2003; Shy et al., 2008). Thus, macrophages are putative targets for immune-modulatory therapeutic strategies in a mouse model for CMT1A focusing on the modulation of the relevant signaling pathways.

As described before, animal models for the different subtypes of CMT1 implicate that inflammatory mechanisms affect the demyelination processes. A valid argument for the involvement of immune cells in human CMT1 is the subgroup of patients which exhibit inflammatory infiltrates within peripheral nerves and respond to anti-inflammatory treatment, e.g. with glucocorticosteroids (Martini and Toyka, 2004 for review). Some of these patients with “treatable” CMT1 show sensory signs like pain and paraesthesia which are usually untypical symptoms of CMT1. However, most of the CMT1 patients do not develop an improved progression caused by anti-inflammatory treatments. Therefore, different studies focus on experimental therapies in models for CMT1A which are not aimed at immune cells as direct targets.

Based on the observation that the steroid hormone progesterone stimulates the expression of myelin genes *in vitro*, onapristone – a selective progesterone receptor antagonist – was used in a PMP22-overexpressing rat model. By the use of this treatment, the transcriptional overexpression of PMP22 was reduced by 15% and the CMT phenotype was improved (Sereda et al., 2003). Interestingly, a similar uncoupling of demyelination and axonopathic alterations as in the PMP22tg/MCP-1 double mutant mice was observed (Meyer zu Horste et al., 2007). Further studies focus on the administration of ascorbic acid (vitamin C) as therapeutic approach. Ascorbic acid is required for the synthesis of collagen, for the formation of the basal lamina and for the myelin formation in neuron-Schwann cell cocultures (Carey and Todd, 1987; Podratz et al., 2001; Podratz et al., 2004). In the more severe affected PMP22-overexpressing mouse model from the C22 strain administration of oral ascorbic acid resulted in an improvement of myelination and of motor performance (Passage et al., 2004). High doses of ascorbic acid diminish the PMP22 mRNA expression via decreasing the adenylate cyclase activity and intracellular cAMP levels (Kaya et al., 2007).

To proof this treatment strategy in human patients, trials of ascorbic acid in CMT1A have been initiated in North America with 120 individuals.

Other putative treatment strategies focus on the administration of coenzyme Q10, neurotrophin-3 or mark RNA and gene-based therapies in preclinical CMT models (Herrmann, 2008 for review). Thus, the development of new therapeutic approaches for inherited neuropathies is a permanent challenge. Hereby, it would be worthwhile to focus on both the demyelinating alterations and the axonopathic changes as well as on the influence of the immune system on this pathology.

Appendix

A. Equipment and materials

A.1 Equipment

BioPhotometer 6131	Eppendorf (Hamburg, Germany)
Biosphere Filter Tips	Sarstedt (Nuernbrecht, Germany)
CellQuest Pro	BD Bioscience Pharmingen (San Jose, CA, USA)
Cell cultures bottles	Sarstedt (Nuernbrecht, Germany)
Centrifuges: Biofuge 15R	Heraeus (Hanau, Germany)
Biofuge pico	Heraeus (Hanau, Germany)
Centrifuge 5810R	Eppendorf (Hamburg, Germany)
Rotofix 32	Hettich Zentrifugen (Tuttlingen, Germany)
Centrifuge 5424	Eppendorf (Hamburg, Germany)
Device for electrophysiology: MS92a	Medelec (Old Woking, Surrey, UK)
Dry-Block Thermostate TDB-120	Hartenstein (Wuerzburg, Germany)
ELISA reader Original Multiskan EX	Labsystems (Frankfurt, Germany)
FACSCalibur	BD Biosciences Pharmingen (San Jose, CA, USA)
FACS Tubes	BD Biosciences Pharmingen (San Jose, CA, USA)
Gel chamber (horizontal)	PeqLab (Erlangen, Germany)
Incubator: HeraCell150	Heraeus (Hanau, Germany)
Kryostats: CM 1900	Leica (Wetzlar, Germany)
CM 3050S	Leica (Wetzlar, Germany)
Microscopes: CX31	Olympus (Hamburg, Germany)
BH2	Olympus (Hamburg, Germany)
CKX41	Olympus (Hamburg, Germany)
Axiophot 2	Zeiss (Oberkochen, Germany)
906 E	Zeiss (Oberkochen, Germany)
TCS SP2 mounted to a	
DM RE-7 SDK microscope	Leica Microsystems (Wetzlar, Germany)
Minirocker MR-1	New England Biolabs (Ipswich, MA, USA)
Object slides superfrost	Langenbrinck (Teningen, Germany)

PapPen	SCI (Munich, Germany)
PCR tubes	Sarstedt (Nuernbrecht, Germany)
Pipettes:	Abimed (Berlin, Germany)
	Eppendorf (Hamburg, Germany)
	Gilson (Bad Camberg, Germany)
Perfusion pump "Reglo"	Ismatec (Glattbrugg-Zuerich Swiss)
Power Pac Basic	Biorad (Hercules, CA, USA)
Power Pac 200	Biorad (Hercules, CA, USA)
ProScan Slow Scan CCD camera	Pro Scan (Lagerlechfeld, Germany)
Reaction tubes (0.5ml - 50ml)	Sarstedt (Nuernbrecht, Germany)
Shaker: KS250 basic	IKA Labortechnik (Staufen, Germany)
Speedvac: Univapo 100H	UniEquip (Martinsried, Germany)
Sonoplus HD60	Bandelin Electronic (Berlin, Germany)
Speed Vac: Vacobox	KNF Neuberger (Freiburg i. Br., Germany)
	Unicryo MC 2L -60.0C
	mounted to Univapo 100 H
Thermocycler: Mastercycler	Unicryo (Planegg, Germany)
	Unicryo (Planegg, Germany)
	Eppendorf (Hamburg, Germany)
	Primus 96 advanced
Thermoshaker TS1	PeqLab (Erlangen, Germany)
Ultracut	Biometra (Göttingen, Germany)
UV Crosslinker 1800	Leica (Wetzlar, Germany)
	Stratagene (La Jolla, CA, USA)

A.2 Reagents

Acetone	Invitrogen (Karlsruhe, Germany)
Ammonium chloride	Merck (Darmstadt, Germany)
Agarose	Sigma (Munich, Germany)
AmpliTaq DNA Polymerase	Applied Biosystems (Darmstadt, Germany)
Aquatex	Merck (Darmstadt, Germany)
Boric acid	Merck (Darmstadt, Germany)
Bovine Serum albumine (BSA) 96	Sigma (Munich, Germany)
Chloroform	J.T. Baker (Deventer, Netherlands)
Diaminobenzidine (DAB)	KemEnTecDiagnostics (Copenhagen, Denmark)
1,4-Dithiothreitol (DTT)	Sigma (Munich, Germany)
Dulbecco`s Modified Eagle`s medium	Gibco Invitrogen (Karlsruhe, Germany)

Ethanol	J.T. Baker (Deventer, Netherlands)
Ethidium bromide	Sigma (Munich, Germany)
EDTA	Merck (Darmstadt, Germany)
Fetal Calf Serum (FCS)	Gibco Invitrogen (Karlsruhe, Germany)
Glutamat	Gibco Invitrogen (Karlsruhe, Germany)
Glycine	Sigma (Munich, Germany)
Glycerol	Merck (Darmstadt, Germany)
Heparin	Ratiopharm (Ulm, Germany)
Hepes	Carl Roth (Karlsruhe, Germany)
Ketanest	Parke-Davis (Karlsruhe, Germany)
Lowry powder	Sigma (Munich, Germany)
Methanol	J.T.Baker (Deventer, Netherlands)
2-Methylbutane	Carl Roth (Karlsruhe, Germany)
Nonidet P-40 substitute (NP-40)	Fluka (Buchs, Swiss)
O.C.T. matrix	DiaTec (Nuernberg, Germany)
O Range Ruler 600bp DNA ladder	Fermentas (St. Leon-Rot, Germany)
Orange Loading Dye (6x)	Fermentas (St. Leon-Rot, Germany)
Penicillin/Streptomycin	Invitrogen (Karlsruhe, Germany)
Phosphate-buffered saline (PBS)	Biochrom AG (Berlin, Germany)
Primers	Sigma (Munich, Germany)
Potassium di-hydrogen phosphate	Merck (Darmstadt, Germany)
Potassium chloride	Merck (Darmstadt, Germany)
Potassium hydrogen carbonate	Merck (Darmstadt, Germany)
Polyacrylamid	Carl Roth (Karlsruhe, Germany)
Rompun	BayerVital (Leverkusen, Germany)
StreptABComplex kit	DakoCytomation (Hamburg, Germany)
Sodium azide	Merck (Darmstadt, Germany)
Sodium chloride solution	Merck (Darmstadt, Germany)
SDS	Carl Roth (Karlsruhe, Germany)
Temed	Sigma (Munich, Germany)
Tris	Merck (Darmstadt, Germany)
TritonX-100	Carl Roth (Karlsruhe, Germany)
Trypsin	Invitrogen (Karlsruhe, Germany)
Tween20	Carl Roth (Karlsruhe, Germany)
Vinyl/ERL4221D	ServaElectrophoresis (Heidelberg, Germany)
Vitro-Clud	Langenbrinck (Teningen, Germany)

A.3 Solutions, buffers and media

Anesthetic:	0.6% Ketanest 0.08% Rompun 8.3% NaCl
DABCO:	25% 1xPBS 75% Glycerol 25mg/ml 1,4-diazabicyclo[2.2.2]octane Store at 4°C protected from light.
DEPC-H ₂ O:	0.01% diethyl pyrocarbonate (DEPC) Dissolve in distilled water, autoclave.
Erythrocyte lysis buffer (pH 7.4):	0.15M NH ₄ Cl 1mM KHCO ₃ 0.1mM Na ₂ EDTA Dissolve in distilled water, filtrate through 0.2µm filter.
FACS buffer:	1xPBS 0.1-1% BSA 0.1% NaAzide Store at 4°C.
Freeze medium (cell culture):	20% (v/v) FCS 20% DMSO Dissolve in DMEM, store at -20°C.
Medium (NIH 3T3):	10-20% FCS 1% Glutamate 1% Penicillin/Streptomycin Dissolve in DMEM, store at 4°C and use at 37°C.
PBS (1x, pH 7.4):	137mM NaCl 2.7mM KCl 1.5mM KH ₂ PO ₄ 8.1mM Na ₂ HPO ₄

PBST (1x):	0.1% Tween20 Dissolve in 1xPBS.
Ponceau S:	1% Trichloroacetic acid 0.1% Ponceau S Store protected from light.
RIPA lysis buffer:	25mM Tris pH 8 10mM Hepes pH 4.4 150mM NaCl 5mM MgCl ₂ 145mM KCl 0.4% EDTA 0.1% SDS 1% Nonidet P40 10% Glycerol Store at 4°C.
SDS PAGE buffer (10x):	0.25M Tris 1.92M Glycine 1% SDS Store at 4°C.
Separating gel buffer (4x, pH 8.8):	1.5M Tris 0.4% SDS 0.4% TEMED Store at 4°C.
Spurr`s medium:	10g ERL 4206 (3,4-Epoxy-cyclohexylmethyl-3,4-epoxy- cyclohexylcyclohexylcarboxylate) 6g DER 736 26g NSA (Nonenylsuccinicanhydride) 0.4g DMAE (Dimethylaminoethanol)

Stacking gel buffer (4x, pH 6.8):	0.5M Tris 0.4% SDS 0.4% TEMED Store at 4°C.
Stripping-buffer (pH 2.1):	0.2M Glycine 0.1% SDS 20mM Dithiotreitol 1% Tween20 Store at 4°C.
Transfer buffer (10x):	0.25M Tris 1.92M Glycine Store at 4°C.
Transfer buffer (1x):	20% Methanol Dissolve in 1x Transfer buffer.
TBE (pH 8.0):	89mM Tris 89mM Borate 2mM EDTA
Gel running buffer (10x)	0.25M Tris 1.92M Glycin 1% SDS Store at 4°C, use of diluted solution (1:10).

Unless otherwise mentioned, distilled water was used as solvent and solutions were stored at room temperature.

A.4 Antibodies for western blot analyses

Primary antibody	Dilution	Company (product number)	Modification in protocol
Rabbit anti-actin	1:500	Sigma (A2066)	---
Mouse anti-p-ERK1/2	0.2µg/ml	Santa Cruz (7383)	2h, RT
Rabbit anti-ERK1/2	0.02µg/ml	Santa Cruz (94)	2h, RT
Rabbit anti-p-IkBa (Ser32)	1:200	Cell Signalling (9241)	---
Rabbit anti-IkBa	1:200	Cell Signalling (9242)	---
Mouse anti-p-JNK	0.2µg/ml	Santa Cruz (6254)	---
Rabbit anti-JNK1	0.2µg/ml	Santa Cruz (571)	---
Rabbit anti-p-MEK1/2 (Ser 218/222)	1:200	Cell Signalling (9121)	diluted in 1xPBST
Rabbit anti-MEK1/2	1:1000	Cell Signalling (9122)	diluted in 1xPBST
Rabbit anti-p-p38 (Thr180/Tyr182)	1:1000	Chemicon (AB3828)	diluted in 1xPBST
Rabbit anti-p38	1:1000	Chemicon (AB3188)	diluted in 1xPBST
Rabbit anti-p-PKCα (Ser657)	0.2µg/ml	Santa Cruz (12356)	---
Rabbit anti-PKCα	0.2µg/ml	Santa Cruz (10800)	---
Rabbit anti-p-STAT (Tyr701)	10µg/ml	Chemicon (AB3892)	---
Rabbit anti-STAT	2µg/ml	Chemicon (AB16951)	---

Secondary antibody	Dilution	Company (product number)	Modification in protocol
Sheep anti-rabbit IgG (HRP conjugated)	1:2000	Chemicon (AP322P)	---
Sheep anti-mouse IgG (HRP conjugated)	1:4000	Chemicon (AP300P)	---

B. References

- Aguayo AJ, Attiwell M, Trecarten J, Perkins S, Bray GM (1977) Abnormal myelination in transplanted Trembler mouse Schwann cells. *Nature* 265:73-75.
- Al-Thihli K, Rudkin T, Carson N, Poulin C, Melancon S, Der Kaloustian VM (2008) Compound heterozygous deletions of PMP22 causing severe Charcot-Marie-Tooth disease of the Dejerine-Sottas disease phenotype. *Am J Med Genet A* 146A:2412-2416.
- Anzini P, Neuberg DH, Schachner M, Nelles E, Willecke K, Zielasek J, Toyka KV, Suter U, Martini R (1997) Structural abnormalities and deficient maintenance of peripheral nerve myelin in mice lacking the gap junction protein connexin 32. *J Neurosci* 17:4545-4551.
- Arroyo EJ, Scherer SS (2000) On the molecular architecture of myelinated fibers. *Histochem Cell Biol* 113:1-18.
- Balice-Gordon RJ, Bone LJ, Scherer SS (1998) Functional gap junctions in the schwann cell myelin sheath. *J Cell Biol* 142:1095-1104.
- Barbaria EM, Kohl B, Buhren BA, Hasenpusch-Theil K, Kruse F, Kury P, Martini R, Muller HW (2008) The alpha-chemokine CXCL14 is up-regulated in the sciatic nerve of a mouse model of Charcot-Marie-Tooth disease type 1A and alters myelin gene expression in cultured Schwann cells. *Neurobiol Dis*.
- Ben Othmane K, Middleton LT, Loprest LJ, Wilkinson KM, Lennon F, Rozear MP, Stajich JM, Gaskell PC, Roses AD, Pericak-Vance MA, et al. (1993) Localization of a gene (CMT2A) for autosomal dominant Charcot-Marie-Tooth disease type 2 to chromosome 1p and evidence of genetic heterogeneity. *Genomics* 17:370-375.
- Berghoff M, Samsam M, Muller M, Kobsar I, Toyka KV, Kiefer R, Maurer M, Martini R (2005) Neuroprotective effect of the immune system in a mouse model of severe dysmyelinating hereditary neuropathy: enhanced axonal degeneration following disruption of the RAG-1 gene. *Mol Cell Neurosci* 28:118-127.

- Bergoffen J, Scherer SS, Wang S, Scott MO, Bone LJ, Paul DL, Chen K, Lensch MW, Chance PF, Fischbeck KH (1993) Connexin mutations in X-linked Charcot-Marie-Tooth disease. *Science* 262:2039-2042.
- Beuche W, Friede RL (1985) Millipore diffusion chambers allow dissociation of myelin phagocytosis by non-resident cells and of allogenic nerve graft rejection. *J Neurol Sci* 69:231-246.
- Boekhoudt GH, Guo Z, Beresford GW, Boss JM (2003) Communication between NF-kappa B and Sp1 controls histone acetylation within the proximal promoter of the monocyte chemoattractant protein 1 gene. *J Immunol* 170:4139-4147.
- Bosse F, Brodbeck J, Muller HW (1999) Post-transcriptional regulation of the peripheral myelin protein gene PMP22/gas3. *J Neurosci Res* 55:164-177.
- Brancolini C, Marzinotto S, Edomi P, Agostoni E, Fiorentini C, Muller HW, Schneider C (1999) Rho-dependent regulation of cell spreading by the tetraspan membrane protein Gas3/PMP22. *Mol Biol Cell* 10:2441-2459.
- Bruck W, Huitinga I, Dijkstra CD (1996) Liposome-mediated monocyte depletion during wallerian degeneration defines the role of hematogenous phagocytes in myelin removal. *J Neurosci Res* 46:477-484.
- Carenini S, Neuberg D, Schachner M, Suter U, Martini R (1999) Localization and functional roles of PMP22 in peripheral nerves of P0-deficient mice. *Glia* 28:256-264.
- Carenini S, Maurer M, Werner A, Blazyca H, Toyka KV, Schmid CD, Raivich G, Martini R (2001) The role of macrophages in demyelinating peripheral nervous system of mice heterozygously deficient in p0. *J Cell Biol* 152:301-308.
- Carey DJ, Todd MS (1987) Schwann cell myelination in a chemically defined medium: demonstration of a requirement for additives that promote Schwann cell extracellular matrix formation. *Brain Res* 429:95-102.
- Chance PF, Alderson MK, Leppig KA, Lensch MW, Matsunami N, Smith B, Swanson PD, Odelberg SJ, Distèche CM, Bird TD (1993) DNA deletion associated with hereditary neuropathy with liability to pressure palsies. *Cell* 72:143-151.
- Cheepudomwit T, Guzelsu E, Zhou C, Griffin JW, Hoke A (2008) Comparison of cytokine expression profile during Wallerian degeneration of myelinated and unmyelinated peripheral axons. *Neurosci Lett* 430:230-235.

- Chomczynski P, Sacchi N (1987) Single-step method of RNA isolation by acid guanidinium thiocyanate-phenol-chloroform extraction. *Anal Biochem* 162:156-159.
- Colucci-D'Amato L, Perrone-Capano C, di Porzio U (2003) Chronic activation of ERK and neurodegenerative diseases. *Bioessays* 25:1085-1095.
- D'Urso D, Ehrhardt P, Muller HW (1999) Peripheral myelin protein 22 and protein zero: a novel association in peripheral nervous system myelin. *J Neurosci* 19:3396-3403.
- De S, Trigueros MA, Kalyvas A, David S (2003) Phospholipase A2 plays an important role in myelin breakdown and phagocytosis during Wallerian degeneration. *Mol Cell Neurosci* 24:753-765.
- Filbin MT, Tennekoon GI (1993) Homophilic adhesion of the myelin P0 protein requires glycosylation of both molecules in the homophilic pair. *J Cell Biol* 122:451-459.
- Fischer S, Weishaupt A, Troppmair J, Martini R (2008a) Increase of MCP-1 (CCL2) in myelin mutant Schwann cells is mediated by MEK-ERK signaling pathway. *Glia* 56:836-843.
- Fischer S, Kleinschnitz C, Muller M, Kobsar I, Ip CW, Rollins B, Martini R (2008b) Monocyte chemoattractant protein-1 is a pathogenic component in a model for a hereditary peripheral neuropathy. *Mol Cell Neurosci* 37:359-366.
- Fischer S (2008c) Regulation and functional consequences of MCP-1 expression in a model of Charcot-Marie-Tooth 1B disease. Doctoral thesis.
- Fortun J, Li J, Go J, Fenstermaker A, Fletcher BS, Notterpek L (2005) Impaired proteasome activity and accumulation of ubiquitinated substrates in a hereditary neuropathy model. *J Neurochem* 92:1531-1541.
- Frederick MJ, Henderson Y, Xu X, Deavers MT, Sahin AA, Wu H, Lewis DE, El-Naggar AK, Clayman GL (2000) In vivo expression of the novel CXC chemokine BRAK in normal and cancerous human tissue. *Am J Pathol* 156:1937-1950.
- Gabreels-Festen AA, Joosten EM, Gabreels FJ, Jennekens FG, Janssen-van Kempen TW (1992) Early morphological features in dominantly inherited demyelinating motor and sensory neuropathy (HMSN type I). *J Neurol Sci* 107:145-154.
- Giese KP, Martini R, Lemke G, Soriano P, Schachner M (1992) Mouse P0 gene disruption leads to hypomyelination, abnormal expression of recognition molecules, and degeneration of myelin and axons. *Cell* 71:565-576.

- Goebeler M, Gillitzer R, Kilian K, Utzel K, Brocker EB, Rapp UR, Ludwig S (2001) Multiple signaling pathways regulate NF-kappaB-dependent transcription of the monocyte chemoattractant protein-1 gene in primary endothelial cells. *Blood* 97:46-55.
- Greenfield S, Brostoff S, Eylar EH, Morell P (1973) Protein composition of myelin of the peripheral nervous system. *J Neurochem* 20:1207-1216.
- Griffin JW, George R, Ho T (1993) Macrophage systems in peripheral nerves. A review. *J Neuropathol Exp Neurol* 52:553-560.
- Guenard V, Montag D, Schachner M, Martini R (1996) Onion bulb cells in mice deficient for myelin genes share molecular properties with immature, differentiated non-myelinating, and denervated Schwann cells. *Glia* 18:27-38.
- Hanemann CO, Gabreels-Festen AA, Stoll G, Muller HW (1997) Schwann cell differentiation in Charcot-Marie-Tooth disease type 1A (CMT1A): normal number of myelinating Schwann cells in young CMT1A patients and neural cell adhesion molecule expression in onion bulbs. *Acta Neuropathol* 94:310-315.
- Hanemann CO, D'Urso D, Gabreels-Festen AA, Muller HW (2000) Mutation-dependent alteration in cellular distribution of peripheral myelin protein 22 in nerve biopsies from Charcot-Marie-Tooth type 1A. *Brain* 123 (Pt 5):1001-1006.
- Harding AE, Thomas PK (1980) The clinical features of hereditary motor and sensory neuropathy types I and II. *Brain* 103:259-280.
- Hasse B, Bosse F, Hanenberg H, Muller HW (2004) Peripheral myelin protein 22 kDa and protein zero: domain specific trans-interactions. *Mol Cell Neurosci* 27:370-378.
- Hayasaka K, Takada G, Ionasescu VV (1993) Mutation of the myelin P0 gene in Charcot-Marie-Tooth neuropathy type 1B. *Hum Mol Genet* 2:1369-1372.
- Henry EW, Cowen JS, Sidman RL (1983) Comparison of Trembler and Trembler-J mouse phenotypes: varying severity of peripheral hypomyelination. *J Neuropathol Exp Neurol* 42:688-706.
- Herrmann DN (2008) Experimental therapeutics in hereditary neuropathies: the past, the present, and the future. *Neurotherapeutics* 5:507-515.
- Hildebrand C, Hahn R (1978) Relation between myelin sheath thickness and axon size in spinal cord white matter of some vertebrate species. *J Neurol Sci* 38:421-434.

- Holtmann B, Wiese S, Samsam M, Grohmann K, Pennica D, Martini R, Sendtner M (2005) Triple knock-out of CNTF, LIF, and CT-1 defines cooperative and distinct roles of these neurotrophic factors for motoneuron maintenance and function. *J Neurosci* 25:1778-1787.
- Hromas R, Broxmeyer HE, Kim C, Nakshatri H, Christopherson K, 2nd, Azam M, Hou YH (1999) Cloning of BRAK, a novel divergent CXC chemokine preferentially expressed in normal versus malignant cells. *Biochem Biophys Res Commun* 255:703-706.
- Huxley C, Passage E, Manson A, Putzu G, Figarella-Branger D, Pellissier JF, Fontes M (1996) Construction of a mouse model of Charcot-Marie-Tooth disease type 1A by pronuclear injection of human YAC DNA. *Hum Mol Genet* 5:563-569.
- Huxley C, Passage E, Robertson AM, Youl B, Huston S, Manson A, Saberan-Djoniedi D, Figarella-Branger D, Pellissier JF, Thomas PK, Fontes M (1998) Correlation between varying levels of PMP22 expression and the degree of demyelination and reduction in nerve conduction velocity in transgenic mice. *Hum Mol Genet* 7:449-458.
- Ip CW, Kroner A, Bendszus M, Leder C, Kobsar I, Fischer S, Wiendl H, Nave KA, Martini R (2006) Immune cells contribute to myelin degeneration and axonopathic changes in mice overexpressing proteolipid protein in oligodendrocytes. *J Neurosci* 26:8206-8216.
- Jenkins SM, Bennett V (2001) Ankyrin-G coordinates assembly of the spectrin-based membrane skeleton, voltage-gated sodium channels, and L1 CAMs at Purkinje neuron initial segments. *J Cell Biol* 155:739-746.
- Jenkins SM, Bennett V (2002) Developing nodes of Ranvier are defined by ankyrin-G clustering and are independent of paranodal axoglial adhesion. *Proc Natl Acad Sci U S A* 99:2303-2308.
- Jessen KR, Mirsky R (2005) The origin and development of glial cells in peripheral nerves. *Nat Rev Neurosci* 6:671-682.
- Jetten AM, Suter U (2000) The peripheral myelin protein 22 and epithelial membrane protein family. *Prog Nucleic Acid Res Mol Biol* 64:97-129.
- Jung H, Toth PT, White FA, Miller RJ (2008) Monocyte chemoattractant protein-1 functions as a neuromodulator in dorsal root ganglia neurons. *J Neurochem* 104:254-263.

- Jutila MA, Kroese FG, Jutila KL, Stall AM, Fiering S, Herzenberg LA, Berg EL, Butcher EC (1988) Ly-6C is a monocyte/macrophage and endothelial cell differentiation antigen regulated by interferon-gamma. *Eur J Immunol* 18:1819-1826.
- Kaya F, Belin S, Bourgeois P, Micaleff J, Blin O, Fontes M (2007) Ascorbic acid inhibits PMP22 expression by reducing cAMP levels. *Neuromuscul Disord* 17:248-253.
- Kettenmann H, Ransom B (2005) *Neuroglia*. Oxford University Press, Second Edition.
- Kleinschnitz C, Brinkhoff J, Zelenka M, Sommer C, Stoll G (2004) The extent of cytokine induction in peripheral nerve lesions depends on the mode of injury and NMDA receptor signaling. *J Neuroimmunol* 149:77-83.
- Kobsar I, Maurer M, Ott T, Martini R (2002) Macrophage-related demyelination in peripheral nerves of mice deficient in the gap junction protein connexin 32. *Neurosci Lett* 320:17-20.
- Kobsar I, Hasenpusch-Theil K, Wessig C, Muller HW, Martini R (2005) Evidence for macrophage-mediated myelin disruption in an animal model for Charcot-Marie-Tooth neuropathy type 1A. *J Neurosci Res* 81:857-864.
- Kobsar I, Oetke C, Kroner A, Wessig C, Crocker P, Martini R (2006) Attenuated demyelination in the absence of the macrophage-restricted adhesion molecule sialoadhesin (Siglec-1) in mice heterozygously deficient in P0. *Mol Cell Neurosci* 31:685-691.
- Kobsar I, Berghoff M, Samsam M, Wessig C, Maurer M, Toyka KV, Martini R (2003) Preserved myelin integrity and reduced axonopathy in connexin32-deficient mice lacking the recombination activating gene-1. *Brain* 126:804-813.
- Kroner A, Schwab N, Ip CW, Sommer C, Wessig C, Wiendl H, Martini R (2008) The co-inhibitory molecule PD-1 modulates disease severity in a model for an inherited, demyelinating neuropathy. *Neurobiol Dis*.
- Kunkel-Bagden E, Dai HN, Bregman BS (1993) Methods to assess the development and recovery of locomotor function after spinal cord injury in rats. *Exp Neurol* 119:153-164.
- Kurth I, Willimann K, Schaerli P, Hunziker T, Clark-Lewis I, Moser B (2001) Monocyte selectivity and tissue localization suggests a role for breast and kidney-expressed chemokine (BRACK) in macrophage development. *J Exp Med* 194:855-861.

- Liang SC, Latchman YE, Buhlmann JE, Tomczak MF, Horwitz BH, Freeman GJ, Sharpe AH (2003) Regulation of PD-1, PD-L1, and PD-L2 expression during normal and autoimmune responses. *Eur J Immunol* 33:2706-2716.
- Lopez-Vales R, Navarro X, Shimizu T, Baskakis C, Kokotos G, Constantinou-Kokotou V, Stephens D, Dennis EA, David S (2008) Intracellular phospholipase A(2) group IVA and group VIA play important roles in Wallerian degeneration and axon regeneration after peripheral nerve injury. *Brain* 131:2620-2631.
- Lowry OH, Rosebrough NJ, Farr AL, Randall RJ (1951) Protein measurement with the Folin phenol reagent. *J Biol Chem* 193:265-275.
- Lu B, Rutledge BJ, Gu L, Fiorillo J, Lukacs NW, Kunkel SL, North R, Gerard C, Rollins BJ (1998) Abnormalities in monocyte recruitment and cytokine expression in monocyte chemoattractant protein 1-deficient mice. *J Exp Med* 187:601-608.
- Lupski JR, de Oca-Luna RM, Slaugenhaupt S, Pentao L, Guzzetta V, Trask BJ, Saucedo-Cardenas O, Barker DF, Killian JM, Garcia CA, Chakravarti A, Patel PI (1991) DNA duplication associated with Charcot-Marie-Tooth disease type 1A. *Cell* 66:219-232.
- Magyar JP, Martini R, Ruelicke T, Aguzzi A, Adlkofer K, Dembic Z, Zielasek J, Toyka KV, Suter U (1996) Impaired differentiation of Schwann cells in transgenic mice with increased PMP22 gene dosage. *J Neurosci* 16:5351-5360.
- Manfioletti G, Ruaro ME, Del Sal G, Philipson L, Schneider C (1990) A growth arrest-specific (gas) gene codes for a membrane protein. *Mol Cell Biol* 10:2924-2930.
- Martini R (1997) Animal models for inherited peripheral neuropathies. *J Anat* 191 (Pt 3):321-336.
- Martini R, Schachner M (1997) Molecular bases of myelin formation as revealed by investigations on mice deficient in glial cell surface molecules. *Glia* 19:298-310.
- Martini R, Toyka KV (2004) Immune-mediated components of hereditary demyelinating neuropathies: lessons from animal models and patients. *Lancet Neurol* 3:457-465.
- Martini R, Fischer S, Lopez-Vales R, David S (2008) Interactions between Schwann cells and macrophages in injury and inherited demyelinating disease. *Glia* 56:1566-1577.
- Martini R, Zielasek J, Toyka KV, Giese KP, Schachner M (1995) Protein zero (P0)-deficient mice show myelin degeneration in peripheral nerves characteristic of inherited human neuropathies. *Nat Genet* 11:281-286.

- Masu Y, Wolf E, Holtmann B, Sendtner M, Brem G, Thoenen H (1993) Disruption of the CNTF gene results in motor neuron degeneration. *Nature* 365:27-32.
- Maurer M, Kobsar I, Berghoff M, Schmid CD, Carenini S, Martini R (2002) Role of immune cells in animal models for inherited neuropathies: facts and visions. *J Anat* 200:405-414.
- Maurer M, Muller M, Kobsar I, Leonhard C, Martini R, Kiefer R (2003) Origin of pathogenic macrophages and endoneurial fibroblast-like cells in an animal model of inherited neuropathy. *Mol Cell Neurosci* 23:351-359.
- Maurer M, Schmid CD, Bootz F, Zielasek J, Toyka KV, Oehen S, Martini R (2001) Bone marrow transfer from wild-type mice reverts the beneficial effect of genetically mediated immune deficiency in myelin mutants. *Mol Cell Neurosci* 17:1094-1101.
- Melik-Parsadaniantz S, Rostene W (2008) Chemokines and neuromodulation. *J Neuroimmunol* 198:62-68.
- Meyer Zu Horste G, Nave KA (2006) Animal models of inherited neuropathies. *Curr Opin Neurol* 19:464-473.
- Meyer zu Horste G, Prukop T, Liebetanz D, Mobius W, Nave KA, Sereda MW (2007) Antiprogestosterone therapy uncouples axonal loss from demyelination in a transgenic rat model of CMT1A neuropathy. *Ann Neurol* 61:61-72.
- Mombaerts P, Iacomini J, Johnson RS, Herrup K, Tonegawa S, Papaioannou VE (1992) RAG-1-deficient mice have no mature B and T lymphocytes. *Cell* 68:869-877.
- Mueller M, Leonhard C, Wacker K, Ringelstein EB, Okabe M, Hickey WF, Kiefer R (2003) Macrophage response to peripheral nerve injury: the quantitative contribution of resident and hematogenous macrophages. *Lab Invest* 83:175-185.
- Muller HW (2000) Tetraspan myelin protein PMP22 and demyelinating peripheral neuropathies: new facts and hypotheses. *Glia* 29:182-185.
- Muller M, Berghoff M, Kobsar I, Kiefer R, Martini R (2007) Macrophage colony stimulating factor is a crucial factor for the intrinsic macrophage response in mice heterozygously deficient for the myelin protein P0. *Exp Neurol* 203:55-62.
- Murakami M, Nakatani Y, Atsumi G, Inoue K, Kudo I (1997) Regulatory functions of phospholipase A2. *Crit Rev Immunol* 17:225-283.

- Myers JK, Mobley CK, Sanders CR (2008) The peripheral neuropathy-linked Trembler and Trembler-J mutant forms of peripheral myelin protein 22 are folding-destabilized. *Biochemistry* 47:10620-10629.
- Nave KA, Sereda MW, Ehrenreich H (2007) Mechanisms of disease: inherited demyelinating neuropathies--from basic to clinical research. *Nat Clin Pract Neurol* 3:453-464.
- Nguyen T, Mehta NR, Conant K, Kim KJ, Jones M, Calabresi PA, Melli G, Hoke A, Schnaar RL, Ming GL, Song H, Keswani SC, Griffin JW (2009) Axonal protective effects of the myelin-associated glycoprotein. *J Neurosci* 29:630-637.
- Nicholson GA, Valentijn LJ, Cherryson AK, Kennerson ML, Bragg TL, DeKroon RM, Ross DA, Pollard JD, McLeod JG, Bolhuis PA, et al. (1994) A frame shift mutation in the PMP22 gene in hereditary neuropathy with liability to pressure palsies. *Nat Genet* 6:263-266.
- Niemann A, Berger P, Suter U (2006) Pathomechanisms of mutant proteins in Charcot-Marie-Tooth disease. *Neuromolecular Med* 8:217-242.
- Nishimura H, Minato N, Nakano T, Honjo T (1998) Immunological studies on PD-1 deficient mice: implication of PD-1 as a negative regulator for B cell responses. *Int Immunol* 10:1563-1572.
- Notterpek L, Ryan MC, Tobler AR, Shooter EM (1999) PMP22 accumulation in aggresomes: implications for CMT1A pathology. *Neurobiol Dis* 6:450-460.
- Notterpek L, Roux KJ, Amici SA, Yazdanpour A, Rahner C, Fletcher BS (2001) Peripheral myelin protein 22 is a constituent of intercellular junctions in epithelia. *Proc Natl Acad Sci U S A* 98:14404-14409.
- Okabe M, Ikawa M, Kominami K, Nakanishi T, Nishimune Y (1997) 'Green mice' as a source of ubiquitous green cells. *FEBS Lett* 407:313-319.
- Okazaki T, Honjo T (2007) PD-1 and PD-1 ligands: from discovery to clinical application. *Int Immunol* 19:813-824.
- Okazaki T, Iwai Y, Honjo T (2002) New regulatory co-receptors: inducible co-stimulator and PD-1. *Curr Opin Immunol* 14:779-782.
- Pareek S, Notterpek L, Snipes GJ, Naef R, Sossin W, Laliberte J, Iacampo S, Suter U, Shooter EM, Murphy RA (1997) Neurons promote the translocation of peripheral myelin protein 22 into myelin. *J Neurosci* 17:7754-7762.

- Passage E, Norreel JC, Noack-Fraissignes P, Sanguedolce V, Pizant J, Thirion X, Robaglia-Schlupp A, Pellissier JF, Fontes M (2004) Ascorbic acid treatment corrects the phenotype of a mouse model of Charcot-Marie-Tooth disease. *Nat Med* 10:396-401.
- Pedrola L, Espert A, Valdes-Sanchez T, Sanchez-Piris M, Sirkowski EE, Scherer SS, Farinas I, Palau F (2008) Cell expression of GDAP1 in the nervous system and pathogenesis of Charcot-Marie-Tooth type 4A disease. *J Cell Mol Med* 12:679-689.
- Perrin FE, Lacroix S, Aviles-Trigueros M, David S (2005) Involvement of monocyte chemoattractant protein-1, macrophage inflammatory protein-1alpha and interleukin-1beta in Wallerian degeneration. *Brain* 128:854-866.
- Podratz JL, Rodriguez E, Windebank AJ (2001) Role of the extracellular matrix in myelination of peripheral nerve. *Glia* 35:35-40.
- Podratz JL, Rodriguez EH, Windebank AJ (2004) Antioxidants are necessary for myelination of dorsal root ganglion neurons, in vitro. *Glia* 45:54-58.
- Poliak S, Peles E (2003) The local differentiation of myelinated axons at nodes of Ranvier. *Nat Rev Neurosci* 4:968-980.
- Previtali SC, Quattrini A, Bolino A (2007) Charcot-Marie-Tooth type 4B demyelinating neuropathy: deciphering the role of MTMR phosphatases. *Expert Rev Mol Med* 9:1-16.
- Quarles RH (2007) Myelin-associated glycoprotein (MAG): past, present and beyond. *J Neurochem* 100:1431-1448.
- Raeymaekers P, Timmerman V, Nelis E, De Jonghe P, Hoogendijk JE, Baas F, Barker DF, Martin JJ, De Visser M, Bolhuis PA, et al. (1991) Duplication in chromosome 17p11.2 in Charcot-Marie-Tooth neuropathy type 1a (CMT 1a). The HMSN Collaborative Research Group. *Neuromuscul Disord* 1:93-97.
- Rasband MN, Peles E, Trimmer JS, Levinson SR, Lux SE, Shrager P (1999) Dependence of nodal sodium channel clustering on paranodal axoglial contact in the developing CNS. *J Neurosci* 19:7516-7528.
- Robertson AM, Huxley C, King RH, Thomas PK (1999) Development of early postnatal peripheral nerve abnormalities in Trembler-J and PMP22 transgenic mice. *J Anat* 195 (Pt 3):331-339.

- Roux KJ, Amici SA, Notterpek L (2004) The temporospatial expression of peripheral myelin protein 22 at the developing blood-nerve and blood-brain barriers. *J Comp Neurol* 474:578-588.
- Roux KJ, Amici SA, Fletcher BS, Notterpek L (2005) Modulation of epithelial morphology, monolayer permeability, and cell migration by growth arrest specific 3/peripheral myelin protein 22. *Mol Biol Cell* 16:1142-1151.
- Saada A, Reichert F, Rotshenker S (1996) Granulocyte macrophage colony stimulating factor produced in lesioned peripheral nerves induces the up-regulation of cell surface expression of MAC-2 by macrophages and Schwann cells. *J Cell Biol* 133:159-167.
- Salzer JL (1997) Clustering sodium channels at the node of Ranvier: close encounters of the axon-glia kind. *Neuron* 18:843-846.
- Samsam M, Mi W, Wessig C, Zielasek J, Toyka KV, Coleman MP, Martini R (2003) The Wlds mutation delays robust loss of motor and sensory axons in a genetic model for myelin-related axonopathy. *J Neurosci* 23:2833-2839.
- Sancho S, Young P, Suter U (2001) Regulation of Schwann cell proliferation and apoptosis in PMP22-deficient mice and mouse models of Charcot-Marie-Tooth disease type 1A. *Brain* 124:2177-2187.
- Scherer SS, Deschenes SM, Xu YT, Grinspan JB, Fischbeck KH, Paul DL (1995) Connexin32 is a myelin-related protein in the PNS and CNS. *J Neurosci* 15:8281-8294.
- Scherer SS, Xu YT, Nelles E, Fischbeck K, Willecke K, Bone LJ (1998) Connexin32-null mice develop demyelinating peripheral neuropathy. *Glia* 24:8-20.
- Schlueter AJ, Glasgow JK (2006) Phenotypic comparison of multiple monocyte-related populations in murine peripheral blood and bone marrow. *Cytometry A* 69:281-290.
- Schmid CD, Stienekemeier M, Oehen S, Bootz F, Zielasek J, Gold R, Toyka KV, Schachner M, Martini R (2000) Immune deficiency in mouse models for inherited peripheral neuropathies leads to improved myelin maintenance. *J Neurosci* 20:729-735.
- Sereda M, Griffiths I, Puhlhofer A, Stewart H, Rossner MJ, Zimmerman F, Magyar JP, Schneider A, Hund E, Meinck HM, Suter U, Nave KA (1996) A transgenic rat model of Charcot-Marie-Tooth disease. *Neuron* 16:1049-1060.

- Sereda MW, Meyer zu Horste G, Suter U, Uzma N, Nave KA (2003) Therapeutic administration of progesterone antagonist in a model of Charcot-Marie-Tooth disease (CMT-1A). *Nat Med* 9:1533-1537.
- Shapiro L, Doyle JP, Hensley P, Colman DR, Hendrickson WA (1996) Crystal structure of the extracellular domain from P0, the major structural protein of peripheral nerve myelin. *Neuron* 17:435-449.
- Sharpe AH, Wherry EJ, Ahmed R, Freeman GJ (2007) The function of programmed cell death 1 and its ligands in regulating autoimmunity and infection. *Nat Immunol* 8:239-245.
- Sheng WS, Hu S, Ni HT, Rowen TN, Lokensgard JR, Peterson PK (2005) TNF-alpha-induced chemokine production and apoptosis in human neural precursor cells. *J Leukoc Biol* 78:1233-1241.
- Shurin GV, Ferris RL, Tourkova IL, Perez L, Lokshin A, Balkir L, Collins B, Chatta GS, Shurin MR (2005) Loss of new chemokine CXCL14 in tumor tissue is associated with low infiltration by dendritic cells (DC), while restoration of human CXCL14 expression in tumor cells causes attraction of DC both in vitro and in vivo. *J Immunol* 174:5490-5498.
- Shy ME (2006) Peripheral neuropathies caused by mutations in the myelin protein zero. *J Neurol Sci* 242:55-66.
- Shy ME, Garbern JY, Kamholz J (2002) Hereditary motor and sensory neuropathies: a biological perspective. *Lancet Neurol* 1:110-118.
- Shy ME, Arroyo E, Sladky J, Menichella D, Jiang H, Xu W, Kamholz J, Scherer SS (1997) Heterozygous P0 knockout mice develop a peripheral neuropathy that resembles chronic inflammatory demyelinating polyneuropathy (CIDP). *J Neuropathol Exp Neurol* 56:811-821.
- Shy ME, Chen L, Swan ER, Taube R, Krajewski KM, Herrmann D, Lewis RA, McDermott MP (2008) Neuropathy progression in Charcot-Marie-Tooth disease type 1A. *Neurology* 70:378-383.
- Shy ME, Blake J, Krajewski K, Fuerst DR, Laura M, Hahn AF, Li J, Lewis RA, Reilly M (2005) Reliability and validity of the CMT neuropathy score as a measure of disability. *Neurology* 64:1209-1214.

- Skre H (1974) Genetic and clinical aspects of Charcot-Marie-Tooth's disease. *Clin Genet* 6:98-118.
- Sleeman MA, Fraser JK, Murison JG, Kelly SL, Prestidge RL, Palmer DJ, Watson JD, Kumble KD (2000) B cell- and monocyte-activating chemokine (BMAC), a novel non-ELR alpha-chemokine. *Int Immunol* 12:677-689.
- Stanley ER, Berg KL, Einstein DB, Lee PS, Pixley FJ, Wang Y, Yeung YG (1997) Biology and action of colony-stimulating factor-1. *Mol Reprod Dev* 46:4-10.
- Street VA, Bennett CL, Goldy JD, Shirk AJ, Kleopa KA, Tempel BL, Lipe HP, Scherer SS, Bird TD, Chance PF (2003) Mutation of a putative protein degradation gene LITAF/SIMPLE in Charcot-Marie-Tooth disease 1C. *Neurology* 60:22-26.
- Stubgen JP (2008) Tumor necrosis factor-alpha antagonists and neuropathy. *Muscle Nerve* 37:281-292.
- Sunderkotter C, Nikolic T, Dillon MJ, Van Rooijen N, Stehling M, Drevets DA, Leenen PJ (2004) Subpopulations of mouse blood monocytes differ in maturation stage and inflammatory response. *J Immunol* 172:4410-4417.
- Suter U, Snipes GJ (1995a) Biology and genetics of hereditary motor and sensory neuropathies. *Annu Rev Neurosci* 18:45-75.
- Suter U, Snipes GJ (1995b) Peripheral myelin protein 22: facts and hypotheses. *J Neurosci Res* 40:145-151.
- Suter U, Scherer SS (2003) Disease mechanisms in inherited neuropathies. *Nat Rev Neurosci* 4:714-726.
- Suter U, Moskow JJ, Welcher AA, Snipes GJ, Kosaras B, Sidman RL, Buchberg AM, Shooter EM (1992a) A leucine-to-proline mutation in the putative first transmembrane domain of the 22-kDa peripheral myelin protein in the trembler-J mouse. *Proc Natl Acad Sci U S A* 89:4382-4386.
- Suter U, Welcher AA, Ozelik T, Snipes GJ, Kosaras B, Francke U, Billings-Gagliardi S, Sidman RL, Shooter EM (1992b) Trembler mouse carries a point mutation in a myelin gene. *Nature* 356:241-244.

- Suter U, Snipes GJ, Schoener-Scott R, Welcher AA, Pareek S, Lupski JR, Murphy RA, Shooter EM, Patel PI (1994) Regulation of tissue-specific expression of alternative peripheral myelin protein-22 (PMP22) gene transcripts by two promoters. *J Biol Chem* 269:25795-25808.
- Taskinen HS, Roytta M (2000) Increased expression of chemokines (MCP-1, MIP-1alpha, RANTES) after peripheral nerve transection. *J Peripher Nerv Syst* 5:75-81.
- Thomas PK, King RH, Small JR, Robertson AM (1996) The pathology of charcot-marie-tooth disease and related disorders. *Neuropathol Appl Neurobiol* 22:269-284.
- Toews AD, Barrett C, Morell P (1998) Monocyte chemoattractant protein 1 is responsible for macrophage recruitment following injury to sciatic nerve. *J Neurosci Res* 53:260-267.
- Tofaris GK, Patterson PH, Jessen KR, Mirsky R (2002) Denervated Schwann cells attract macrophages by secretion of leukemia inhibitory factor (LIF) and monocyte chemoattractant protein-1 in a process regulated by interleukin-6 and LIF. *J Neurosci* 22:6696-6703.
- Traka M, Dupree JL, Popko B, Karagogeos D (2002) The neuronal adhesion protein TAG-1 is expressed by Schwann cells and oligodendrocytes and is localized to the juxtaparanodal region of myelinated fibers. *J Neurosci* 22:3016-3024.
- Trapp BD, Quarles RH (1982) Presence of the myelin-associated glycoprotein correlates with alterations in the periodicity of peripheral myelin. *J Cell Biol* 92:877-882.
- Ulzheimer JC, Peles E, Levinson SR, Martini R (2004) Altered expression of ion channel isoforms at the node of Ranvier in P0-deficient myelin mutants. *Mol Cell Neurosci* 25:83-94.
- Vance JM, Nicholson GA, Yamaoka LH, Stajich J, Stewart CS, Speer MC, Hung WY, Roses AD, Barker D, Pericak-Vance MA (1989) Linkage of Charcot-Marie-Tooth neuropathy type 1a to chromosome 17. *Exp Neurol* 104:186-189.
- Vass K, Hickey WF, Schmidt RE, Lassmann H (1993) Bone marrow-derived elements in the peripheral nervous system. An immunohistochemical and ultrastructural investigation in chimeric rats. *Lab Invest* 69:275-282.
- Vital A, Vital C, Julien J, Fontan D (1992) Occurrence of active demyelinating lesions in children with hereditary motor and sensory neuropathy (HMSN) type I. *Acta Neuropathol* 84:433-436.

- Vital A, Vital C, Lagueny A, Ferrer X, Ribiere-Bachelier C, Latour P, Petry KG (2003) Inflammatory demyelination in a patient with CMT1A. *Muscle Nerve* 28:373-376.
- Voyvodic JT (1989) Target size regulates calibre and myelination of sympathetic axons. *Nature* 342:430-433.
- Waetzig V, Czeloth K, Hidding U, Mielke K, Kanzow M, Brecht S, Goetz M, Lucius R, Herdegen T, Hanisch UK (2005) c-Jun N-terminal kinases (JNKs) mediate pro-inflammatory actions of microglia. *Glia* 50:235-246.
- Waller A (1850) Experiments on the section of the glossopharyngeal and hypoglossal nerves of the frog, and observations of the alterations produced thereby in the structure of their primary fibers. *Phil Trans R Soc London (Biol)* 140:423-429.
- Yoo JK, Kwon H, Khil LY, Zhang L, Jun HS, Yoon JW (2005) IL-18 induces monocyte chemotactic protein-1 production in macrophages through the phosphatidylinositol 3-kinase/Akt and MEK/ERK1/2 pathways. *J Immunol* 175:8280-8286.
- Yoshihara T, Kanda F, Yamamoto M, Ishihara H, Misu K, Hattori N, Chihara K, Sobue G (2001) A novel missense mutation in the early growth response 2 gene associated with late-onset Charcot-Marie-Tooth disease type 1. *J Neurol Sci* 184:149-153.
- Young P, Wiebusch H, Stogbauer F, Ringelstein B, Assmann G, Funke H (1997) A novel frameshift mutation in PMP22 accounts for hereditary neuropathy with liability to pressure palsies. *Neurology* 48:450-452.
- Zielasek J, Martini R, Toyka KV (1996) Functional abnormalities in P0-deficient mice resemble human hereditary neuropathies linked to P0 gene mutations. *Muscle Nerve* 19:946-952.
- Zorzano A, Bach D, Pich S, Palacin M (2004) [Role of novel mitochondrial proteins in energy balance]. *Rev Med Univ Navarra* 48:30-35.
- Zubair S, Holland NR, Beson B, Parke JT, Prodan CI (2008) A novel point mutation in the PMP22 gene in a family with Roussy-Levy syndrome. *J Neurol* 255:1417-1418.
- Zuchner S, Mersiyanova IV, Muglia M, Bissar-Tadmouri N, Rochelle J, Dadali EL, Zappia M, Nelis E, Patitucci A, Senderek J, Parman Y, Evgrafov O, Jonghe PD, Takahashi Y, Tsuji S, Pericak-Vance MA, Quattrone A, Battaloglu E, Polyakov AV, Timmerman V, Schroder JM, Vance JM (2004) Mutations in the mitochondrial GTPase mitofusin 2 cause Charcot-Marie-Tooth neuropathy type 2A. *Nat Genet* 36:449-451.

C. Abbreviations

APC	allophycocyanin
BDNF	brain-derived neurotrophic factor
BMAC	B-cell- and monocyte-activating chemokine
BMC	bone marrow chimera
bp	base pairs
BRAK	breast and kidney-expressed chemokine
BSA	bovine serum albumin
Caspr	contactin associated protein
CCL2	chemokine (C-C-motif) ligand 2
CCR2	chemokine (C-C-motif) ligand 2
CD	cluster of differentiation
cDNA	complementary desoxyribonucleic acid
CMAP	compound muscle action potential
CMT	Charcot-Marie-Tooth disease
CMTNS	CMT neuropathy score
CNS	central nervous system
CXCL14	CXC chemokine ligand 14
Cx32	Connexin-32
Cy3	Indocarbocyanin
DAB	diaminobenzidine-HCl
DABCO	1,4Diazobicyclo[222]octan
DAPI	4',6-diamidino-2-phenylindole
DEPC	diethyl pyrocarbonate
DMEM	Dulbecco`s Modified Eagle`s medium
DMSO	dimethylsulfoxid
DNA	Desoxyribonucleic acid
DSS	Dejerine-Sottas syndrome
DTT	1,4-Dithiothreitol
E	embryonic day
ECL	enhanced chemiluminescence
EGR-2	early growth response
ELISA	enzyme-linked immunosorbent assay

ER	endoplasmic reticulum
ERK1/2	extracellular signal-regulated kinase 1/2
FACS	fluorescence activated cell sorting
FCS	fetal calf serum
FITC	fluorescein-5-isothiocyanat
GDAP1	ganglioside-induced differentiation-associated protein-1
GJB1	Gap junction protein, beta-1
GFP	green fluorescent protein
HIV	human immuno deficiency virus
HMSN	hereditary motor and sensory neuropathy
HNPP	hereditary neuropathy with liability to pressure palsies
HSAN	hereditary sensory and autonomy neuropathy
HSN	hereditary sensory neuropathy
hPMP22	human peripheral myelin protein-22
IFN γ	Interferon-gamma
IgG	Immunglobuline
IL	interleukin
I κ B α	I κ B α Nuclear factor of kappa light polypeptide gene enhancer in B-cells inhibitor, alpha
JNK	c-jun N-terminal kinase
K ⁺ channels	potassium channels
kDa	kilo-Dalton
LIF	leukaemia inhibitory factor
LITAF	lipopolysaccharide-induced tumor necrosis factor- α factor
LPS	lipopolysaccharide
MAC-2	macrophage galactose-specific lectin-2
MAG	myelin-associated glycoprotein
MAPK	mitogen-activated protein kinase
MBP	myelin basic protein
MCP-1	monocyte chemoattractant protein-1
MEK1/2	MAPK-ERK-kinase
MFN2	mitofusin-2
MPZ	myelin protein zero
mRNA	messenger ribonucleid acid
M-SCF	macrophage-colony stimulating factor
MTMR2	myotubularin-related protein-2

Na ⁺ channels	sodium channels
NCV	nerve conduction velocity
op	osteopetrotic
PBS	phosphate buffered saline
PBST	phosphate buffered saline / Tween
PCR	polymerase chain reaction
PD-1	programmed death-1
PE	phycoerythrin
PERCP	peridinin chlorophyll protein
PFA	paraformaldehyde
PKC α	protein kinase C-alpha
PLA ₂	phospholipase A ₂
PMP22	peripheral myelin protein-22
PNS	peripheral nervous system
P	postnatal day
qRT-PCR	semiquantitative real-time PCR
RAG-1	recombination-activating gene-1
RIPA	radio-immuno precipitation assay
RNA	ribonucleid acid
RT	room temperature
SD	standard deviation
SDS	sodium dodecyl sulphate
Sn	sialoadhesin
STAT	signal transducer and activator of transcription
tg	transgenic
TBE	Tris-borate-EDTA
TGF β	tumor growth factor-beta
T _H	T-helper cell
TNF α	tumor necrosis factor-alpha
Tr	Trembler
Tr ^J	Trembler-J
wt	wild type
YAC	yeast artificial chromosome

D. Curriculum vitae

Persönliche Daten

Bianca Dorothea Kohl
geb. am 16.11.1978 in Miltenberg
ledig

Berufliche Tätigkeiten

- | | |
|-------------------|---|
| 06/2005 – 07/2009 | Wissenschaftliche Mitarbeiterin, Neurologische Klinik und Poliklinik, Experimentelle Entwicklungsneurobiologie, Prof. Dr. Rudolf Martini, Julius-Maximilians-Universität, Würzburg |
| 08/2004 – 05/2005 | Diplomarbeit, Neurologische Klinik und Poliklinik, Experimentelle Entwicklungsneurobiologie, Prof. Dr. Rudolf Martini, Julius-Maximilians-Universität, Würzburg; Titel: „Die Blut-Hirn-Schranke im Mausmodell einer PLP-überexprimierenden Myelinmutante“ |
| 07/2003 – 12/2003 | Studentische Hilfskraft, Neurologische Klinik und Poliklinik, Experimentelle Entwicklungsneurobiologie, Prof. Dr. Rudolf Martini, Julius-Maximilians-Universität, Würzburg |

Studium

- | | |
|-------------------|---|
| 04/1999 – 05/2005 | Studium der Biologie (Diplom), Julius-Maximilians-Universität Würzburg; Schwerpunkte: Neurobiologie, Verhaltensphysiologie und Biotechnologie |
|-------------------|---|

Schulbildung

- | | |
|-------------------|---|
| 09/1995 – 07/1998 | Allgemeine Hochschulreife; Wirtschaftsgymnasium, Walldürn |
| 09/1991 – 07/1995 | Mittlere Reife; Realschule, Miltenberg |
| 09/1985 – 07/1991 | Grund- und Volksschule Kleinheubach |

E. List of Publications

Publications

Kohl B., Fischer S., Wessig C., Martini R.; American Journal of Pathology, *submitted*.

MCP-1 mediates axonopathy in a PMP22-overexpressing mouse model for Charcot-Marie-Tooth 1A neuropathy.

Barbaria E. M., Kohl B., Buhren B. A. , Hasenpusch-Theil K., Kuery P., Martini R., Mueller H. W.; Neurobiology of Disease, March 2009, Volume 33, Issue 3: 448-458:

The α -chemokine CXCL14 is up-regulated in the sciatic nerve of a mouse model of Charcot-Marie-Tooth disease type 1A and alters myelin gene expression in cultured Schwann cells.

Ip, C. W., Kroner A., Kohl B., Wessig C., Martini R.; Neurobiology of Disease, February 2009, Volume 33, Issue 2: 207-212:

Tacrolimus (FK506) causes disease aggravation in models for inherited peripheral myelinopathies.

Ip, C. W., Kohl B., Kleinschnitz, C., Reuss, B., Nave, K. A., Kroner, A., Martini, R.; Molecular and Cellular Neuroscience; 2008 Aug; 38(4):489-94:

Origin of CD11b⁺ macrophage-like cells in the CNS of PLP-overexpressing mice: Low influx of haematogenous macrophages and unchanged blood-brain-barrier in the optic nerve.

Poster presentations

Kohl B., Fischer S., Wessig C., Martini R.; Biennial Meeting 2009, Wuerzburg, Germany:

Functional impairment, but not demyelination, is correlated with MCP-1 expression in a mouse model for CMT1A

Kohl B., Fischer S., Groh J., Weishaupt A., Troppmair J., Martini R.; Society for Neuroscience, 38th Annual Meeting, November 2008, Washington, D.C., USA:

The monocyte chemoattractant protein-1 is a pathogenetically relevant modulator of inherited peripheral neuropathies in animal models for Charcot-Marie-Tooth Type-1 disorders.

Fischer S., Kohl B., Groh J., Troppmair J., Martini R.; Immunology Training Network, Wildbad/Rothenburg ob der Tauber, July 2008:

Characterization of the pathological impact and regulation of MCP-1 in three different myelin mutants of the peripheral nervous system.

Kroner A., Kohl B., Kobsar I., Martini R., Mäurer M.; Federation of Clinical Immunology Societies, Boston, USA; Clinical Immunology, May 2005:

Endoneurial CD34-positive macrophages activation in the peripheral nerve?

Danksagung

An dieser Stelle möchte ich mich bei all jenen bedanken, die zum erfolgreichen Gelingen dieser Arbeit beigetragen haben:

Beginnen möchte ich mit Prof. Dr. Rudolf Martini und mich für die Möglichkeit, auf diesem Gebiet arbeiten zu können, bedanken. Nicht nur im Zuge der Doktorarbeit, sondern schon auch als Student habe ich sein umfangreiches Wissen, sein zielorientiertes Denken und seine Begeisterungsfähigkeit zu schätzen gelernt. Danken möchte ich ihm auch für die optimale Anleitung und Betreuung, die entscheidend für diese Arbeit war, sowie für zukunftsweisende Ratschläge.

Bei Prof. Dr. Erich Buchner bedanke ich mich für die Tätigkeit als zweiter Gutachter dieser Arbeit. Außerdem möchte ich mich bei Prof. Dr. Hans Werner Müller und Dr. Elena Barbaria für eine angenehme und erfolgreiche Zusammenarbeit bedanken, sowie für interessante Diskussionen und Anregungen.

Ein besonderer Dank geht an Dr. Stefan Fischer, der mir in den letzten Jahren auch außerhalb des Labors ein wichtiger Freund geworden ist. Er hat mir nicht nur bei der Einarbeitung in neue Methoden geholfen, sondern war mir stets ein wertvoller Ratgeber und Diskussionspartner im Laboralltag. Selbst in Momenten, in denen er kaum Zeit hatte, war er immer für meine Gedanken offen und hatte oft hilfreiche Anregungen. Obwohl sein Beistand bei meinem Kaffee-Entzug zu einer neuen Kräutertee-Abhängigkeit führte, werde ich mich immer gerne an die schöne Zeit zurück erinnern. Bei Dr. Antje Kroner möchte ich mich ebenfalls für viele gute Ratschläge, Diskussionen und die Hilfe bei der Durchführung der PD-1-Studie bedanken. Die Zusammenarbeit mit ihr hat großen Spaß gemacht, was nicht zuletzt an ihrem besonderen Humor gelegen hat. Auch mit ihr verbindet mich eine Freundschaft, die über „Schreibtisch-Grenzen“ hinaus reichen wird.

Bedanken möchte ich mich auch bei Karl-Heinz Aulenbach für die sehr gute Pflege und die optimale Organisation der Mäuse, sowie seine unermüdliche Ausdauer bei der Verpaarung unwilliger Mausböcke. Helga Brünner sage ich ebenso Danke für die optimale Organisation der Mäuse, ihre Hilfe bei Sonderwünschen und die nette Zusammenarbeit. Außerdem geht ein großes Dankeschön an alle Personen der aktuellen und ehemaligen AG Martini,

besonders an Dr. Carsten Wessig, der trotz seines vollen Arbeitstags immer Zeit für präzise elektrophysiologische Messungen hatte, auch wenn ein paar Sonderwünsche dabei waren; an Janos Groh, bei dem zuletzt nur ein flüchtiger Blick gereicht hat, um ihn zu einem Kaffee „zu überreden“; an Silke Loserth, deren „Hmmm“ ich immer äußerst nett fand und mit der die Zusammenarbeit aufgrund ihrer Begeisterungsfähigkeit besonders Spaß gemacht hat; an Bettina Meyer, die die PMP22-Genotypisierung immer wieder geduldig wiederholt hat, wenn die Primer mal nicht so wollten, wie sie eigentlich sollten und an Nadine Weckesser, die als Frühaufsteherin schon immer alles am Laufen hatte, bevor das Labor voll wurde. Mein besonderer Dank geht an Heinrich Blazyca und Carolin Kiesel, die mir vor sechs Jahren als Laborfrischling alles gezeigt und mich ausgezeichnet in den Laboralltag eingearbeitet haben. Im Laufe der Zeit habe ich in beiden gute Freunde gefunden, auch außerhalb des Laborlebens.

Bei Sabine Matschl und Annina Seitz möchte ich mich besonders bedanken für die leider viel zu wenigen, dafür aber umso längeren Telefongespräche. Ich könnte mir keine besseren Freundinnen vorstellen, da sie nie den Glauben an mich verloren haben und mir immer wieder zeigten, was mir wirklich wichtig ist. Ein großer Dank geht auch an Martin Kiesel und an Klaus Mittendorfer, die als sehr enge Freunde ebenfalls alle Höhen und Tiefen der letzten Jahre mitbekommen haben.

Ganz besonders bedanken möchte ich mich bei den Menschen, denen auch diese Arbeit gewidmet ist, meiner Familie und Martin. Meine Familie war besonders in den letzten Jahren eine „Insel“ für mich, wohin ich mich zurückziehen und erholen konnte. Insbesondere meinen Eltern möchte ich für ihre ausdauernde Unterstützung, Ratschläge und Liebe danken, ohne die ich nicht so weit gekommen wäre. Herzlicher Dank geht an Martin, der mir stets Halt, Ruhe, Ausgleich und eine wunderbare „WG“ gegeben hat. Besonders habe ich in der Zeit meiner Doktorarbeit sein enormes Verständnis, seine ausdauernde Geduld, die wertvollen Ratschläge und seinen grenzenlosen Optimismus zu schätzen gelernt.